

THE DESIGN, ASSEMBLY AND TESTING OF A LARGE
SCALE MODEL RISER FOR VORTEX INDUCED
VIBRATIONS

GILLIAN STONE



**The Design, Assembly and Testing of a
Large Scale Model Riser for Vortex Induced Vibrations**

by

©Gillian Stone, B.Eng.

A thesis submitted to the School of Graduate Studies
in partial fulfillment of the requirements for the degree of
Master of Engineering

Faculty of Engineering and Applied Science

Memorial University of Newfoundland

September 2008

St. John's, Newfoundland, Canada

Abstract

Offshore oil and gas exploration has been moving into ever increasing water depths. On the East Coast of Canada exploration is being done in depths of up to 2,000m in the Orphan Basin region and deepwater exploration and development is ongoing in the water zones of 56 countries worldwide, in and adjacent to every continent.

Marine risers are pipes used to transport oil and gas from producing fields to surface platforms, tanker loading systems or back down to the ocean floor for export through a subsea pipeline. One of the growing issues facing deepwater risers is Vortex Induced Vibration (VIV), or large amplitude oscillations which occur when the vortex shedding frequency is approximately equal to the structures' natural frequency.

The focus of this research was to design, assemble and test a Large Scale deepwater riser model (130m in length) for VIV for two main purposes. The first was to be a learning process for the VIV team at Memorial University with the insight gathered in designing and assembling a large scale model in a field situation being invaluable to future projects.

The second was through the development of the large scale model, to provide an intermediate step between the common riser models (8-10m in length) that have mainly been used to research and predict VIV to date and the actual 3,000m deepwater risers currently being used in industry.

The Large Scale Model Riser (LS – Model Riser) that was developed was relatively robust and the assembly and testing went well. Small changes in the parts, instrumentation and assembly process were necessary to aid in assembly and to help the

model function properly. The LS – Model Riser was to be outfitted with 65 modules along its length, however, due to problems during assembly and testing, only 28 of those modules were operational during testing. It was felt that although the large drop out rate was unfortunate, the working modules were still located along the entire length of the model and would yield useful data, so testing was carried out with the remaining 28 working modules. The resulting data that was collected was analyzed and determined to be useful, proving that the model could be used as a base for future VIV analysis projects.

Acknowledgments

I would like to thank my supervisor Dr. Neil Bose and Xiangqun Li for their input and suggestions throughout the tenure of this degree program. This project was undertaken with a grant and the financial assistance of Petroleum Research Atlantic Canada (PRAC), the National Sciences and Engineering Research Council, Canada (NSERC), and the National Research Council, Canada (NRCC). Also, I would like to thank Memorial University of Newfoundland (MUN) for the use of their facilities, especially the Technical Services Department. Specifically, I would like to thank Roy Crocker, Chris Batten and Fred Walsh of the MUN Engineering Technical Services Electronics Design and Fabrication Shop, and Jason Miller and David Snook of the MUN Engineering Technical Services Machine Shop. Without their time and knowledge, this research could not have been completed and I greatly appreciate all of the hard work they have put into this project.

I would also like to thank Martin Ordonez, who spent many long nights and weekends designing the electrical system and writing the code to run all of the instrumentation. This project would have been useless without your expertise and hard work and I am indebted to you for this.

Thank you to the Institute for Ocean Technology (IOT) and Wayne Raman-Nair for allowing me to use their Riser Dynamics Code and for helping me apply the code to my own special circumstance.

Thank you to Kean's Pump Shop who helped me design a watertight way to bring the cables from the riser to the vessel and helped me keep the ocean oil free.

To the owner Frank Hutchings and the captain and crew of the *Miss Jacqueline IV*, many thanks for helping to make the test run smoothly and making the test day such an enjoyable experience.

Finally, I would like to acknowledge my family, without whom this research could not have been accomplished. Their time, patience and support, not only during this project, but in every aspect of my life, is over and above what can be expected and for that I am ever grateful.

Table of Contents

ABSTRACT	II
ACKNOWLEDGMENTS	IV
TABLE OF CONTENTS	VI
LIST OF FIGURES	IX
LIST OF TABLES	XIV
LIST OF APPENDICES	XV
1 INTRODUCTION	1
2 LITERATURE REVIEW	5
2.1 LARGE SCALE VIV EXPERIMENTS	7
2.1.1 CASTINE, MAINE EXPERIMENTS	7
2.1.2 ARCTIC OCEAN AND ST. CROIX EXPERIMENTS	8
2.1.3 LAWRENCE, MASSACHUSETTS EXPERIMENTS	9
2.1.4 EXPERIMENTS OF THE 1990's	10
2.1.5 STRIDE JIP EXPERIMENTS	14
2.1.6 DEEPSTAR EXPERIMENTS	18
3 METHODOLOGY	22
3.1 PROTOTYPE RISER	22
3.2 MODEL SCALING AND SIMILARITY THEORY	23
3.2.1 WEIGHT PER UNIT LENGTH AND CURRENT SPEED	24

3.2.2	TENSION AND BENDING STIFFNESS	26
3.3	NATURAL AND SHEDDING FREQUENCIES	28
3.4	INSTITUTE FOR OCEAN TECHNOLOGY RISER DYNAMICS CODE....	33
3.4.1	INPUT DATA.....	33
3.4.1.1	INPUTS.M	34
3.4.1.2	INPUTS_AUX1.M	35
3.4.1.3	P0.M, PN.M, P0DOT.M AND PNDOT.M.....	35
3.4.1.4	VFLUID.M	37
3.4.2	OUTPUT	38
3.4.2.1	TENSION	38
3.4.2.2	MAXIMUM TENSILE STRESS.....	40
3.4.2.3	PROFILE	41
3.4.2.4	CROSS FLOW VIV RESPONSE.....	45
3.4.3	SENSITIVITY STUDY OF BENDING STIFFNESS	47
3.5	PLACEMENT OF ACCELEROMETERS	50
4	LARGE SCALE MODEL RISER	53
4.1	PARTS	53
4.1.1	PIPE.....	53
4.1.1.1	TENSION TEST.....	55
4.1.2	INSTRUMENTATION	58
4.1.2.1	PRESSURE TEST	60
4.1.3	POWER/GROUND AND COMMUNICATION CABLES.....	61
4.1.4	PLACEMENT PUCKS.....	63
4.1.5	COATED WIRE ROPE	64
4.1.6	EPOXY	65
4.1.7	SOFTWARE.....	66
4.1.8	UNIVIS BIO 40	68
4.1.9	END CONFIGURATIONS	69
4.1.9.1	TOP SECTION	70
4.1.9.2	WIRE MESH GRIPS	71
4.1.9.3	T SECTION	73

4.1.9.4	DUMMY SECTION.....	75
4.1.9.5	BOTTOM SECTION.....	75
4.1.10	RAILWAY WHEEL.....	76
4.1.11	STEEL SPHERICAL BUOY.....	78
4.1.12	PUMP SYSTEM.....	79
5	ASSEMBLY PROCESS.....	81
6	TESTING VIV WITH THE LARGE SCALE MODEL	
	RISER.....	94
6.1	CALIBRATING THE LS - MODEL RISER.....	94
6.2	TRANSPORTING THE LS - MODEL RISER.....	95
6.3	TEST SETUP.....	101
6.3.1	TEST VESSEL - <i>MISS JACQUELINE IV</i>	102
6.3.2	TEST PLAN.....	103
6.4	TEST DAY.....	104
6.5	ACCELEROMETER DATA COLLECTED.....	115
6.6	DATA ANALYSIS.....	118
7	CONCLUSIONS AND RECOMMENDATIONS.....	129
7.1	DESIGN PROCESS.....	129
7.2	ASSEMBLY PROCESS.....	130
7.3	TESTING PROCESS AND DATA COLLECTION/ANALYSIS.....	139
8	REFERENCES.....	143

List of Figures

Figure 1: A Schematic of the Terra Nova Oil Field.....	2
Figure 2: Compliant Vertical Access Riser	12
Figure 3: Steel Catenary Riser	12
Figure 4: Lazy Wave Steel Catenary Riser.....	13
Figure 5: Helical Strakes on Marine Risers	16
Figure 6: Fairings Installed on a Marine Riser	16
Figure 7: Layout of Elastic Catenary Riser in IOT Riser Dynamics Code.....	36
Figure 8: Tension vs. Time Along the Model Length	39
Figure 9: Maximum Tensile Stress vs. Time Along the Model Length	41
Figure 10: X Position vs. Time Along the Model Length	42
Figure 11: Z Position vs. Time Along the Model Length.....	43
Figure 12: Final Profile for Maximum Current Speed 1.5m/s.....	45
Figure 13: Y Position vs. Time Along the Model Length	46
Figure 14: Tension vs. Time for the Sensitivity Study	48
Figure 15: Maximum Tensile Stress vs. Time for the Sensitivity Study	49
Figure 16: Samples of IPEX Pipe with the Stripe.....	53
Figure 17: Pressure Rating Changes with Temperature	54
Figure 18: ASTM Specimen Dimensions for Tension Tests.....	56
Figure 19: Tension Test - Stress vs. Strain Curve	57
Figure 20: Accelerometer Module	59

Figure 21: Full Module	59
Figure 22: Pressure Test Samples	60
Figure 23: Marine Institute Pressure Chamber	61
Figure 24: Internal Cables.....	62
Figure 25: External Cables.....	62
Figure 26: Placement Puck	63
Figure 27: Placement Pucks on a Module after Epoxy has Been Applied	64
Figure 28: Module/Placement Puck Assembly Entering the Pipe.....	65
Figure 29: Modules Drying after Epoxy had Been Applied	66
Figure 30: User Interface for Module Coding	67
Figure 31: The Completed Top Section.....	70
Figure 32: Wire Mesh Grip Strength Test Set-Up.....	72
Figure 33: T Section Being Attached to LS - Model Riser.....	73
Figure 34: Fully Assembled T Section	74
Figure 35: Completed T Section after Fixing Joint Leaks.....	74
Figure 36: Dummy Section.....	75
Figure 37: Bottom Section of the LS - Model Riser.....	76
Figure 38: Railway Wheel	77
Figure 39: Separation Plate, Shackle and Swivel	78
Figure 40: Steel Spherical Buoy	79
Figure 41: Pump System Set-Up.....	80
Figure 42: Pipe Laid out Behind IOT	82

Figure 43: Cables and Instrumentation Laid Out.....	83
Figure 44: Modules Laid Out Beside Power Cables.....	84
Figure 45: Weak Connections on Original Modules	86
Figure 46: Reinforced Soldered Joints.....	87
Figure 47: Tent Setup.....	88
Figure 48: Completed Module Ready to Enter the Pipe.....	89
Figure 49: The Tent After The Storm	90
Figure 50: After The Storm - Unsheltered Work Setup.....	91
Figure 51: The Buried Pipe Uncovered by a Snow Plow	92
Figure 52: The Coiled LS - Model Riser	95
Figure 53: Lifting the Coiled LS - Model Riser	96
Figure 54: Laying the LS - Model Riser on the Truck	96
Figure 55: Securing the LS - Model Riser to the Truck	97
Figure 56: LS - Model Riser Secured to the Boom Truck.....	97
Figure 57: Truck Loaded with Buoy, Railway Wheel and LS - Model Riser	98
Figure 58: Sphere Buoy Being Lifted On Board	99
Figure 59: LS - Model Riser Being Lifted In Over the Starboard Side.....	99
Figure 60: LS - Model Riser Being Lifted In Over the Starboard Side.....	100
Figure 61: Equipment On Board the <i>Miss Jacqueline IV</i> Ready for Testing	100
Figure 62: Test Setup.....	101
Figure 63: End Assembly Sketch.....	102
Figure 64: <i>Miss Jacqueline IV</i>	103

Figure 65: Buoy Attachment Details	105
Figure 66: Buoy Lowered Into The Water.....	106
Figure 67: The Buoy Towed at 60' Behind the Vessel	107
Figure 68: Lowering the LS - Model Riser Overboard.....	108
Figure 69: Lifting the Railway Wheel over the Side	109
Figure 70: Lowering the Railway Wheel into the Water.....	109
Figure 71: The Buoy Winched into the Vessel.....	111
Figure 72: Location of Shackle Causing the CAN Bus to Wear	112
Figure 73: Worn CAN Bus Cable.....	112
Figure 74: Starting to Pull the LS - Model Riser on Board	113
Figure 75: Pulling the LS - Model Riser on Board.....	114
Figure 76: Securing the Completely Coiled LS - Model Riser.....	114
Figure 77: Working and Dead Sensors	116
Figure 78: In-Line Acceleration Time History	119
Figure 79: Cross-Flow Acceleration Time History	119
Figure 80: In-Line Displacement Time History.....	120
Figure 81: Cross-Flow Displacement Time History	120
Figure 82: In-Line Amplitude vs. Reduced Velocity.....	121
Figure 83: In-Line Frequency vs. Reduced Velocity.....	122
Figure 84: In-Line Modal Component Time History - Mode 1.....	123
Figure 85: In-Line Modal Component Time History - Mode 25.....	123
Figure 86: Cross-Flow Modal Component Time History - Mode 1	124

Figure 87: Cross-Flow Modal Component Time History - Mode 25 124

Figure 88: In-Line Displacement Spectra 125

Figure 89: Cross-Flow Displacement Spectra 126

Figure 90: Vibration Trajectory Example 1 127

Figure 91: Vibration Trajectory Example 2 128

Figure 92: Vibration Trajectory Example 3 128

List of Tables

Table 1: Prototype-DCR Dimensions	23
Table 2: Natural Frequency Calculations	30
Table 3: Natural Frequency Calculations using Similitude Bending Stiffness.....	32
Table 4: Maximum Tension (Newtons).....	38
Table 5: Maximum Tensile Stress (Pascals).....	40
Table 6: Number and Distance Between Modules	50
Table 7: Final Position of Modules Inside LS-Model Riser	51
Table 8: Test Plan	104

List of Appendices

Appendix A - Prototype DCR Characteristics	A-1
Appendix B - Bending Stiffness Calculation.....	B-1
Appendix C - Natural Frequency Calculations.....	C-1
Appendix D - IOT Riser Dynamics Code Input Files.....	D-1
Appendix E - IOT Riser Dynamics Code Output	E-1
Appendix F - Tension Test Data and Calculations	F-1
Appendix G - Instrumentation Product Data Sheets.....	G-1
Appendix H - UNIVIS BIO 40 Product Data Sheet	H-1

1 Introduction

The phenomenon of vortex shedding around cylindrical structures is a concern in many different engineering fields. Cylindrical structures are used in a variety of industrial areas from marine mooring lines and offshore marine risers to heat exchangers that use tubes as heating or cooling elements and the cables used to support suspension bridges.

Over the years, experimental and field data have proven that for a range of Reynolds number flows, whether it be the wind flowing over bridge cables, sea currents flowing over mooring lines or fluid flowing through a heat exchanger, vortex shedding is a common occurrence and can lead to large amplitude vibrations, or Vortex Induced Vibrations (VIV), given a specific object geometry and set of operating conditions.

VIV occurs when the vortex shedding frequency is approximately equal to the structure's natural frequency. This can cause the structure to undergo large amplitude oscillations, which can in turn increase fatigue and even cause clashing (impact) with other nearby structures. This VIV phenomenon is of great importance to the offshore oil and gas industry due to their use of cylindrical risers to transport product and other fluids.

Marine risers are used to transport oil and gas from producing fields to a surface platform and back down for export through a subsea pipeline or a tanker loading system. In Figure 1 of the Terra Nova field off the coast of Newfoundland [17], development risers can be seen extending from the ocean floor to the FPSO on the surface.

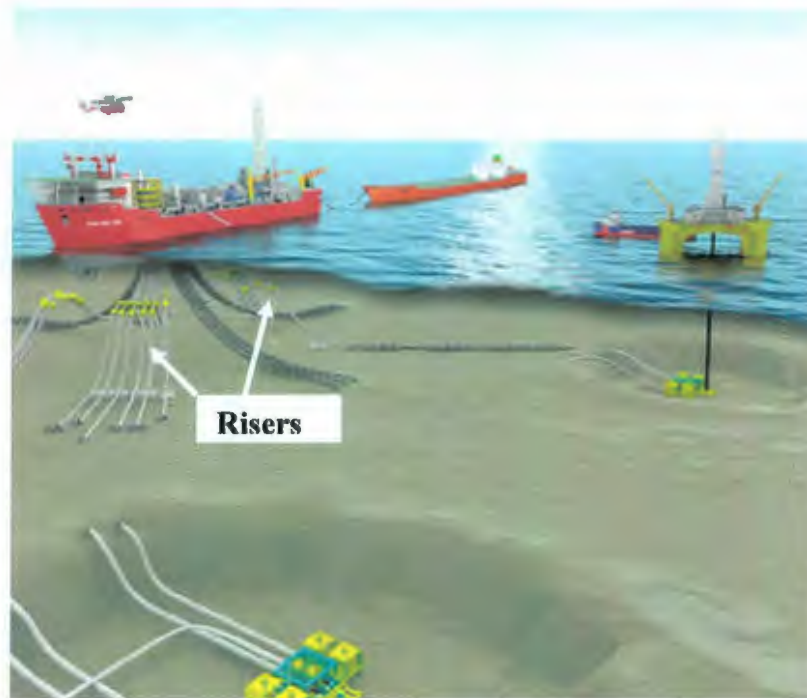


Figure 1: A Schematic of the Terra Nova Oil Field

Offshore oil and gas exploration has been moving into ever increasing water depths. Off the East Coast of Canada deepwater exploration is being done in the Orphan Basin region to the north east of the Grand Banks and off the Scotian Shelf. There were two deepwater wells drilled off the coast of Newfoundland by 2003 and three on the Scotian Slope by 2002 and deepwater drilling is expected to be a significant factor in the future of not only the Canadian, but also the worldwide offshore oil and gas industry [1]. Hence there is a strong need to address deepwater issues on marine risers.

Due to the increased water depth, a riser in a deepwater system will encounter more technological challenges than a shallow water riser. Firstly, the deepwater riser will encounter a more complex environment. In addition to waves, currents will also become an important factor affecting riser behavior. In some deepwater areas, current velocities

are not only very high (up to 2m/s), but they are usually non-uniform over water depth [26]. Secondly, deepwater risers are subjected to extremely large and non-uniform tension forces due to their long length and complex structural nature compared with their shallow-water equivalents. Finally, and of most interest to this work, high-mode VIV can occur with deepwater risers due to their excitation from these current forces and high tension. While shallow water riser spans often experience only first mode vibration, deepwater risers can experience very high modes of vibration and can also experience more than one mode of vibration at a time. A riser is said to be “locked in” when the frequency of oscillation is equal to the frequency of vortex shedding [27]. This is normally when the largest amplitude oscillations occur.

The focus of this research was to design, assemble and test a large scale deepwater riser model for VIV. This is valuable information for future analysis as this large scale model provides an intermediate step between the common 8 – 10m riser models that have frequently been used to research VIV and the actual 3,000m deepwater risers being used in industry today. If the results of this large scale research can be predicted by the available small scale model analysis, then it may be possible to extrapolate to the real life case. However, if the large scale results are quite different from the small scale model, then any extrapolation using the small scale model analysis may not be correct for the real life situation.

This thesis includes a concise overview of some of the initial work done on VIV of circular cylinders and a more detailed look at recent large scale field experiments studying VIV, particularly that of marine risers. It then describes a detailed design

methodology for modeling a large scale riser that has been developed using first principal calculations and a Riser Dynamics Code from the Institute for Ocean Technology. A detailed description of the parts of the model as well as the assembly process is given along with the testing procedure and the resulting data. Finally, a summary of conclusions and recommendations have been included with regard to improving every aspect of the project, from design to assembly and testing.

2 Literature Review

This section gives a concise overview of some of the initial work done on VIV of circular cylinders and a more detailed look at recent large scale field experiments studying VIV, particularly that of marine risers. There is a large body of literature available dealing with VIV, a majority of which in recent years deals specifically with VIV of marine risers. An overview of the subject can be found in [23]. The following researchers [24] have carried out extensive reviews dealing with the difficulties in defining the nature, occurrence and characteristics of VIV, Parkinson, Sarpkaya, Griffin and Ramberg, Bearman, Parkinson, Pantazopoulos, Sarpkaya and in books by Chen, Blevins, Naudascher and Rockwell, Sumer and Fredsoe and Au-Yang.

The study of circular cylinders excited into vibration by a flowing fluid was first explored by Strouhal and Rayleigh [22]. Their major findings were the initial basis for all VIV experiments that followed and a few of their important findings are still valid today, such as:

- The dimensionless group $S = \frac{f_s D}{U}$ (Strouhal number) is dependent upon the Reynolds number. Where f_s is the vortex shedding frequency, D is the cylinder outer diameter, and U is the current velocity.
- The cylinder does not need to vibrate in order for the fluid to apply a fluctuating force to it.

Since then, research done in this area was in part a refinement of these findings, and it was discovered that besides the mean drag, there are fluctuating lift and drag forces being exerted on the cylinder causing vibration [22]. These fluctuating lift and drag forces were not measured directly during this early research due to the lack of suitable instruments able to read such small forces, and therefore very few results were available. Once the technology had advanced and the measurement of these forces was possible, many different experiments have been done on VIV of circular cylinders. In the beginning, these experiments were done by measuring the lift, drag and steady (average) drag forces exerted by a fluid on a stationary cylinder [22]. As interest grew and technology progressed, the majority of experiments regarding the VIV of circular cylinders used fixed cylinders forced to vibrate at a fixed frequency, amplitude and Reynolds number. These experiments are referred to as “forced oscillation” experiments and still today much of the information available concerning the VIV of circular cylinders is based on these tests. Although useful in isolating different elements of VIV, these forced oscillation experiments do not completely explain the phenomenon and have been found to be quite different from the real life occurrence, where a cylinder is not fixed, but free to vibrate in response to the forces produced by its wake. In recent years, more work has been done on the VIV of circular cylinders for this more realistic case of “self-excited” or “free oscillation” experiments. The data from these experiments are useful and valid, but it is not known if the validity of extrapolating from these small scale experiments to the behavior of the actual large scale systems in the real world is entirely correct.

2.1 Large Scale VIV Experiments

Due to the movement of the oil and gas industry into deeper water, experiments have been taken further than small scale laboratory experiments and larger scale model risers have been designed and tested in different field situations.

2.1.1 Castine, Maine Experiments

Historically, it has been difficult to interpret the data obtained from larger scale systems, due to complications such as the inconsistent distribution of mass along the length of the riser model or non-uniform current velocity and tension over the length of the model. A field study was conducted by Vandiver and Mazel (1976) to address these problems and to try and find a link between the theoretical and small scale experimental data and actual large scale systems [11]. The study, located on a sandbar at the mouth of Holbrook Cove in Castine, Maine, tested 76.5 foot lengths of various cables with fixed ends held under constant tension in a uniform flow. They found that the moderately long cables behaved similarly to the small scale laboratory experiments and that lock-in was the dominant feature that controlled the response of the cables. If the Strouhal number was far from a natural frequency, the vortex shedding drove the vibration at the Strouhal frequency, but as the Strouhal frequency approached the cable's natural frequency, or frequencies, the phenomena of lock-in occurred at the natural frequency. Over a smaller band within this lock-in range, where the shedding frequency and the natural frequency were very close, the vibrations were self excited and "resonant lock-in" occurred. They also found that the largest single displacement peaks were found for non-resonant and

non-locked-in conditions, with resonant lock-in producing larger mean vibration amplitudes. The maximum Reynolds number tested was 6850, and the ratio of length to diameter ranged from 1892 to 5960, acceptable values by today's experimental standards. However, deepwater risers encounter multi-mode vibrations and can achieve very high mode numbers, whereas the maximum mode number achieved in these tests were 6 to 7 and there were only 2 accelerometers used to measure model displacements. The site near Castine, Maine was again used for a field experiment by Vandiver (1983) to extend the knowledge of VIV under field conditions [12]. Again acceptable values of Reynolds numbers up to 22,000 and length to diameter ratios of 750 were obtained, as well as drag coefficients which had never been measured on flexible cylinders undergoing significant vibration up to this point in time. Drag coefficients larger than 3 were found for the model experiencing lock-in under uniform flow conditions. Vandiver suggests that this may not be a practical design consideration for a number of reasons such as: these high drag coefficients were only observed in uniform flow during lock-in; and for actual field conditions the flow will not be uniform. Again, only the seventh mode was achieved, and only 7 pairs of accelerometers were used over the 75 foot model length.

2.1.2 Arctic Ocean and St. Croix Experiments

Kim et al. (1983) conducted field experiments in the Arctic Ocean and at St. Croix [7]. The tests used Kevlar cables ranging in length from 100 to 9,050 feet and 0.094 to 0.162 inches in diameter, which were hung over the side of a vessel where ocean currents provided the incoming flow velocity. It was found that the vibration response of a long

cable is essentially that of an infinite string and single mode lock-in was not observed in a shear current. As well, a parameter, N_s , which includes the effects of shear current on response, was proposed to predict the possibility of lock-in. However, only 3 accelerometers were used over the 875 foot model to determine modal displacements and there were problems reading the inflowing current correctly. An analysis of the drag coefficient for long cables in sheared flow revealed that for a range of Reynolds numbers from 200 to 2,000, the drag coefficients ranged from 1.40 to 1.58 with an average drag coefficient of approximately 1.49. As predicted by Vandiver, these values were much less than those obtained in the previously mentioned Castine experiments where the cables were in uniform flow and were experiencing lock-in.

2.1.3 Lawrence, Massachusetts Experiments

A historic mill canal in Lawrence, Massachusetts was used by Vandiver and Chung (1988) to conduct sheared current tests on an instrumented cable arranged horizontally across the width of the 58 foot canal [13]. The test cable was a 1.125 inch diameter rubber hose with 6 pairs of accelerometers along the length. Once again the tests were conducted under realistic field conditions, acceptable values of Reynolds numbers and length to diameter ratios, but with only a maximum mode number of 11 being achieved. An important conclusion from this experiment was that the highly turbulent shear flow did not alter the vibration of the cable when compared to Vandiver's prior work, such as the testing in Castine, Maine. However, the vibration response did have a broader frequency bandwidth due to the turbulence, and this prevented single mode lock-in even in the nearly uniform current profile. Another important finding was that with the

exception of single mode lock-in, the hydrodynamic modal damping was 10 to 100 times larger than the structural damping, with the highest modes having the least damping. This showed that hydrodynamic damping is important in determining flow-induced vibration response.

2.1.4 Experiments of the 1990's

In the late 1990's, the oil and gas industry was flourishing and many different projects were being completed by joint industry and academic groups to study VIV of deepwater marine risers. In July 1996, Lie et al. (1998) conducted tests on a bare riser model for different shear profiles and speeds using a rotating arm tank at MARINTEK, the results of which appeared along with those of an additional test using the same rig for a staggered buoyancy riser [9]. A staggered buoyancy riser has modules attached along the length of the riser to provide buoyancy. This mimics an actual deepwater riser, as buoyancy modules are used frequently to achieve different riser configurations. The buoyancy modules may be situated at differing intervals along the riser and may have bare sections of riser between them. Therefore, the flow around the riser will actually be flowing around two different diameter cylinders, the bare riser diameter and the buoyancy module diameter. One of the main conclusions of the tests was that only one peak frequency was observed in the transverse displacement spectra for the bare riser, in both uniform and shear currents, whereas the staggered buoyancy riser test found at least two peaks. This suggested that the riser had locked into both the vortex shedding frequency related to the bare riser diameter, as well as the vortex shedding frequency related to the buoyancy module diameter. One of the important results of this work was

the Strouhal number was found to be 0.15, which differs from the accepted value of 0.2 up to this point. This is important when designing deepwater risers, as the estimated VIV response is a result of the assumed Strouhal number and will differ with any variation, leading to a riser which could experience VIV when it has not been accounted for in the design.

In August of 1997, a 90m long riser model was tested in a Norwegian fjord by Huse et al. (1998). The resulting paper focuses on the concern that VIV can cause considerable fluctuations in axial tension which can lead to high fatigue stresses [6]. They developed a theory that indicates if VIV occurs at a frequency that will excite the first axial resonance, then very high and possibly dangerous stresses can occur. Although this is an important discovery regarding the design of deepwater risers, in particular with regard to fatigue life, it is beyond the scope of this research. However, it is important to note this finding, and perhaps in the future research can be done using the model riser designed in this research to carry out fatigue analysis.

Another large scale riser model test was carried out by Grant et al. (1999) using three Highly Compliant Rigid (HCR) riser configurations [2]. The tests were done in Lake Pend Oreille in Idaho using a Compliant Vertical Access Riser (CVAR), a Steel Catenary Riser (SCR) and a Lazy Wave SCR.

A Compliant Vertical Access Riser (CVAR), shown in Figure 2 [19], is a concept riser for deepwater. A double-curvature shape, obtained by buoyancy attached to the lower section of the riser, is used to achieve vertical compliancy which allows relative heave motion between the upper and lower ends of the riser.

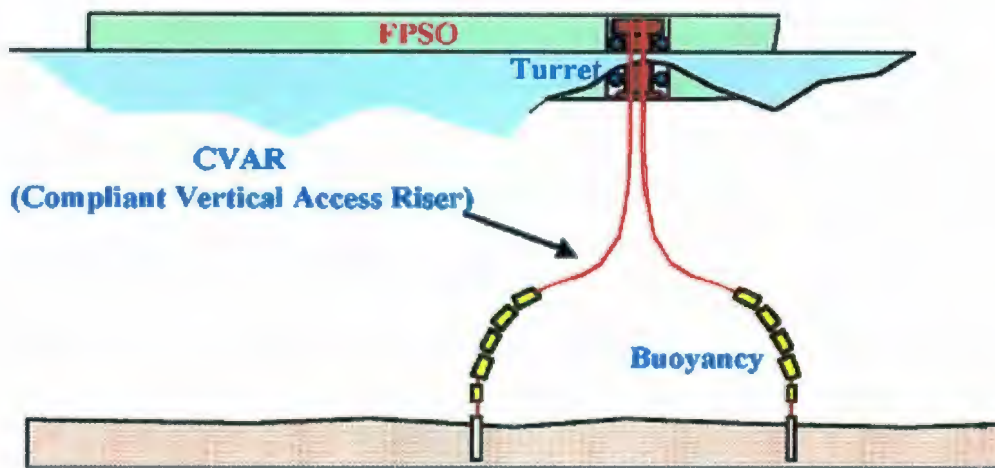


Figure 2: Compliant Vertical Access Riser

A Steel Catenary Riser (SCR), shown in Figure 3 [20], is a long steel pipe that hangs freely and gently curves down to the seabed from a floating production system. This is the simplest of all riser configurations.

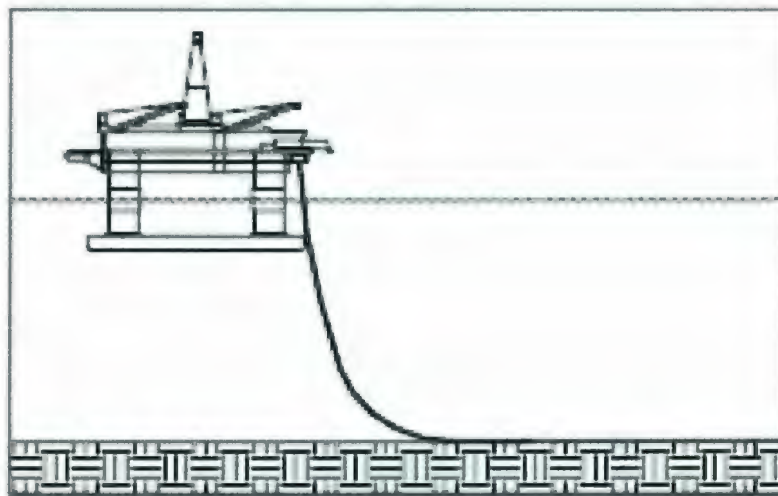


Figure 3: Steel Catenary Riser

A Lazy Wave SCR, shown in Figure 4 [20], is similar to a Steel Catenary Riser but has support provided at about midwater by distributed buoyancy modules. 'Lazy' refers to

the riser centerline which is parallel with the seabed on contact while 'Wave' refers to the line shape as a result of the buoyancy modules.

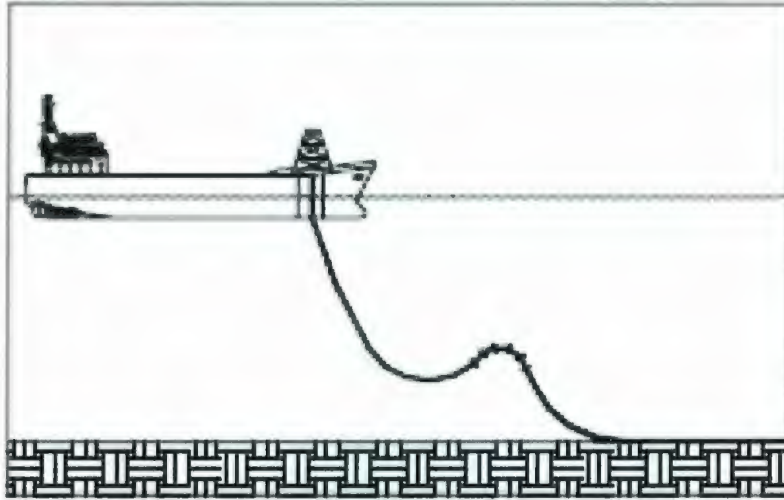


Figure 4: Lazy Wave Steel Catenary Riser

The key objective of the tests carried out by Grant was to determine if the buckling that is predicted by riser analysis programs really occurs on a large scale riser [2]. Although the riser models studied were rigid, many of the results apply to flexible risers as well. In particular, they found that HCR risers exhibited intermittent VIV which was influenced by soil interaction at the touch down point. However, the available riser analysis programs up to this point were unable to model intermittent VIV and could only model soil in a limited capacity. Therefore, any results found using the available analysis programs may not have been completely correct. This is important to note when using any program to analyze extremely complex real life situations such as deepwater riser motions.

2.1.5 STRIDE JIP Experiments

In 1998 Phase I of the STRIDE JIP project (STeel RISers for Deepwater Environments Joint Industry Project) was completed by Hatton and Willis (1998). The main objective of the STRIDE JIP was to develop steel catenary technology to a level where it could be applied with confidence in a harsh deepwater environment [4]. Phase I specifically dealt with riser system design and installation methods, from pipe sizing and material selection to VIV and fatigue analysis. Although there was no model testing done in Phase I, there were a number of important conclusions. First, VIV was found to be the single most important design issue for steel catenary risers, in particular for high current locations. The VIV analysis was carried out using SHEAR7, an analysis program developed at Massachusetts Institute of Technology (MIT) and used extensively for the study of riser response [4]. The program has been validated by model tests for vertically tensioned risers, but up to that point, there was much uncertainty for catenary shapes which occur in actual riser configurations. Again, this stresses the importance of not depending solely on riser analysis programs as they can not completely model the complex riser systems and therefore may not be entirely correct when predicting VIV in real life situations. Many software tools have been developed to perform VIV analysis, the majority of which are based on empirical formulas that rely heavily on model test data [26]. As mentioned, the majority of these model tests have been on small scale 8-10m riser models, which may provide acceptable VIV predictions for small length to diameter ratio shallow water risers. However, when deepwater risers are considered, the

empirical formulas may not be applicable due to the complex motions associated with deepwater riser VIV [26].

Another conclusion from [4] found that suppression systems are necessary and can reduce VIV fatigue by over 80% when they appear over long sections of the suspended length. Suppression systems are used when the geometry of a system can not be optimized so that the natural frequency of the system will avoid the vortex shedding frequency and therefore VIV is a possibility. These suppression systems can work in a number of ways, by increasing the damping of the system, by staggering the vortices that are developed, by introducing other vortices into the flow, by dephasing the separation that occurs, or by adding other structures into the wake. All of these systems will cause the vortices to be weakened or destroyed, thereby reducing or removing the structural vibrations.

Strakes are commonly used in the offshore marine industry as an effective way of reducing vortex induced vibrations on marine risers. Figure 5 [21], shows marine risers with helical strakes before (left) and during (right) installation.



Figure 5: Helical Strakes on Marine Risers

As technology for offshore marine applications has advanced, many companies have come up with alternatives to the helical strake. One such alternative, fairings, are airfoil shaped fittings that wrap around cylinders, and are used to streamline the flow so that the forces from vortex shedding are minimized. Figure 6 [18] shows the cross section of a riser surrounded by a fairing (left) and a fairing installed on a marine riser (right).



Figure 6: Fairings Installed on a Marine Riser

However, the two most common systems, strakes and fairings, are costly to develop and install and they introduce handling difficulties. As well, strakes, although the most common suppression device used today, increase riser drag and are partially responsible for the need for heavier, higher-grade pipes. It was found in [4] that it is possible that programs, such as SHEAR7, are over conservative and it would be of use to the industry to validate these programs for catenary shapes. In Phase II of STRIDE JIP, these issues were to be considered and both tow tank and large scale VIV testing was proposed to help validate the VIV response of inclined, skewed and curved pipes [16]. For the purpose of this thesis, the large scale VIV tests will be discussed. In this test by Willis (1999) both bare pipe and helical straked riser models, 650ft long and 10.75" outer diameter, were towed in currents up to 3m/s at angles up to 75 degrees between two tugs in a Norwegian fjord [16]. The test setup allowed the riser to be towed in a variety of different ways to mimic various catenary shapes. Willis concluded that the results of these tests will provide a better understanding of riser VIV response and will validate VIV software, in turn allowing less conservative, lower cost risers to be developed. However, formal approval from the JIP group is required for distribution of the results and therefore they are not available for the present research. Along with the study of fatigue as previously discussed, various catenary shapes as well as the use of VIV suppression devices may also be valid tests to be carried out in the future on the model riser being developed for this research.

2.1.6 Deepstar Experiments

Most recently and closest in design and objective to the research done in this project, J. Kim Vandiver's MIT research team conducted field experiments on large scale riser models working in conjunction with an industry research group known as "Deepstar" [14]. The tests by Vandiver et al. (2005) took place in the summer of 2004 and were conducted at the Naval Underwater Warfare Center Lake Seneca Test Facility. It involved two composite fiberglass pipes, 201ft and 401ft long, and 1.31 inches in diameter. The main objectives of the experiments were [14]:

- To gather vortex-induced vibration response data on a densely instrumented circular pipe at high mode number.
- To investigate mean drag coefficients at high mode number.
- To validate or improve drag coefficient prediction formulas.
- To test the efficacy of helical strakes at high mode numbers.
- To obtain statistics on the distribution of single-mode vs. multi-mode response of a pipe at high mode number.
- To determine the relative contribution to damage rate from the in-line and cross-flow VIV.
- To improve knowledge of damping factors.

The resulting paper specifically dealt with RMS response, reduced velocities, drag coefficients and damping factors [14]. As with this project, the length, diameter and tension of the pipe were chosen to excite as high a mode number as possible and 24 tri-axial accelerometers were spaced evenly along the length of the model. The maximum

possible towing speed with the system at Lake Seneca was approximately 1.1m/s and allowed for a cross-flow excitation of up to the 25th mode. However, a general rule of thumb when determining the number of accelerometers to include in VIV test models in order to properly map each mode shape, is to have no less than five sets of accelerometers per cycle. When dealing with the 25th mode, or 12.5 cycles, this yields an accelerometer count of at least 62.5. Therefore, the Lake Seneca model, with 24 evenly spaced accelerometers, may not have been densely enough instrumented to properly map all 25 modes. In a field testing situation, there will also tend to be accelerometers which do not function properly and so the number of accelerometers should be increased to account for this dropout rate. Nonetheless, the paper found that the experimental setup, using a suspended weight to provide tension and which is the basis of the design for this research, was useful and worked well. As well, they found that SHEAR7 was a good predictor of drag coefficient and finally, they found that the observed RMS in-line displacement was 30 – 50% of the cross-flow displacement [14]. Even though it was not presented in full in [14], they found that single mode cross-flow vibration was observed only a fraction of the time and multi-mode vibration was the primary response. Up to this point, the analysis of the single versus multi-mode vibration has not been released.

A second project by Vandiver et al. (2006) was completed for Deepstar in the Gulf Stream near Miami, Florida [15]. Again a composite pipe, 485.3 ft long and 1.4 inches in diameter, was towed behind a boat with a railroad wheel at the bottom to provide tension. Along with the previously mentioned objectives of the Lake Seneca tests, the

main objective of the Gulf Stream test was to measure the efficacy of helical strakes at high mode numbers and to determine the changes, if any, in damage rate due to helical strakes. Again, the analysis of single versus multi-mode vibration was not discussed in [15] and therefore can not be included here. The results for the test showed that strakes do reduce the amplitude of vibration and the frequency content of the vibration at high mode numbers. They also showed that the fatigue damage rate is lowered by using strakes, but that regions of long straked pipe next to bare pipe tend to cause stress concentrations. This again means that the use of VIV suppression devices, specifically helical strakes, would be a valid test to be carried out in the future on the model riser being developed for this research.

Due to many causes, such as sparse instrumentation, small length to diameter ratios, low Reynolds numbers, low current velocities, high turbulence, and low maximum mode numbers of vibration, there are still many questions surrounding VIV of deepwater risers and there is still much work to be done in this area. The research presented in this paper is the design, development and implementation of a densely instrumented large scale riser model at a high Reynolds number and high maximum modes of vibration. The hope is to develop a large scale riser model that will yield useful information about the behavior of long flexible deepwater risers responding to high mode vortex shedding. As previously mentioned, this is valuable information for future analysis as it will provide an intermediate step between the common 8 – 10m riser models, which have frequently been used to date to develop VIV prediction tools, and the actual 3,000m deepwater risers being used in industry today. If the results of this large scale research can be predicted by

the available small scale model VIV prediction tools, then it may be possible to extrapolate to the real life case. However, if the large scale results are quite different from the small scale model, then any extrapolation using the small scale model prediction tools may not be correct for the real life situation and further work can be done on the prediction tools to correct any discrepancies.

3 Methodology

This section gives a detailed overview of the approach and calculations used to design the Large Scale Model Riser (referred to as “LS-Model Riser” from here on) developed for the VIV experiments. First a prototype riser was chosen to base the design upon and similarity theory was used to achieve initial riser dimensions and characteristics. Next detailed calculations, done both from first principals and using original software based on 3D multibody dynamics formulation, were completed to determine the final LS-Model Riser characteristics.

3.1 *Prototype Riser*

The riser used as the prototype was taken from Gupta (2002), an Offshore Technology Conference Paper entitled “Spar Riser Alternatives for 10,000 ft Water Depth”. The Dual Casing Riser (DCR) from this paper was chosen as the prototype riser (referred to as “Prototype-DCR” from here on) for the following reasons:

- Offshore production is moving into ultra deepwater (10,000 ft or 3,000 m) and therefore designing a model that would help study VIV for these ultra deepwater risers was considered to be practical and important work that has not been entirely completed up to this point.
- The Dual Casing Riser (DCR) is a popular riser option already being used in several field developments.

- There was a great deal of data available for the DCR. In general, most sources give only a few riser characteristics which deal with the specific issues being discussed. However, this paper gave most of the riser dimensions and characteristics and therefore was the most complete source of information found. For instance, the weight per unit length, top tension and stiffness were all available in the published record; this has been found to be rare.

The important Prototype-DCR dimensions used in calculating the dimensions of the LS-Model Riser can be seen in Table 1 below and the complete list of characteristics for the Prototype-DCR can be found in Appendix A.

Length	m	3,048
Outer Diam	m	0.3239
Inner Diam	m	0.2445
Weight per Length	kg/m	145
Top Tension	kN	5,834
Net Riser Stiffness	N/m	1,298,857
Elastic Modulus	N/m ²	1.12E+11
Bending Stiffness	N m ²	4.07E+07
Current Velocity	m/s	2.25

Table 1: Prototype-DCR Dimensions

3.2 Model Scaling and Similarity Theory

The actual length of a deepwater riser can be up to 3,000m with an outer diameter as small as 0.32m. These large lengths and relatively small diameters are difficult to model given that most testing is done in towing tanks or other indoor facilities. The length of the model is often limited by the tanks, making one scaling factor useless due to the fact

that the model diameter would become impractically small. The model would be too small to instrument and the Reynolds number would be very low.

Conducting the tests outside in a field situation allows the riser to be designed at a much larger scale. However, since the Prototype-DCR is extremely long, when it is scaled to a realistic model length, 130m in this case, it will yield an outer diameter of only 0.014m. Instrumentation in this small a diameter riser may be possible, but it is very impractical and would be costly. As well, if testing was conducted at 1.0m/s, the Reynolds number would be only 1.2×10^4 , which is below the “acceptable” minimum value of 2.0×10^4 . This “acceptable” value was determined by consulting industry leaders in the field of VIV research and other members of the Memorial University VIV Research Team.

In order to remedy this, a distorted model can be designed that uses different scaling factors for the length and diameter. In the paper, “Multi-modal Vortex Induced Vibration Tests on a Flexible Model Riser” [8], Li discuss the important parameters for multi-modal VIV and develop a similarity theory to show that a riser model and its prototype are similar. These parameters were used here to help develop similarity between the Prototype-DCR and the LS-Model Riser.

3.2.1 Weight per Unit Length and Current Speed

The first two non-dimensional parameters to determine the weight per unit length and current speed for the LS-Model Riser were as follows:

$$\left[\frac{m_s}{D^2} \right]^{(m)} = \left[\frac{m_s}{D^2} \right]^{(p)} \quad (1)$$

$$\left[\frac{U^2}{D} \right]^{(m)} = \left[\frac{U^2}{D} \right]^{(p)} \quad (2)$$

Where:

- $m_s^{(m)}$ = mass per unit length of model (kg/m)
- $m_s^{(p)}$ = mass per unit length of prototype (kg/m)
- $D^{(m)}$ = outer diameter of model (m)
- $D^{(p)}$ = outer diameter of prototype (m)
- $U^{(m)}$ = current speed of model (m/s)
- $U^{(p)}$ = current speed of prototype (m/s)

where the superscripts (*m*) and (*p*) represent the LS-Model Riser and the Prototype-DCR respectively. The first step in using this theory is to determine at least one characteristic for the LS-Model Riser. The outer diameter was chosen to maximize the Reynolds number while maintaining an achievable current speed and yet be large enough to place instrumentation within the pipe. After considering a number of available materials, a 2" nominal diameter plumbing pipe was chosen as the basis for the model design with an outer diameter of 0.053m (See Section 4.1.1 for pipe details). Using the non-dimensional equation (1) with the Prototype-DCR characteristics, the LS-Model Riser mass per unit length was found to be:

$$\left[\frac{m_s}{D^2} \right]^{(m)} = \left[\frac{m_s}{D^2} \right]^{(p)}$$

$$\left[\frac{m_s}{(0.053)^2} \right]^{(m)} = \left[\frac{145}{(0.324)^2} \right]^{(p)}$$

$$m_s^{(m)} = 3.87 \text{ kg / m}$$

Li also found that a distorted model length only influences the modeling of the frequency ratio, and not the modeling of other parameters. Therefore, the length of the LS-Model

Riser was determined independently based on practical test restrictions and the ability to achieve maximum mode numbers. The current velocity was then determined solely by the Reynolds number similarity condition equation (2) as follows:

$$\left[\frac{U^2}{D} \right]^{(m)} = \left[\frac{U^2}{D} \right]^{(p)}$$

$$\left[\frac{U^2}{0.053} \right]^{(m)} = \left[\frac{(2.25)^2}{0.324} \right]^{(p)}$$

$$U^{(m)} = 0.91 \text{ m/s}$$

A current speed of 0.91m/s is considered a practical design speed and results in a Reynolds number of 4.1×10^4 . This Reynolds number is within the range: 5,000 to 3×10^5 which results in “subcritical high Reynolds number flow”, where the wake is turbulent but the boundary layer itself is laminar [31]. This Reynolds number range has been discussed by the Project Team and found to be acceptable for this research.

Equation (6) in Section 3.3 shows that as the tension is increased, the natural frequency for each mode number is decreased, allowing the same model to achieve a higher mode number at a given shedding frequency. To increase the tension, and in turn increase the maximum achievable mode number, the speed must be increased. A higher speed will be set as the maximum during actual testing to try and achieve as high a mode number as possible.

3.2.2 Tension and Bending Stiffness

Li also gives a way to scale the tension if the bending stiffness can be determined by other means. However, the tension for this model will be determined not only by the

bending stiffness, length, and current speed but also by the railway wheel that was hung from of the end of the model to ensure the pipe remained as close as possible to vertical while it was being towed (See Section 6.3 for an explanation of the test setup). This complicates the design and these basic non-dimensional parameters may not be a good indication of the tension the model will actually experience. The non-dimensional parameters are based on a “perfect” system, where the bend stiffness, current profile and tension along the riser are constant. In field conditions, it can be assumed that this will not be the case and there will be variation in all of the model parameters. Therefore, a riser analysis program, developed at the Institute for Ocean Technology (IOT) was used to obtain an estimate of the tension for the LS-Model Riser. This is explained in detail in Section 3.4 of this thesis

This leaves only the bending stiffness to be determined for the LS-Model Riser. Li also developed a non-dimensional parameter for this as follows:

$$\left[\frac{k_b}{\rho g D^5} \right]^{(m)} = \left[\frac{k_b}{\rho g D^5} \right]^{(p)} \quad (3)$$

$$\left[\frac{k_b}{(0.053)^5} \right]^{(m)} = \left[\frac{4.07 \times 10^7}{(0.324)^5} \right]^{(p)}$$

$$k_b^{(m)} \cong 4700 \text{ Nm}^2$$

Where: $k_b^{(m)}$ = bending stiffness of the model (N m²)
 $k_b^{(p)}$ = bending stiffness of the prototype (N m²)

The actual bending stiffness of the LS – Model Riser was obtained by completing a common bending stiffness test where a section of the pipe was treated as a cantilever beam fixed at one end with a force applied to the free end. The deflection was measured

and the following equation for a cantilever beam was used to find an estimate of the bending stiffness.

$$k_b = \frac{\Delta PL^3}{3\Delta H}$$

where ΔP is the applied force in Newtons, L is the length of the pipe sample in meters, and ΔH is the deflection measured at the free end of the beam in meters. The calculation can be seen in Appendix B. The resulting bending stiffness, 126.6 N m^2 , was not comparable to the required similarity bending stiffness calculated in equation (3) above. However, for long cylinders the tension has a larger effect on the model than the bending stiffness and the model will act as an infinite string. This is shown in the next section of this thesis by comparing the results for finding the natural frequencies of the model using equations that both include and exclude the bending stiffness. As well, a sensitivity test using the riser analysis program developed at IOT was done to verify this assumption and this is discussed in Section 3.4.3 of this thesis.

3.3 Natural and Shedding Frequencies

In addition to the similarity theory, Li et al. (2005) also derived the modal natural frequencies from first principals.

$$f_k = \left(\sqrt{\frac{k_b \left(\frac{k\pi}{L}\right)^4 + T \left(\frac{k\pi}{L}\right)^2}{m_s + \frac{\pi}{4} \rho C_m D^2}} \right) \div 2\pi \quad (5)$$

Where:

f_k = Modal Natural Frequency (Hz)

k = Mode Number

T = Tension (N)

C_m = Added Mass Coefficient

Equation (5) was used here to find the LS-Model Riser's natural frequencies of vibration which are then compared to the vortex shedding frequency to determine the model's highest expected mode of vibration. There is some error due to the fact that the equation was derived for a fixed-fixed end condition and the test setup for this analysis is for a fixed-free end condition. However, the LS-Model Riser is so long that it was felt that only a small portion of the riser would be affected by this "free" end.

The following simplified equation to find the natural frequencies was taken from [14] and is for a long flexible cylinder, towed by the top end with a weight at the bottom end.

$$f_k = \frac{k}{2L} \sqrt{\frac{T}{m_s + \frac{\pi}{4} \rho C_m D^2}} \quad (6)$$

By inspection it can be seen that if the bending stiffness is very small compared to the tension, equation (6) can be derived easily from equation (5). However, it can also be seen that as the mode number k increases, the error between the results will be greater due to the fourth power term in equation (5) which does not appear in equation (6). Table 2 shows the natural frequencies calculated for a range of current speeds and mode

numbers using equation (5), which includes the bending stiffness. Equation (6), which excludes the bending stiffness, was also used to calculate the natural frequencies at the maximum current speed and the % error between the two equations was calculated. The complete table including all variables used in the calculations can be seen in Appendix C.

Material

$\rho = (\text{kg/m}^3) = 1186$
 $E = (\text{N/m}^2) = 4.84\text{E}+08$
 $m_s = (\text{kg/m}) = 2.617$
 $k_b = (\text{Nm}^2) = 126.6$

Re	1.1E+04	5.7E+04	6.8E+04	6.8E+04	
Shedding f	0.71	3.54	4.25	4.25	
Max Speed (m/s)	0.25	1.25	1.50	1.50	
Tension (N)	5,500	7,500	10,000	10,000	
Railway wheel (lbs)	800	800	800	800	
Mode #	Modal Natural Frequencies (Hz) including kb			Freq. (Hz) without kb	% Error
1	0.12	0.14	0.17	0.17	0.00
2	0.25	0.29	0.33	0.33	0.00
3	0.37	0.43	0.50	0.50	0.00
4	0.49	0.58	0.67	0.67	0.01
5	0.62	0.72	0.83	0.83	0.01
6	0.74	0.87	1.00	1.00	0.01
7	0.87	1.01	1.17	1.17	0.02
8	0.99	1.15	1.33	1.33	0.02
16	1.98	2.31	2.67	2.67	0.09
17	2.10	2.46	2.84	2.83	0.11
18	2.23	2.60	3.00	3.00	0.12
19	2.35	2.75	3.17	3.17	0.13
20	2.48	2.89	3.34	3.33	0.15
21	2.60	3.04	3.50	3.50	0.16
22	2.73	3.18	3.67	3.66	0.18
23	2.85	3.33	3.84	3.83	0.19
24	2.98	3.47	4.01	4.00	0.21
25	3.10	3.62	4.17	4.16	0.23
26	3.23	3.76	4.34	4.33	0.25
27	3.35	3.91	4.51	4.50	0.27
28	3.48	4.06	4.68	4.66	0.29
29	3.60	4.20	4.85	4.83	0.31
30	3.73	4.35	5.01	5.00	0.33

Table 2: Natural Frequency Calculations

It can be seen that for the maximum current speed, a Reynolds number of 68,000 would be achieved and the vortex shedding frequency and natural frequency correspond at a maximum mode number of approximately 25. As well, with regard to the assumption that the bending stiffness does not have a major impact on the analysis, it can be seen that the % error is much less than 1%. This was felt to be quite acceptable and show that the tension dominates the effect of bending stiffness in this situation.

Another calculation was done to check if a large change in bending stiffness would have an effect on the calculations. In Table 3 below, the natural frequencies were again calculated using equation (5). However, instead of using the actual bending stiffness of the pipe as before, the much larger bending stiffness from the similitude calculation, equation (3), was used. These results were then compared by % error with the original natural frequencies in Table 2.

Material

$\rho = (\text{kg/m}^3) =$	1186
$E = (\text{N/m}^2) =$	1.80E+10
$m_s = (\text{kg/m}) =$	2.617
$k_b = (\text{Nm}^2) =$	4710

1.1E+04	5.7E+04	6.8E+04
0.71	3.54	4.25
0.25	1.25	1.50
5,500	7,500	10,000
800	800	800
Modal Natural Frequencies (Hz) $k_b = 4710 \text{ Nm}^2$		
0.12	0.14	0.17
0.25	0.29	0.33
0.37	0.43	0.50
0.50	0.58	0.67
0.62	0.72	0.84
0.75	0.87	1.00
0.88	1.02	1.17
1.00	1.17	1.34
2.10	2.41	2.76
2.25	2.58	2.94
2.40	2.75	3.13
2.55	2.92	3.32
2.71	3.09	3.51
2.87	3.27	3.70
3.03	3.44	3.90
3.20	3.63	4.10
3.37	3.81	4.30
3.54	4.00	4.51
3.72	4.19	4.72
3.90	4.39	4.93
4.08	4.58	5.14
4.27	4.79	5.36
4.46	4.99	5.58

0.25	1.25	1.50
5,500	7,500	10,000
800	800	800
% Error		
0.02	0.02	0.01
0.10	0.07	0.05
0.22	0.16	0.12
0.39	0.28	0.21
0.60	0.44	0.33
0.86	0.64	0.48
1.17	0.86	0.65
1.52	1.12	0.85
5.68	4.27	3.25
6.35	4.78	3.65
7.03	5.31	4.06
7.74	5.86	4.50
8.47	6.43	4.94
9.22	7.02	5.41
9.98	7.63	5.89
10.76	8.25	6.38
11.55	8.88	6.89
12.35	9.53	7.41
13.16	10.18	7.94
13.98	10.85	8.49
14.80	11.53	9.04
15.63	12.22	9.60
16.46	12.91	10.17

Table 3: Natural Frequency Calculations using Similitude Bending Stiffness

It can be seen that even with a large value of the bending stiffness, the % error for mode 25 was still only approximately 6 – 10 %. This was assumed to be acceptable for planning as the equations are a very simplified way to look at this complex system and are only an initial way to estimate the maximum modes the riser will encounter.

3.4 Institute for Ocean Technology Riser Dynamics Code

As previously mentioned, the tension for the LS – Model Riser will be determined not only by the bending stiffness, length, and current speed, but also by the wet weight of the railway wheel that was hung at the end of the model. The basic non-dimensional parameters used to predict the characteristics of the model may not be an accurate depiction of the actual tension the model will experience. Again, these non-dimensional parameters are based on a “perfect” experiment. In a field setting there will be variations on all model, setup and test characteristics and therefore the estimates for the non-dimensional parameters may differ from the actual parameters experienced. A riser analysis program, “IOT Riser Dynamics Code” has been developed by Wayne Raman-Nair of the Institute for Ocean Technology (IOT) and was used to obtain not only an estimate of the tension for the LS-Model Riser, but also for the maximum tensile stress, and the position of the model as a function of time. As previously mentioned, this program was also used to verify the assumption that the bending stiffness had very little effect on the vibration of a long riser.

3.4.1 Input Data

The program runs in MATLAB Version 7.1 and consists of a number of input files in the *.m format.

3.4.1.1 *Inputs.m*

The first input file is called *inputs.m*, an example of which can be seen in Appendix D. In this file, the riser properties are defined, such as the total natural length, mass per unit length, outer and inner diameter, modulus of elasticity, and material density. The modulus of elasticity used in the program was $1.8 \times 10^{10} \text{ N/m}^2$, which yields a bending stiffness of approximately $4,700 \text{ Nm}^2$. This value had been previously calculated by similitude modeling in Section 3.2.2 and as mentioned, it is not the actual bending stiffness of the pipe. However, it was shown by the sensitivity analysis (presented below) that the change in bending stiffness and corresponding Modulus of Elasticity does not greatly influence the results. The file also defines the number of lumped masses the riser will be separated into, and the time values that will be used for the output.

The outer and inner diameter values may appear strange, with the outer diameter of 0.053m matching the outer diameter of the pipe, but with the inner diameter of only 0.001m. This is because the properties of the LS – Model Riser have been determined for the completed model, including the pipe, hydraulic oil and cables. Therefore, by setting the inner diameter at only slightly more than zero, the properties that have been input will be an estimate for the full cross section of the model, and not just the hollow pipe. Also, if the inner diameter was set at exactly zero, the program might have encountered errors through divisions by zero.

There are also values in the file that can be changed, but that were kept constant for the purpose of this analysis. These include acceleration due to gravity, seawater density, kinematic viscosity, and the Strouhal number. The internal fluid flow rate, density and

pressure were also kept constant at zero due to the fact that there was to be no fluid flowing through the pipe, and there were no external forces on any of the lumped masses.

3.4.1.2 Inputs_aux1.m

Another file used for defining the characteristics of the riser is called *Inputs_aux1.m* and a sample of this file can also be seen in Appendix D. This file contains quantities calculated from *inputs.m* and usually is not edited by the user. However, the original program was altered to enable the analysis to include the railway wheel weight and volume. This was done by altering the weight per unit length and volume of the bottom segment of the riser model. Then the extensional stiffness and damping of this segment was set to zero, as well as the bending stiffness and damping between this segment and the one above it. This, in essence, models the railway wheel hanging from the bottom of the model.

3.4.1.3 P0.m, Pn.m, P0dot.m and Pndot.m

This group of input files, also shown in Appendix D, defines the position and velocity of the top (P_n) and bottom (P_o) points of the model. Figure 7 shows the layout of an elastic catenary riser in the original program.

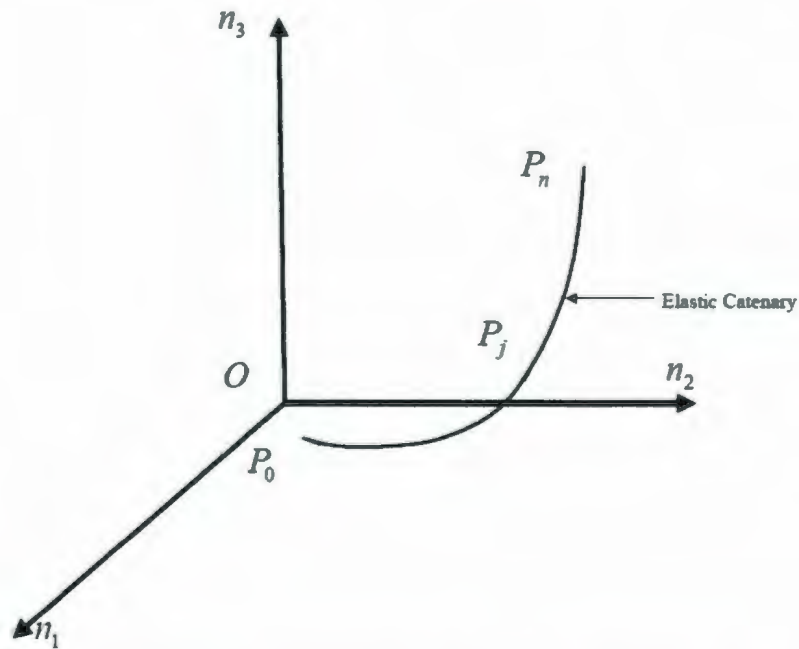


Figure 7: Layout of Elastic Catenary Riser in IOT Riser Dynamics Code

Although the riser above is not exactly how the LS – Model Riser has been modeled in the code, it serves the purpose of showing how the code deals with segments along the riser. It starts with the bottom segment, P_o , and runs along the riser, P_j , where j is from 1 to $(n - 1)$ where n is the number of lumped masses specified in the inputs.m file, finishing at the top segment, P_n . The axes are also shown on Figure 7, where n_1 is the x -direction, n_2 is the y -direction and n_3 is the z -direction.

The LS – Model Riser was modeled vertically, since in the setup it was hung from a buoy and towed behind a vessel. Therefore, P_n is set at $(0,0,150)$ and P_o is set at $(5,0,0)$. The offset of 5 in the x -direction of the bottom point is needed because it was found that when segments are in line directly one on top of the other, the angle between segments can not be found and this causes a computing error. This makes no difference to the overall calculations, as the code needs a number of time steps before it reaches a steady state.

Although the length of the riser is set at 130m, the top point was set at 150m above the ocean floor to ensure the model would not touch down if any stretching occurred.

Keeping the y-coordinate at zero for both the top and bottom points meant that the riser was modeled on the x-z plane.

The velocity for both the top and bottom points was set to zero, as the riser was fixed with a current flowing past it. The code was set up so that the velocity profile of the current was easily input and the resulting riser motions were easy to review. This is, in essence, what was taking place during actual testing by towing the LS – Model Riser at a steady speed.

3.4.1.4 *Vfluid.m*

The last file included in Appendix D and that had to be altered before running the program was *vfluid.m*. This file defines the current profile that the riser will come in contact with. The file is set up so that the current can have any possible profile, from completely constant, to shear, to completely random. For the purpose of this analysis, the current was kept constant each time the program was run and varied from 0.25 to 1.5 m/s. The current was applied along the x-axis (n_1) which is in the same plane as the modeled riser. This means that the riser will tend to “arc” and begin to “float to the surface” in the direction of the flow (along the riser) and any cross flow VIV motions will take place in the y-direction.

3.4.2 Output

The IOT Riser Dynamics Code has numerous output options, however, only those pertinent to this study are discussed here. The output is given as a function of time and position along the riser. For instance, one can examine a calculated value of segment 25 for all points in time, or for just a particular range in time. There is also a file called anim.m which allows the user to animate the response of the riser. By changing the axis in this file, one can look at the riser profile as it is being towed or the riser cross flow VIV response.

3.4.2.1 Tension

One of the driving forces behind using this code was to find a good estimate of the maximum tension along the riser for the highest speeds during testing. This was an invaluable tool when choosing components of the LS – Model Riser, since it was unknown how accurate hand calculations of tension might be for such a complex system. Three current speeds were run with the code, resulting in the following maximum tension values.

	Current Speed (m/s)		
	0.25	1.25	1.50
Max. Tension (N)	5,500	7,500	10,000

Table 4: Maximum Tension (Newtons)

With the top tension in the riser at the top speed reaching a value of approximately 10,000 N, all parts and materials were chosen to withstand at least this amount of tension. The tension results were found by inspecting the tension vs. time graphs for numerous

points along the riser length. The graphs for the top current speed of 1.5 m/s are shown below.

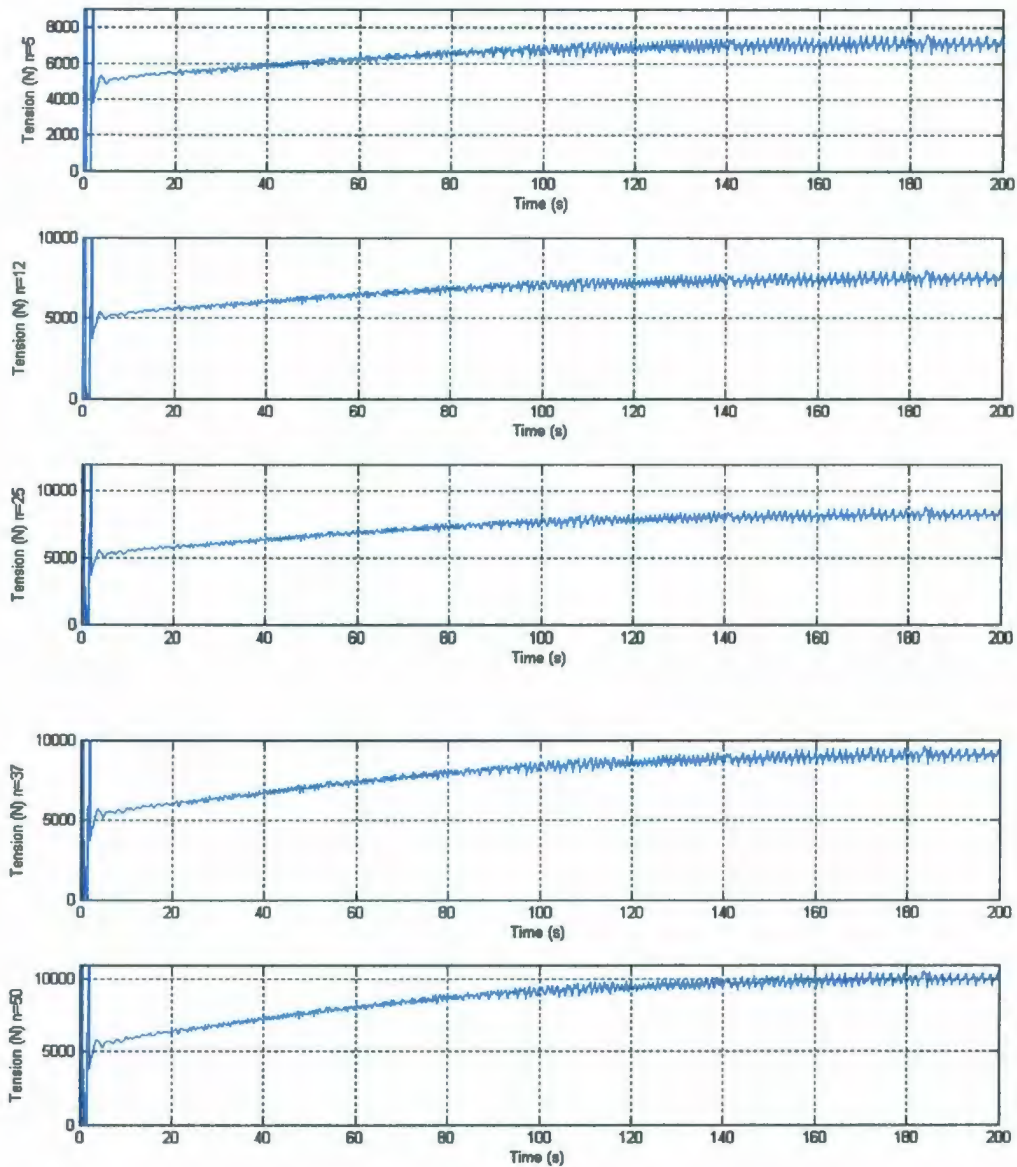


Figure 8: Tension vs. Time Along the Model Length

These graphs show that after an initial period of instability, the riser settles into a steady state. They also show that the maximum tension experienced along the riser is at the top segment $n = 50$, or where the LS – Model Riser attaches to the buoy. This is logical since

the tension of the hanging model and railway wheel will be at a maximum at the top, even without the added tension of the VIV motion. The tension values shown in Table 4 that were used to design the LS – Model Riser were chosen visually from these graphs. The graphs of tension vs. time for the other current speeds can be seen in Appendix E.

3.4.2.2 Maximum Tensile Stress

As with the tension, the maximum tensile stress was found for the four current speeds run in the code. The maximum tensile stress is a combination of the extensional stress plus the bending stress. Table 5 shows the maximum tensile stress values for each current speed.

	Current Speed (m/s)		
	0.25	1.25	1.50
Max. Tensile Stress (Pa)	2.5×10^6	5.5×10^6	6.0×10^6

Table 5: Maximum Tensile Stress (Pascals)

The maximum tensile stress found in the riser was not at the top as with the tension, but at $n=1$ or the bottom of the model. This might be attributed to the fact that there was the most movement in the bottom of the model, where the vibrations and displacements were the largest. However, the tensile stress varied very little along the length of the riser, ranging only from 6.0×10^6 Pa at the bottom to 5.5×10^6 Pa at the top. All parts and materials were chosen to withstand at least 6.0×10^6 Pa of tensile stress. Results for the tensile stress were found by inspecting the stress vs. time graphs for numerous points along the riser length. The graphs of the maximum tensile stress for the top current speed of 1.5 m/s are shown below, and the graphs for the other current speeds can be seen in Appendix E.

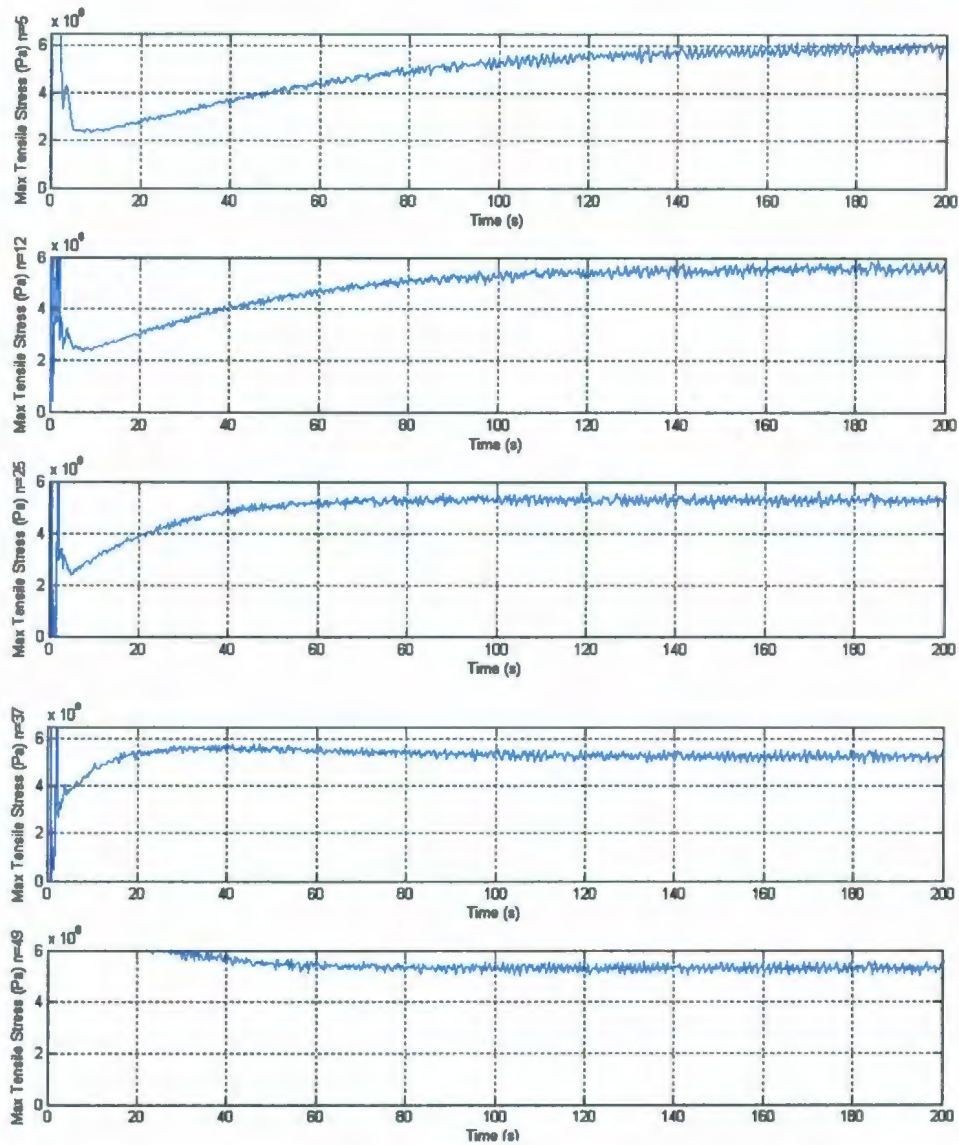


Figure 9: Maximum Tensile Stress vs. Time Along the Model Length

3.4.2.3 Profile

For this analysis, the current speed was set to run along the x-axis. Following the orientation of the riser specified in Figure 7, this current will cause the riser to arc and float to the surface in the x-z plane. The view of the riser in this plane will be referred to

as the “profile” of the riser. As before, representative graphs for the current speed 1.5m/s are included in the discussion here with the remaining graphs for the other current speeds included in Appendix E.

As with the tension and tensile stress, the position of each segment can also be shown as a function of time. The profile is determined by the x and z positions of each segment.

The x position for a number of segments can be seen in Figure 10.

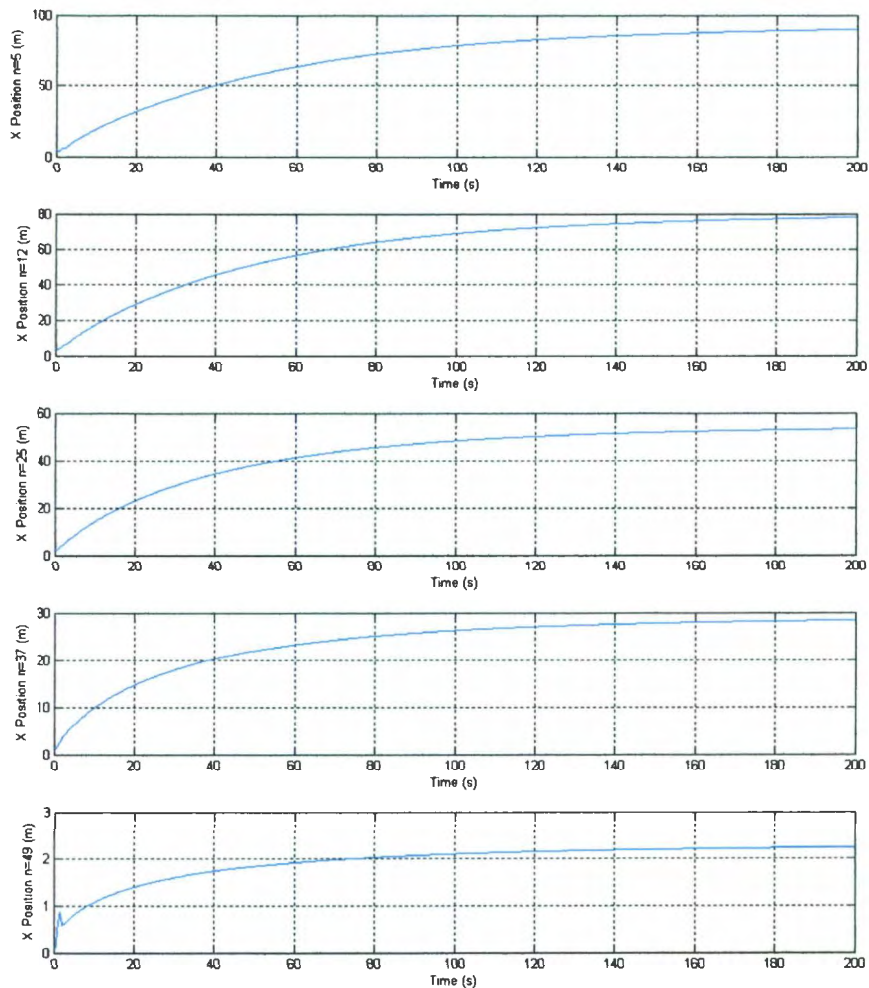


Figure 10: X Position vs. Time Along the Model Length

The $n=49$ segment has the least amount of movement, slightly over 2m, with the $n=1$ segment at the bottom having the most movement over time, almost 100m. Again, this is logical as the top point, $n=50$, has been defined as a fixed point and will not have any change in x , y or z position and the bottom point is free to move.

The z position for the same segments can be seen in Figure 11.

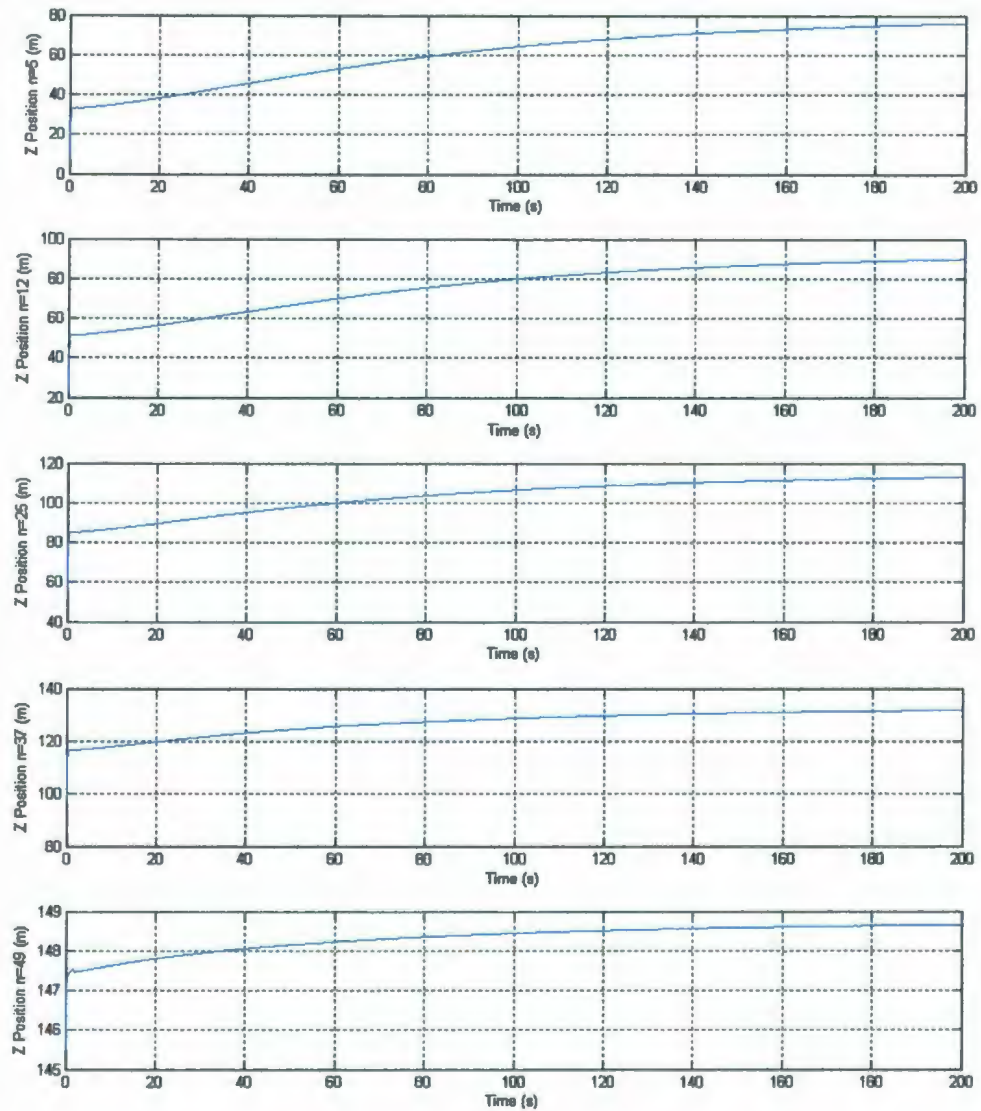


Figure 11: Z Position vs. Time Along the Model Length

The graphs of z position can be somewhat deceptive because all of the segments have different initial z positions. However, this is easily resolved by taking the difference of the reading on the graph and the initial position at $t=0$ for that particular segment. For instance, for $n=49$ in Figure 11, the maximum displacement at $t=200s$ is 148.6m (reading from graph) – 147.2m (initial position at $t=0$) = 1.4m maximum displacement. The top point, $n=50$, was set at 150m above the ocean floor to ensure the model would not touch down if any stretching occurred. This is why the initial position of segment $n=49$ is over 147m. The initial position of $n=1$ can be seen to be 20m, which would correctly make the model 130m long. The largest movement, 45m, occurs at the bottom of the model at $n=1$, again due to the fixed top point and free bottom point.

When the x and z displacements are considered together, the final profile of the riser in the x-z plane can be seen in Figure 12.

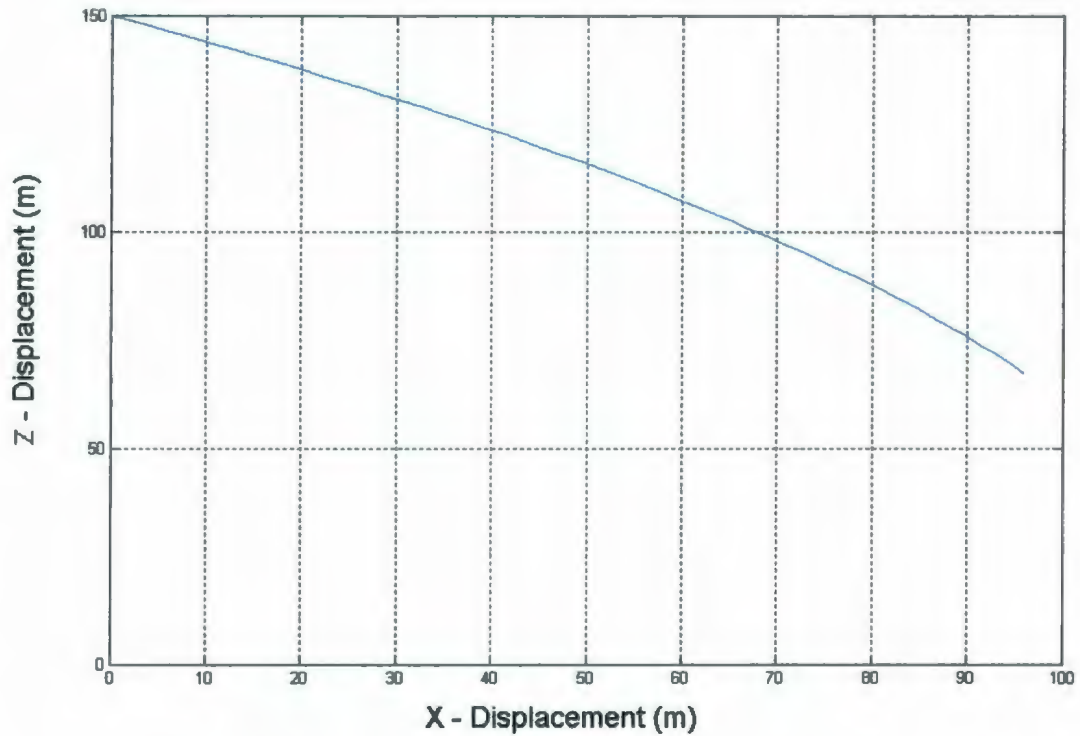


Figure 12: Final Profile for Maximum Current Speed 1.5m/s

Figure 12 also shows that the maximum displacement in the x direction was at the bottom and can be seen to be almost 100m, while in the z direction the maximum displacement was also at the bottom and was close to 45m.

3.4.2.4 Cross Flow VIV Response

The y direction response of the riser is the most interesting from the point of view of this thesis. It is in this direction that the VIV response, known as the cross flow response, will be the strongest and most noticeable. This is easily seen in Figure 13, the y position vs. time graphs for the current speed 1.5m/s. The remaining graphs for the other current speeds can be seen in Appendix E.

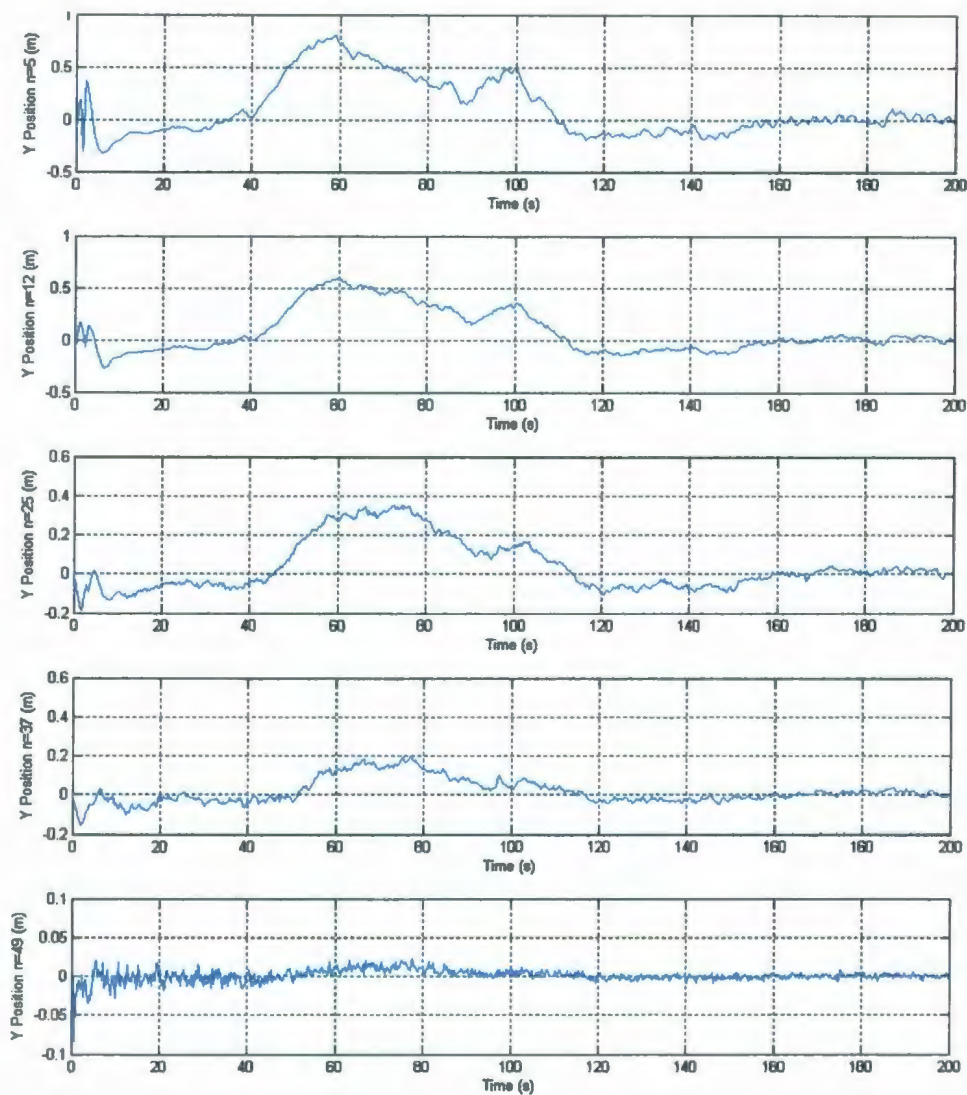


Figure 13: Y Position vs. Time Along the Model Length

The above movement can be broken down into two different types. First, an overall movement of the LS – Model Riser is shown by the large amplitude motions that cause the riser itself to move. Second, the smaller vibrations that are within these larger amplitudes are the vortex induced vibrations. In the analysis of the actual experimental data, the large amplitude motion will be filtered out and only the VIV will remain. If this large motion is removed, the maximum displacement or amplitude of the VIV motion can

be estimated as large as 0.3m for the bottom of the riser where the most movement will occur due to the free end, and 0.005m for the top fixed end. As these values are at the extreme ends of the model, the average VIV amplitude may be closer to 0.1m (1.9D) located at $n=25$ in the middle of the model, which is large when compared to the industry expected values for VIV amplitude which are approximately 1D.

3.4.3 Sensitivity Study of Bending Stiffness

As mentioned in Section 3.2.2, the required bending stiffness found using similarity theory was much higher than the actual pipe bending stiffness. It was felt that since this model is in essence a long cylinder, it will act as an infinite string and the bending stiffness will have very little effect on the vibration. By comparing the results of the natural frequencies, in Section 3.3, using equations (5) and (6) that both include and exclude the bending stiffness respectively, it was found that the bending stiffness was not an important factor. However, to ensure the model would in fact not be affected by such a large change in bending stiffness, a sensitivity study using the "IOT Riser Dynamics Code" was completed to verify this assumption.

All variables in the code were kept constant except for the Modulus of Elasticity. In the original analysis, the Modulus of Elasticity that had been calculated by similitude modeling, $1.8 \times 10^{10} \text{ N/m}^2$ was used. This is the opposite of the natural frequency calculations, where the actual Modulus of Elasticity of the pipe, $4.84 \times 10^8 \text{ N/m}^2$ was used. Therefore, to study the sensitivity of the large change in Modulus of Elasticity the maximum current speed was again run in the code using the actual Modulus of Elasticity

$4.84 \times 10^8 \text{ N/m}^2$. Figure 14 shows the results of the tension vs. time for the sensitivity study.

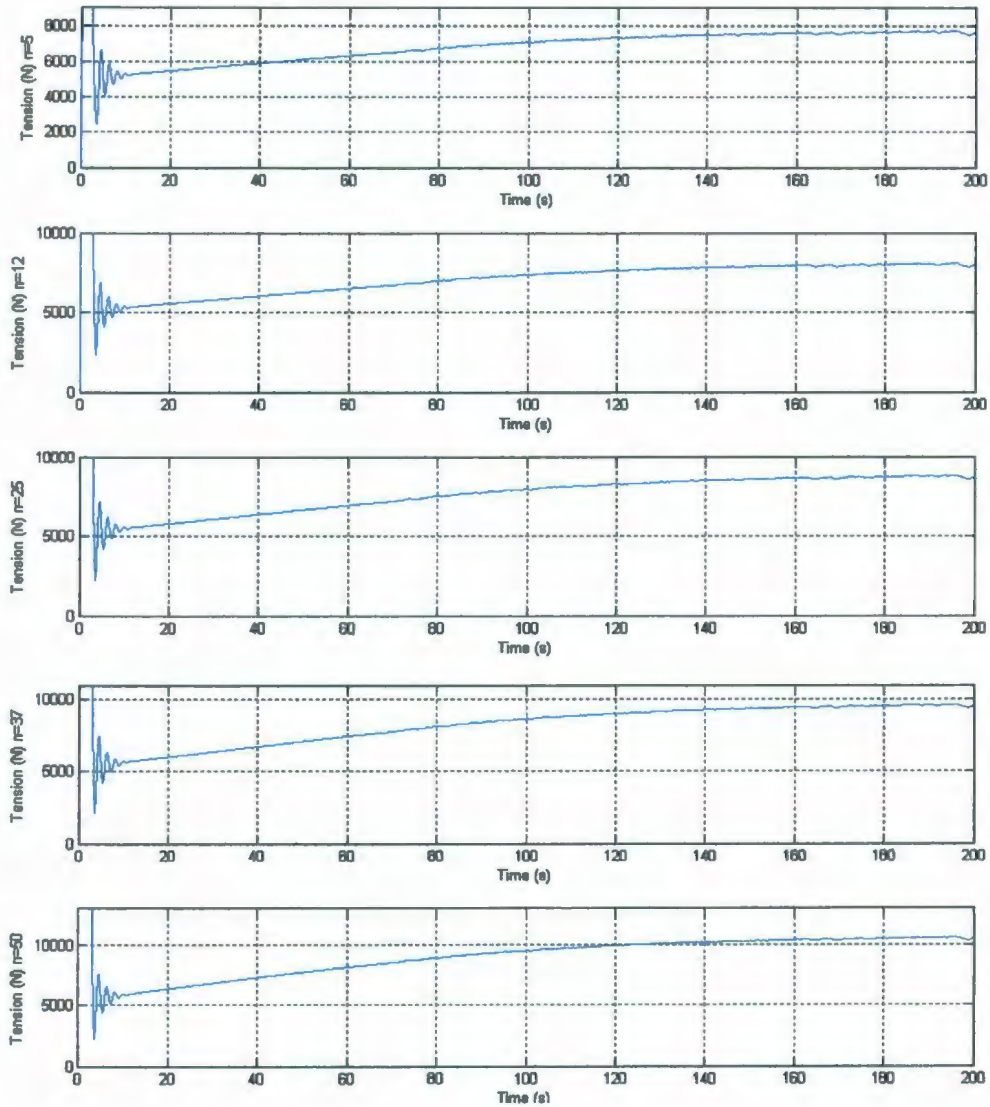


Figure 14: Tension vs. Time for the Sensitivity Study

It can be seen that the maximum tension is just over 10,000 N, which almost exactly matches the original analysis. Figure 15 show the maximum tensile stress for the sensitivity study.

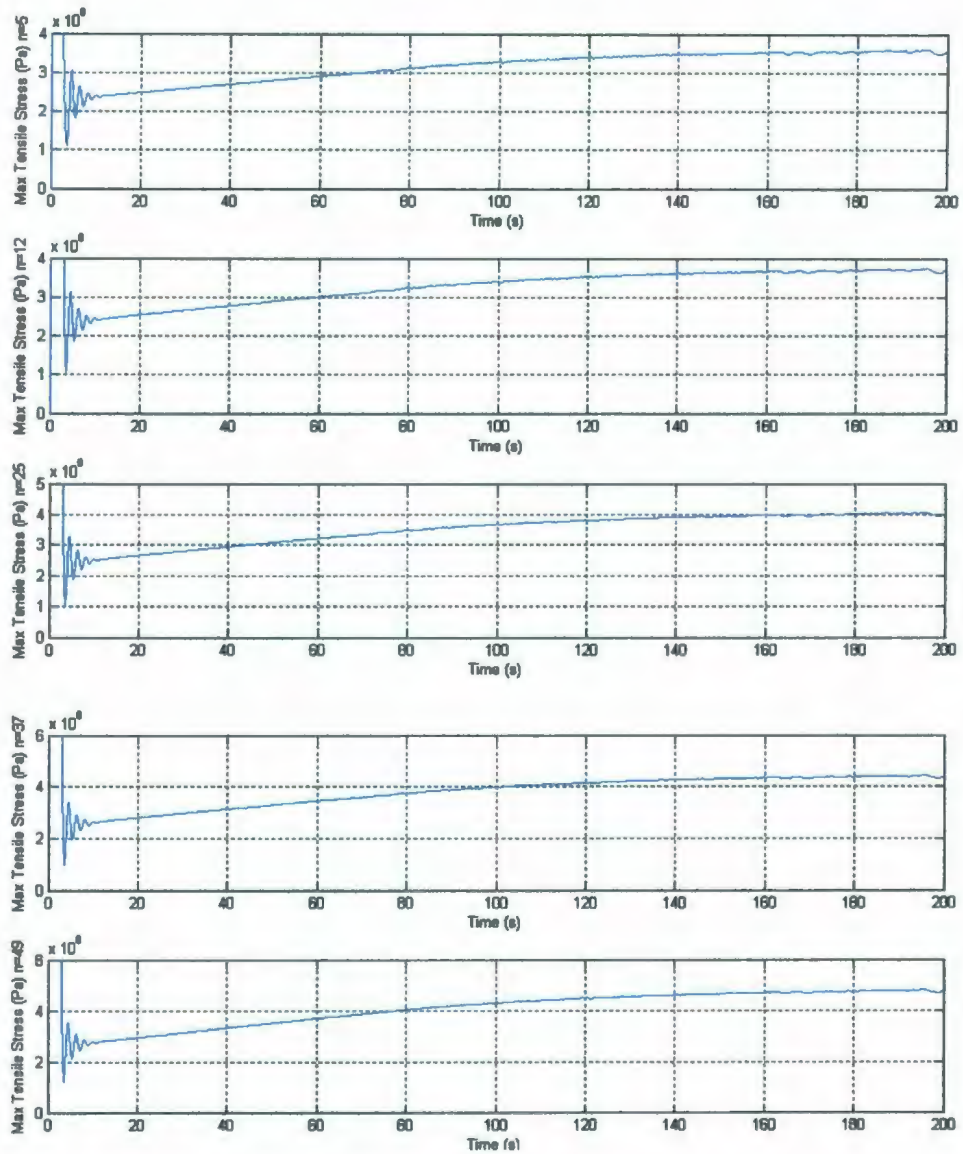


Figure 15: Maximum Tensile Stress vs. Time for the Sensitivity Study

The maximum tensile stress is approximately 5.0×10^6 Pa, which is similar to the original value and is actually a decrease from the original analysis.

Therefore, it has been shown for the maximum values, though the natural frequency equations and the above sensitivity study that the bending stiffness of the LS – Model Riser will not greatly affect the vibration, and in fact our calculations using the similarity

theory bending stiffness have been conservative. However, a more exact estimate of the bending stiffness, testing a sample that includes not only the pipe but all model parts such as cables and hydraulic oil, should be done in the future for completeness.

3.5 Placement of Accelerometers

In order to map the vibration of the LS – Model Riser, accelerometer units, or modules, were placed along the length of the model. The modules and the data they collected are explained in detail later in this thesis. It was felt that to completely map the mode shapes of the riser there should be no less than 5 modules per vibration cycle (1 cycle = mode number/2). This meant, that for this test, which was designed to achieve a maximum mode number of 25 (or 12.5 cycles), no less than 63 modules should be used. The simple calculation to find the distance between each module is shown in Table 6.

Max Mode #	20	25
Cycles	10	12.5
# modules/cycle	5	5
Total Modules	50	62.5
Dist between each module (m)	2.60	2.08

Table 6: Number and Distance Between Modules

It was decided that since the model was 130m long, there would be 65 modules along the length of the model, spaced at a distance of 2.0m.

However, the number of modules and spacing was theoretical and served as a “best case” scenario. Due to problems during assembly, described in detail in Section 5, some of the modules were damaged and only 55 were able to be installed inside the model. As well, assembly issues also caused most of the modules that remained to be placed with a

spacing of 1.9m. The final module locations can be seen in Table 7. It should be noted that the four full modules (which will be described in detail in Section 4) were located, in relation to the table below, at Module Numbers 4, 44, 28 and 9.

Module Number	On Screen Number	Distance from Previous Module (m)	Total Distance From Bottom (m)
Bottom of Pipe		0	0
4	4	2	2
63	62	2	4
62	61	1.9	5.9
61	60	1.9	7.8
60	59	1.9	9.7
59	58	1.9	11.6
58	57	1.9	13.5
57	56	1.9	15.4
54	53	1.9	17.3
53	52	1.9	19.2
52	51	1.9	21.1
50	49	1.9	23
49	48	1.9	24.9
47	46	1.9	26.8
46	45	1.9	28.7
45	44	1.9	30.6
44	43	1.9	32.5
43	42	1.9	34.4
42	41	1.9	36.3
3	3	1.9	38.2
41	40	1.9	40.1
40	39	1.9	42
39	38	1.9	43.9
38	37	1.9	45.8
37	36	1.9	47.7
36	35	1.9	49.6
35	34	1.9	51.5
34	33	1.9	53.4
33	32	1.9	55.3
32	31	1.9	57.2

Module Number	On Screen Number	Distance from Previous Module (m)	Total Distance From Bottom (m)
31	30	1.9	59.1
30	29	1.9	61
29	28	1.9	62.9
28	27	1.9	64.8
27	26	1.9	66.7
26	25	1.9	68.6
25	24	1.9	70.5
24	23	1.9	72.4
1	1	1.9	74.3
23	22	1.9	76.2
21	20	1.9	78.1
20	19	1.9	80
19	18	1.9	81.9
18	17	1.9	83.8
17	16	1.9	85.7
16	15	1.9	87.6
13	12	1.9	89.5
12	11	1.9	91.4
11	10	1.9	93.3
10	9	1.9	95.2
9	8	1.9	97.1
8	7	1.9	99
7	6	1.9	100.9
6	5	1.9	102.8
51	50	1.9	104.7
Top of Pipe		25.3	130

Table 7: Final Position of Modules Inside LS-Model Riser

As can be seen, the top 25.3 meters of the riser model was not instrumented when the model was completed. This was a compromise that could not be helped due to the failure of some modules as well as the decreased distance between modules. It was felt that the top portion of the riser experienced increased noise during testing, due to surface waves and the wake of the boat, and so the bottom portion of the riser was, from a data perspective, felt to be more important. It was expected that the densely instrumented

bottom portion of the LS – Model Riser would be enough to map the high mode vibrations that the riser experienced. The actual data collected from the accelerometer modules is discussed further in Section 6.

4 Large Scale Model Riser

4.1 Parts

This section gives a detailed explanation of the parts used in assembling and testing the LS – model riser.

4.1.1 Pipe

The pipe that was used for the body of the model riser was IPEX Pipe with the Stripe – 160 Series Gold Stripe, a flexible, durable and light weight polyethylene plumbing pipe.

Figure 16 shows some samples of the Pipe with the Stripe.

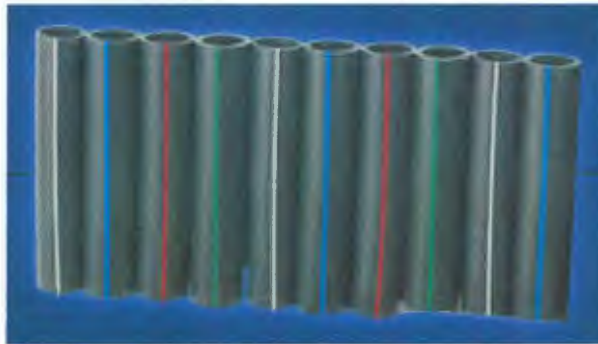


Figure 16: Samples of IPEX Pipe with the Stripe

The following reasons all contributed to choosing the Pipe with the Stripe – 160 Series Gold Stripe as the body of the riser model:

- The extremely smooth interior walls allows for the least resistance when pulling the accelerometer units and wiring through the pipe.
- It is weather resistant in that it has a unique formulation that protects the pipe against excessive ultraviolet rays. As well, the pressure rating for the pipe is

determined at 23 degrees Celsius. If the pipe is used at a lower temperature, such as our testing which was carried out at approximately 0 degrees Celsius, the pressure rating should be increased according to Figure 17 found in the technical manual supplied by the manufacturer.

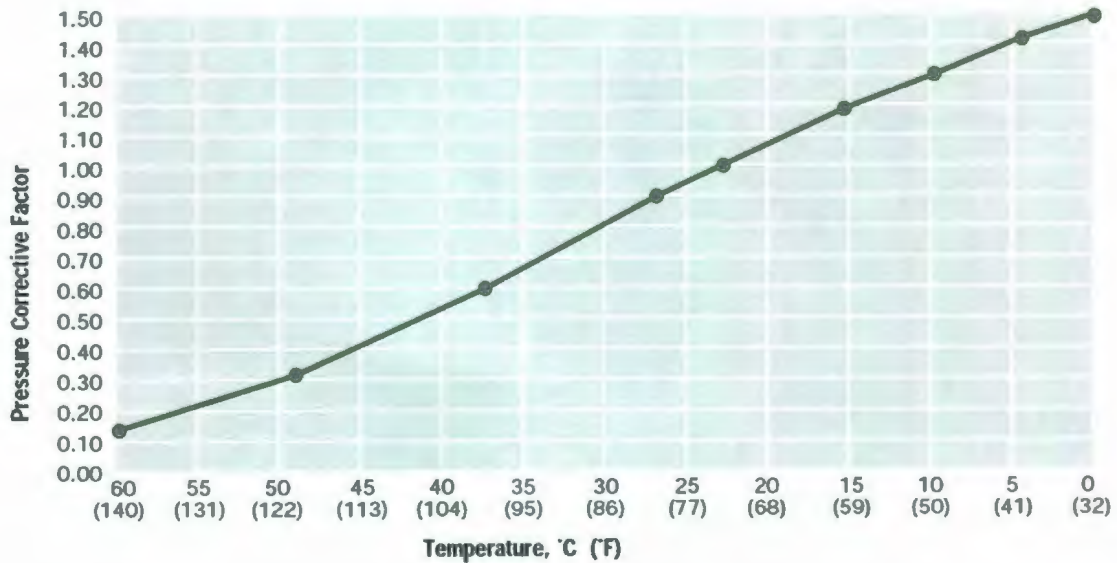


Figure 17: Pressure Rating Changes with Temperature

As shown, the pressure rating will increase by a factor of 1.5 when used at a temperature of 0 degrees Celsius.

- The empty pipe was light weight: approximately 1.5 kg/m. This allowed for easy manipulation and placement of the pipe before and during the assembly process.
- The pipe is chemically resistant, which is important due to the fact it was filled with hydraulic oil and permanently capped at both ends.
- The Gold Stripe was specifically chosen because it had the highest pressure rating, 160 psi, of all the IPEX pipes considered. As mentioned above, this

pressure rating is increased by a factor of approximately 1.5 when it is used in the low temperatures of this test. This will yield a test pressure rating of 240 psi.

- The pipe was available in a nominal 2 inch diameter (outer diameter = 0.053m, inner diameter = 0.040m) which was comparable to initial diameter estimates to achieve a maximum mode number of between 20 and 30.

An important factor in deciding whether the Gold Stripe pipe would be suitable for this test is noticeably missing from the above list. The strength of the pipe in tension was not available from the manufacturer since the sole use of the pipe is for plumbing. Gold Stripe pipe is quite specialized and expensive and therefore is not very common in the plumbing industry. Due to this fact, it is only available in 200 and 500 foot coils, and a sample of the pipe was not available for testing. However, the Blue Stripe 100 Series (rated for 100 psi) was available and therefore testing was done on a sample of this Blue Stripe pipe. The Blue Stripe pipe did satisfy the criteria for testing. Therefore, the Gold Stripe pipe, rated for 160 psi, is much stronger and more than acceptable to use as the body of the LS-riser model.

4.1.1.1 Tension Test

To test the strength of the pipe a common tension test was performed using samples made from the wall of the pipe. The samples, made to follow the ASTM Standards as shown in Figure 18, were placed in a standard automatic tension machine and stretched at a constant rate until fracture.

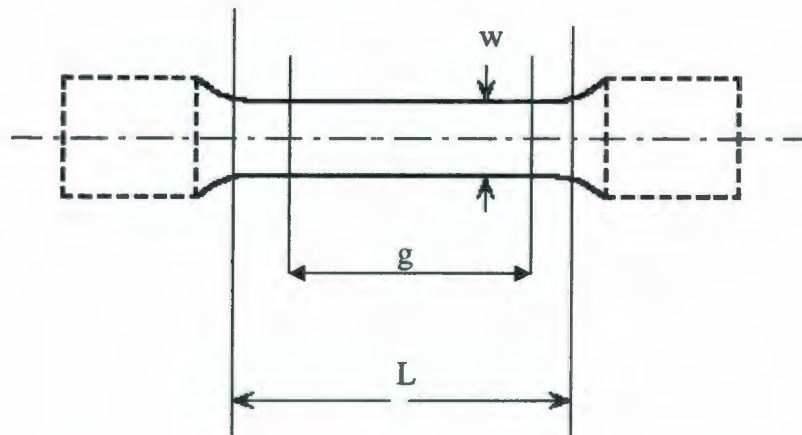


Figure 18: ASTM Specimen Dimensions for Tension Tests

Each specimen was made individually by the Engineering Technical Services Machine Shop, and so each dimension varied slightly from specimen to specimen. A table of the dimensions of each can be seen in the Tension Test Summary Table in Appendix F.

The load in kilograms was recorded along with the extension in centimeters. From this data, the stress in kilopascals and strain in meters/meter were calculated using the cross sectional area and original gauge length, and a stress versus strain curve was developed for each test. The tables of load, extension, stress and strain data for each sample can be seen in the Tension Test Summary Table in Appendix F. The stress vs. strain curve, also included in the Appendix, can be seen in Figure 19 for Samples 3 to 6.

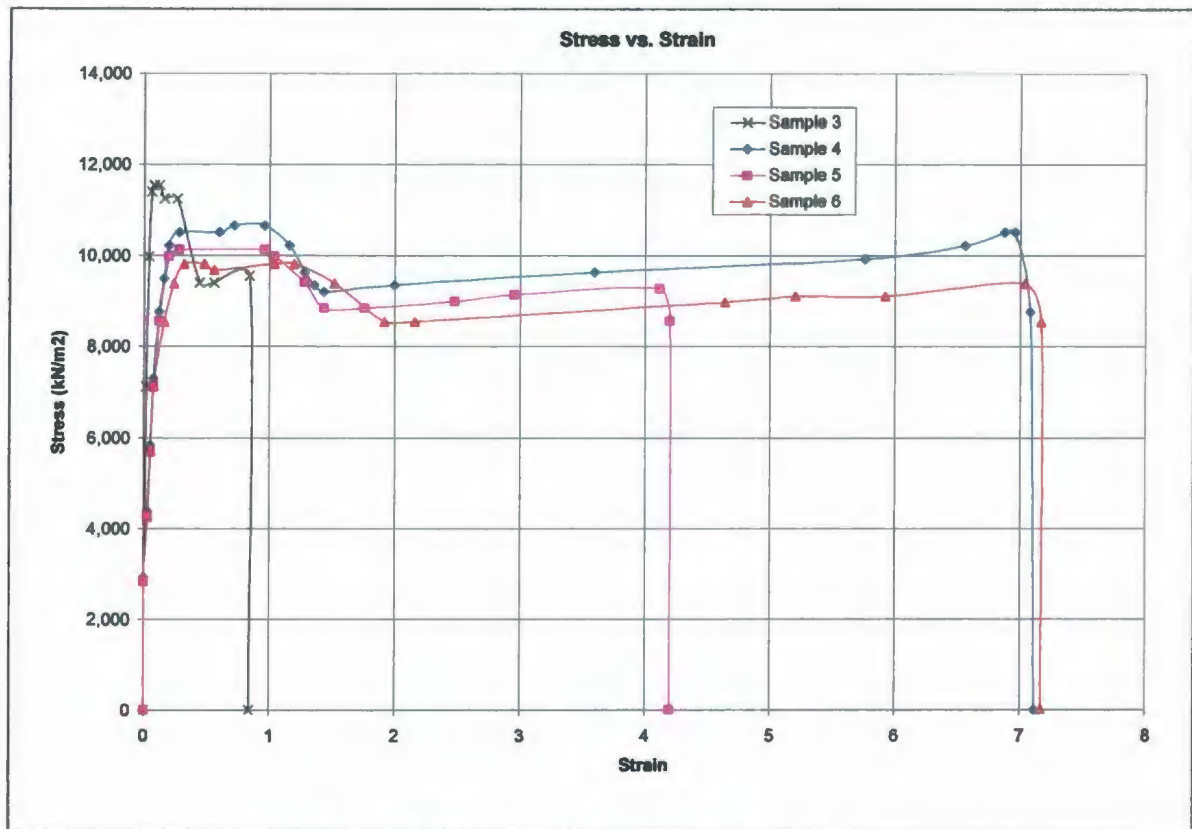


Figure 19: Tension Test - Stress vs. Strain Curve

The curve for Sample 3 can be seen to be quite different from the other samples. This is due to the fact that the load was applied at a rate of 10 cm/min, which was felt to be much too fast for the size of the sample, whereas Samples 4, 5 and 6 had a more acceptable applied rate of 5 cm/min. When the results of Samples 4, 5 and 6 were averaged the pipe was found to break under a load of approximately 7,400 N with a resulting modulus of elasticity for the pipe of 4.71×10^7 Pa. The faster rate caused only a slightly higher break load of approximately 8,000 N but it caused a much higher modulus of elasticity of 1.9×10^8 Pa. However, due to the fact that the rate was extremely fast and the extension only reached 2 cm, it was thought to be less relevant to the performance of the pipe in the conditions expected during the test than the slower 5 cm/min rate.

The estimated tension the pipe will experience, as shown in Section 3.4.2.1, will be 10,000 N. This is higher than the 7,400 N break tension found with the samples. However, the pipe tested was the Blue Stripe 100 Series, not the Gold Stripe 160 Series. The Gold Stripe pipe is already rated for 160 psi, 1.6 times stronger than the Blue Stripe pipe, and with the decreased temperature will be up to approximately 2.4 times stronger. These results were felt to justify the choice to use Gold Stripe pipe as the body of the LS – Model Riser. One final test, shown in Section 4.1.9.2, was done to confirm the strength of the Gold Stripe pipe. In this test, a tension of 14,000 N was applied to the Gold Stripe pipe which established that the strength of the pipe was indeed more than enough to withstand testing.

4.1.2 Instrumentation

All of the instrumentation, wiring and software for this project was designed by Martin Ordonez, an Electrical Engineer. It was implemented by the Engineering Technical Services Electronics Design and Fabrication Shop at Memorial University of Newfoundland. There were two different modules containing instrumentation used for this experiment, an accelerometer module and a full module. Originally, there were 61 accelerometer modules equipped with a three-axis accelerometer on each to record voltage data that was transferred into acceleration data in the in-line and cross-flow directions. The accelerometers, Analog Devices ADXL330, measure a minimum full-scale range of $\pm 3g$'s, and their small profile of 4mm x 4mm x 1.45mm made them attractive from the point of view of trying to fit the entire system inside a small diameter pipe. Figure 20 shows one of the accelerometer modules.

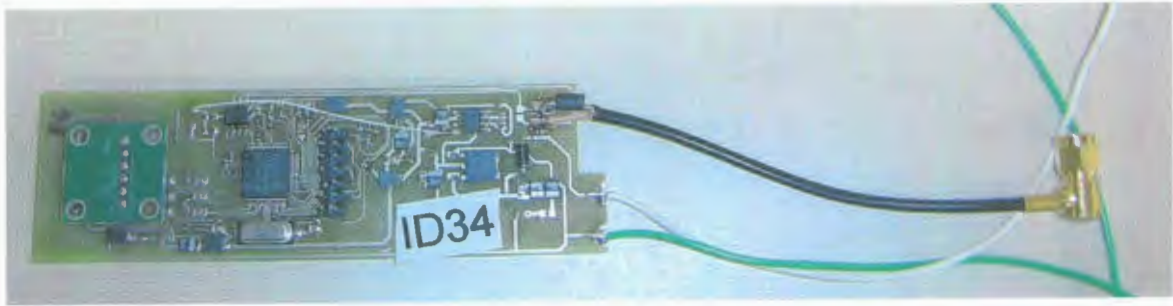


Figure 20: Accelerometer Module

There also were 4 full modules which each contained an accelerometer plus an additional rate sensor and magnetic sensor. Figure 21 shows one of the full modules.

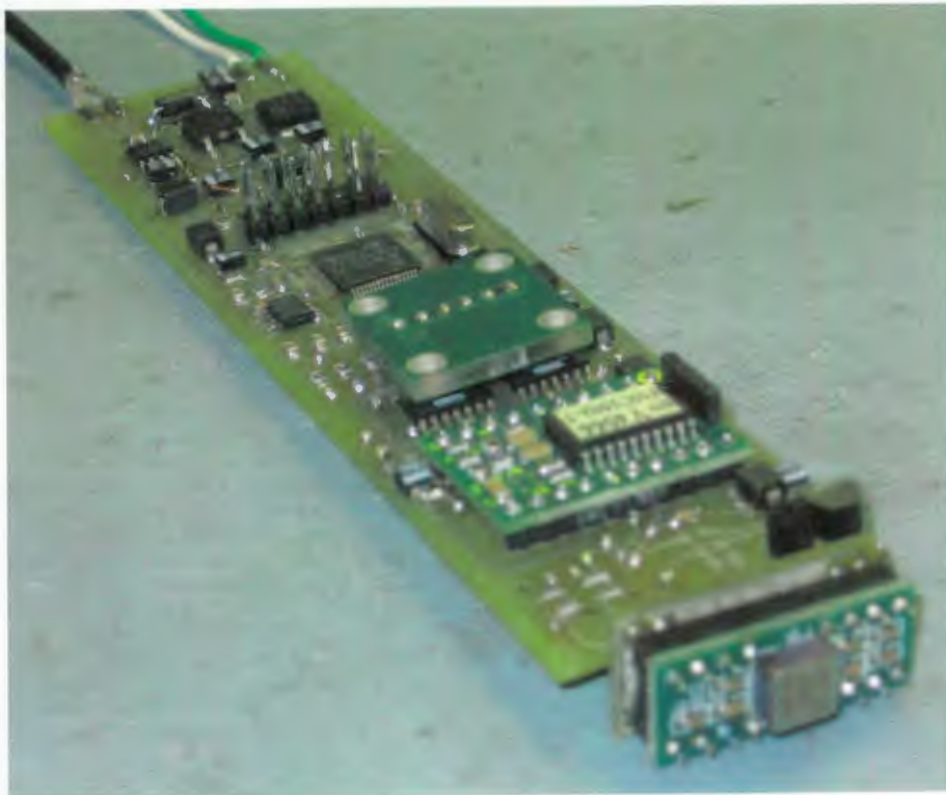


Figure 21: Full Module

The rate sensor (gyroscope), Analog Devices ADXRS300, has an output of voltage that can be transferred into angular rate and a reference and temperature to be used for compensation techniques when analyzing the data. This chip was also attractive due to

its small size of 7mm x 7mm x 3mm. The magnetic sensor, Honeywell HMC 2003, measures the strength and direction of an incident magnetic field along its length, width and height to provide compass heading and attitude. Product data sheets for some of the major parts of the modules can be seen in Appendix G.

4.1.2.1 Pressure Test

It was unknown how all of the components in the modules would stand up against the pressure of being almost 150m underwater. Therefore, two sample modules were created and tested in the Marine Institute Pressure Chamber. Both modules were coated with epoxy, and then one of the modules was placed inside a sample of the IPEX Gold Stripe pipe which was filled with UNIVIS BIO 40 and capped at both ends. These samples can be seen in Figure 22.

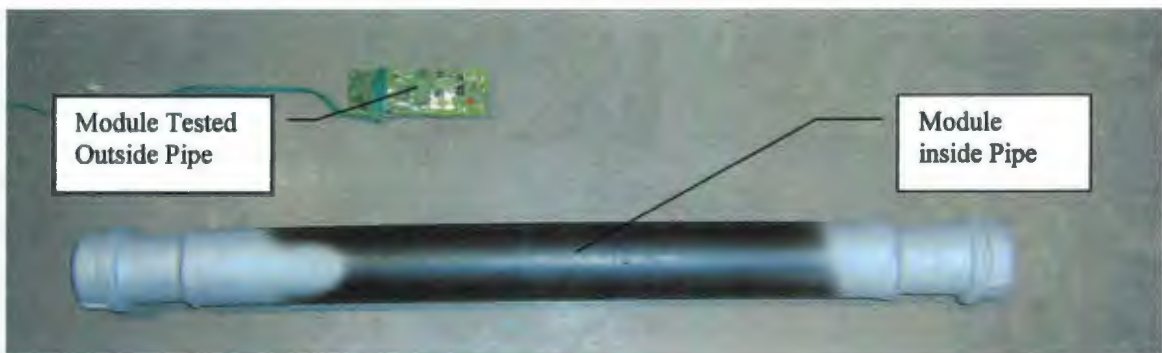


Figure 22: Pressure Test Samples

The samples were then placed inside the pressure chamber and the pressure was set at approximately 290 psi, which is equal to almost 200m of water depth, for approximately 10 minutes.

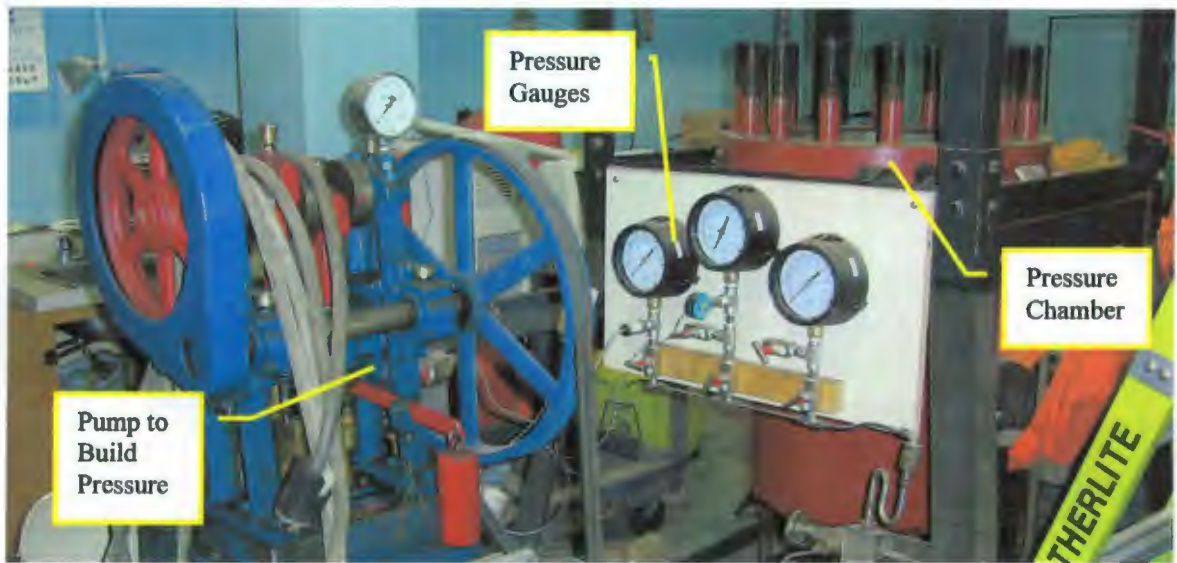


Figure 23: Marine Institute Pressure Chamber

It should be noted that the samples were tested before being placed in the chamber to provide a baseline for this pressure test. The samples were then taken out of the chamber and were tested using the computer which proved the instrumentation still functioned properly. The LS – Model Riser is 130m in length, well above the test 200m water depth, therefore, the pressure at this depth is not expected to influence the modules in a negative fashion.

4.1.3 Power/Ground and Communication Cables

Two sets of cables were used for the LS – Model Riser. The first set, or the internal set, was used to run inside the model, connecting each module to one another, and the second set, or the external set, was spliced into the internal set and ran from the T Section back to the vessel.

The internal set consisted of one CAN Bus cable, Co-ax RG174/U, a group of 4 power cables, Conductor Submersible Cable, 10 Gauge and one power and one ground wire, Type 3051, 22 Gauge.

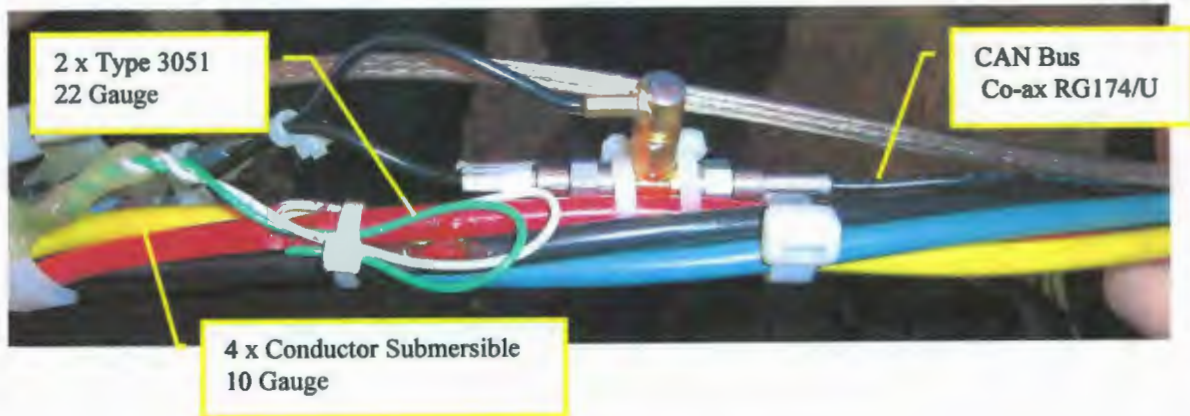


Figure 24: Internal Cables

The external set consisted of a CAN Bus cable, Co-ax RG58/U and a power cable, 10-4 CabTire (10 Gauge, 4 Conductor). These external cables can be seen in Figure 25.

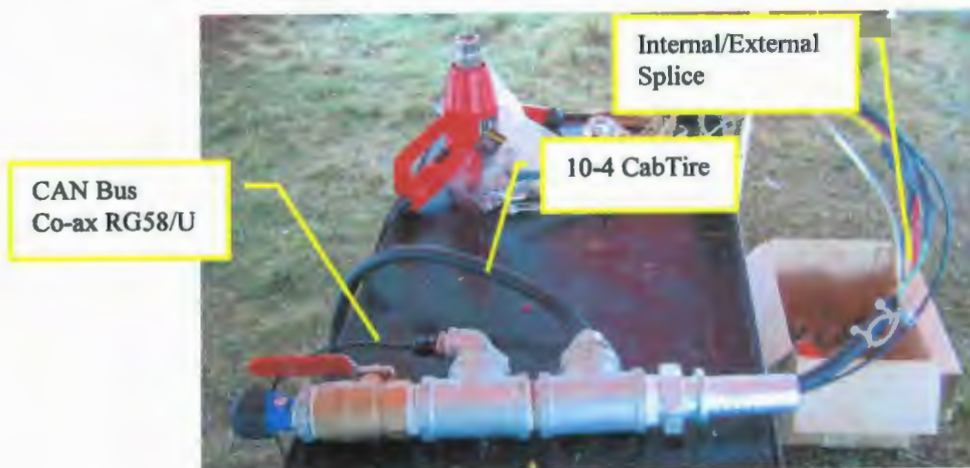


Figure 25: External Cables

4.1.4 Placement Pucks

Placement pucks were developed in conjunction with Jason Miller in the Engineering Technical Services Machine Shop at Memorial University. These pucks, which were made of Delron and can be seen in Figure 26, served a number of purposes within the LS – Model Riser. The outer diameter was made to be slightly smaller than the inner diameter of the pipe. It was thought that the pucks would keep the modules in place fairly close to the center of the pipe while still allowing them to be pulled through the pipe with little friction when lubricated. The inner diameter of the puck was chosen large enough so that the power, ground and communication cables could all fit under the module when mounted, but still allowed for a wall thickness to be large enough to provide ample strength to support the modules. A section of the bottom of the puck was cut out so that they could be added along the length of the cables as it was assembled and did not have to be thread over one end.

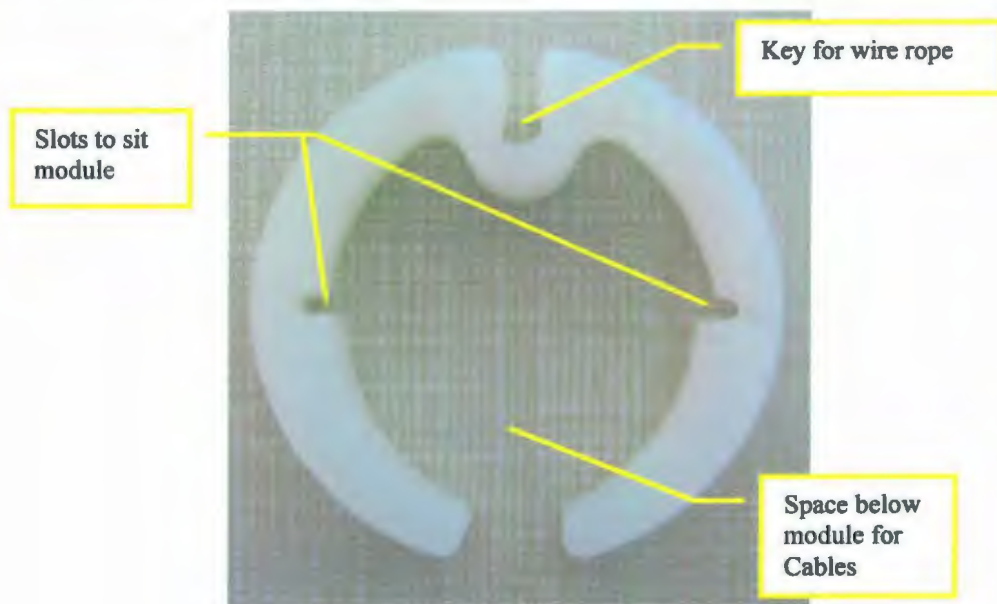


Figure 26: Placement Puck

Also, the puck had a small key hole at the top where a coated wire rope was attached to hold the module in place along the length of the pipe. The pucks were placed on the end of each module after they had been coated with epoxy, fitting snugly into the slots on both sides. Figure 27 shows the module after the epoxy had been applied and the pucks had been put in place.

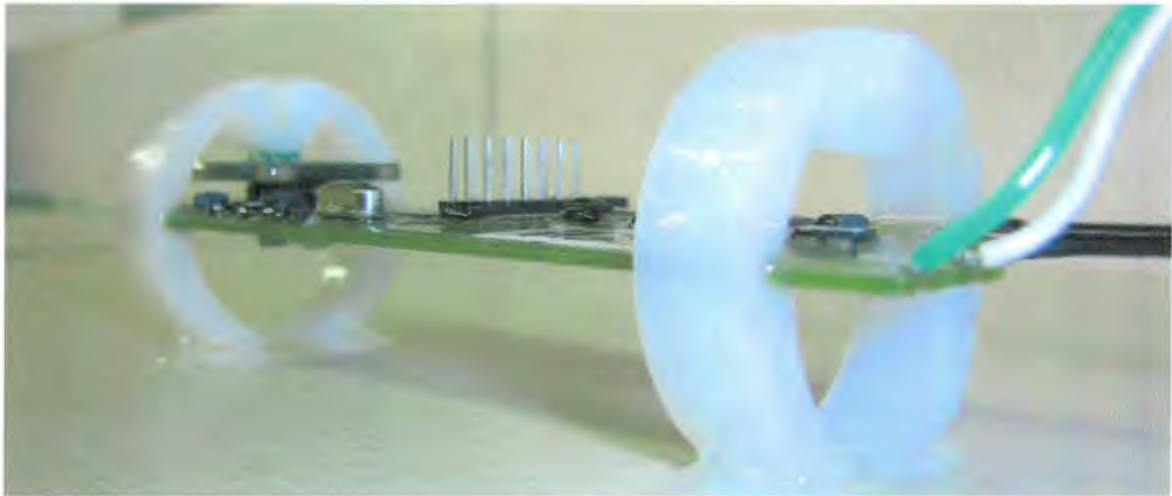


Figure 27: Placement Pucks on a Module after Epoxy has Been Applied

4.1.5 Coated Wire Rope

The coated wire rope is a 1/8" common clothes line, rated for up to 1100 lbs of tension. Initially, a steel wire rope was used, but issues with grounding arose and so a coated wire rope was decided upon for the final assembly. When the wire rope was snapped into the key hole of the placement pucks, crimps were attached at both ends. This produced a way for the modules to be pulled through the pipe without having to pull on any of the power, ground or communication cables. A picture of the module/placement puck assembly attached to the wire rope can be seen in Figure 28.

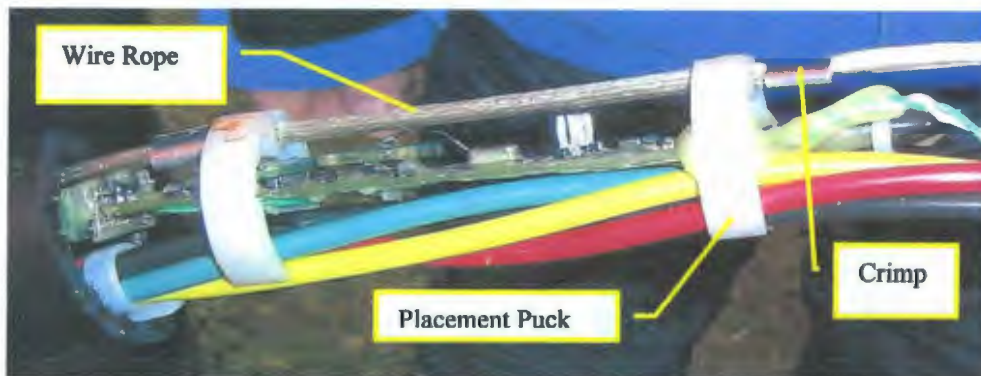


Figure 28: Module/Placement Puck Assembly Entering the Pipe

4.1.6 Epoxy

All modules were coated in epoxy after they had been individually tested and found to be working properly. The epoxy was used to give each component extra strength against the hydrodynamic pressure, as well as to protect each module against water and damage before and during their installation inside the pipe.

The epoxy used was West System epoxy, a high-quality, two part epoxy that will bond to fiberglass, wood, metal, fabrics and other composite materials. It yields superior moisture resistance and high strength and is especially suited for marine applications. The system includes a resin and hardener that must be mixed in a specific proportion to create a high-strength plastic solid. For this project, the 105 Epoxy Resin was used as the base material and the 206 Slow Hardener was added. This slow hardener was chosen to extend working time to 20 to 25 minutes, where the fast hardener would have only given a working time of 9 to 12 minutes. The modules were then coated, taking care to cover the boards completely and give ample time for the epoxy to completely cure. Figure 29 shows some of the modules laid out to dry after the epoxy had been applied.

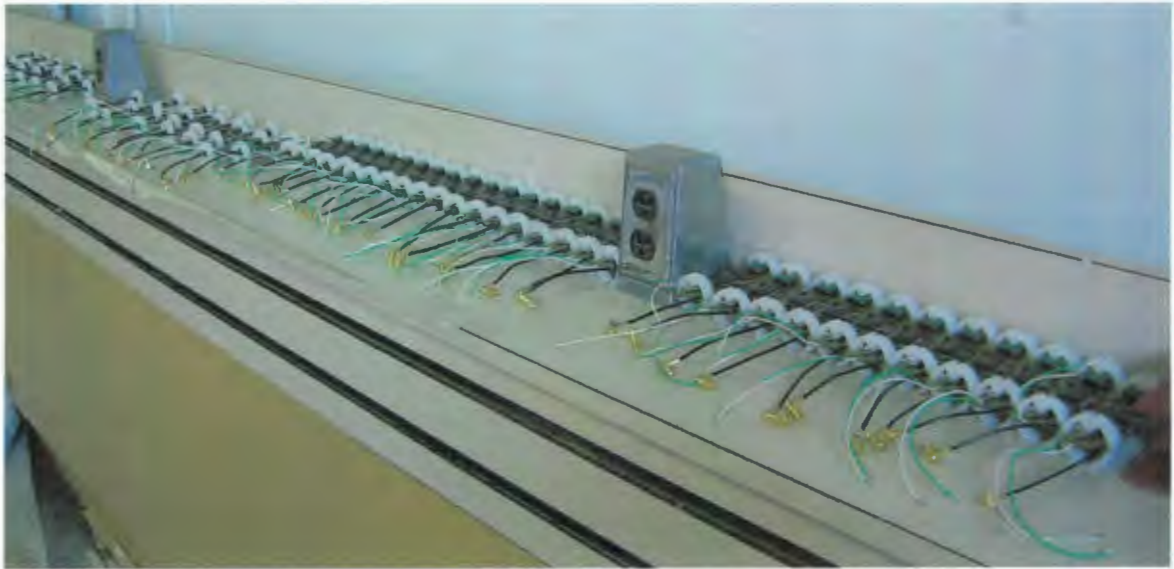


Figure 29: Modules Drying after Epoxy had Been Applied

4.1.7 Software

The software developed for this project was one of a kind custom coding developed by Martin Ordonez. It enabled the user to set the sampling frequency in Hertz, the duration of sampling in seconds, and also gave the user the ability to manually start and stop sampling. The user interface can be seen in Figure 30.

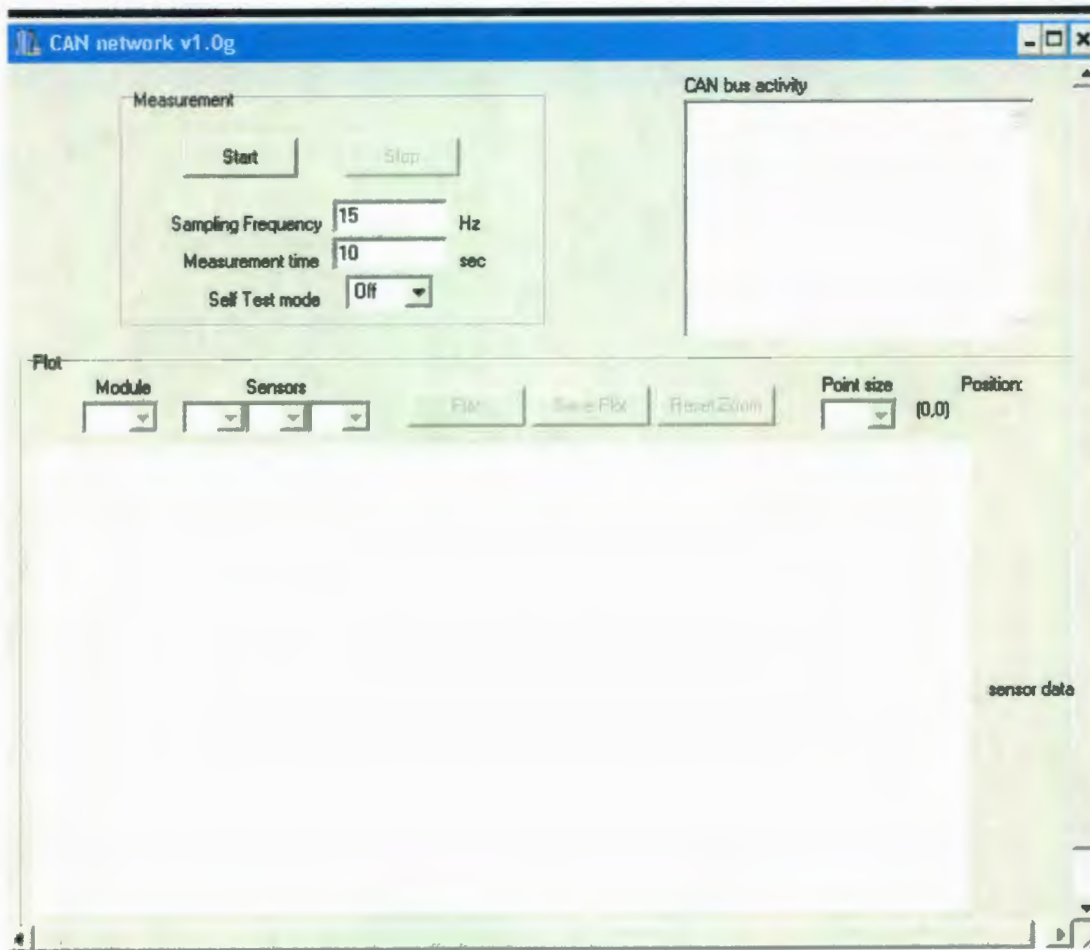


Figure 30: User Interface for Module Coding

As can be seen, there is a large plot area where the data can be reviewed instantly after the sample has been acquired. The “Module” and “Sensors” pull down menus allow the user to select the module of interest and the type of data (sensor) to be plotted, for example the 42nd accelerometer module and the x, y and z axis. The data is then plotted as a function of time giving the user the ability to visually check each module and ensure things are working properly before the next sample is taken. The option is also given to zoom in on any area of the graph or to save the graph.

The CAN Bus activity box is important when sampling the data. This area lists the time step of the sample along with the number of bundles of data that have been acquired.

This is a useful diagnostic tool in that it lets the user know, without having to stop sampling and plot the data, if the system is sampling at a normal rate or if there is a problem. For instance, if the time step keeps increasing but the number of bundles remains constant, the system has stopped reading data for some reason.

4.1.8 UNIVIS BIO 40

After the instrumentation was pulled through the pipe, it was filled with the hydraulic oil, UNIVIS BIO 40. The product data sheet from Esso Imperial Oil for UNIVIS BIO 40 can be seen in Appendix H. The oil was required for various reasons, all of which are listed below:

- The LS-model riser was over 130m in length when completed. The setup required the model to be hung from a steel sphere buoy behind a ship. This meant that at the bottom, the riser saw approximately 200psi of hydrodynamic pressure from the ocean with the pipe itself being rated to only 160 psi. Since there was no evidence to ensure that when testing at 0 degrees Celsius the decrease in temperature did in fact increase the rating of the pipe, it was felt that the pipe could not be assumed to be strong enough to withstand the 200 psi pressure from the ocean. The oil provided extra strength to withstand the hydrodynamic pressure that the pipe was subjected to.
- The oil is a natural insulator which gave protection to the wiring and instrumentation.

- UNIVIS BIO 40 is a non-toxic, biodegradable, vegetable oil based lubricant. If there was a problem and a leak or break in the pipe occurred during the testing, the oil is not harmful to the environment, which is important when testing in a marine situation. As well, when filling the pipe, any spills that occurred were also not an issue.
- The high viscosity of UNIVIS BIO 40 lends itself well to being used as a lubricant when pulling the instrumentation through the pipe.
- The oil has a flash point of 230 degrees Celsius and a pour point of -36 degrees Celsius. After the pipe was filled with the oil, the ends needed to be heated to allow them to be capped properly. The high flash point allowed this to occur without any danger of fire or explosion. As well, the model was assembled outside in the fall/winter in Newfoundland. Although it was cold, with the lowest temperature estimated to be -10 degrees Celsius, the low pour point ensured that it remained workable even in the coldest temperatures experienced.

4.1.9 End Configurations

The ends of the pipe were capped permanently to ensure the oil remained in the pipe.

This poses a problem at the top end due to the cables having to be taken from the model to the vessel, and both ends have to be equipped with a method of attaching the model to a weight at the bottom and a buoy at the top. Therefore, both the top and bottom section were designed specifically to fit these special needs.

4.1.9.1 Top Section

The top section of the LS – Model Riser is the section that is connected to the spherical buoy at the surface that is towed by the vessel. The completed top section, shown in Figure 31, includes a dummy end connected to the T Section which is connected to the pipe itself.

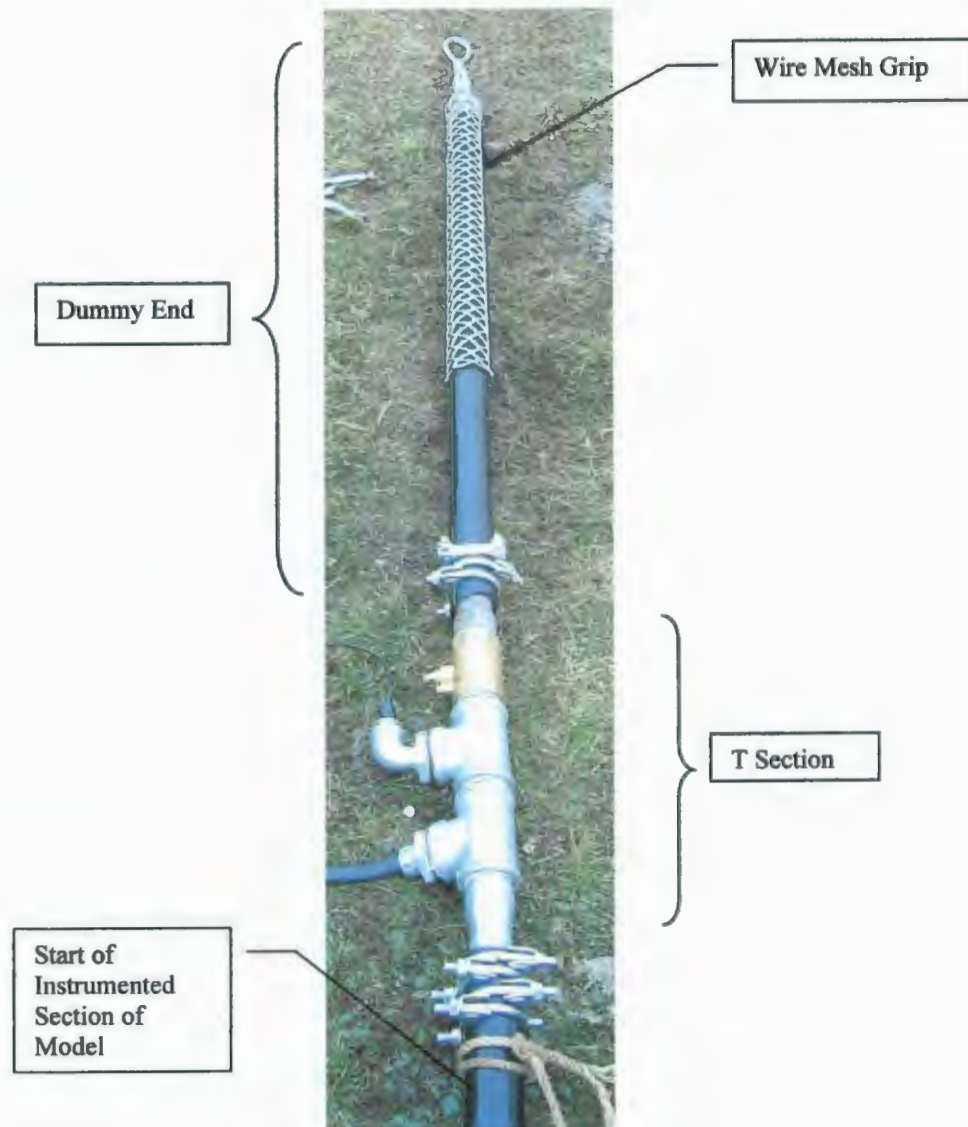


Figure 31: The Completed Top Section

4.1.9.2 Wire Mesh Grips

The wire mesh grips were chosen as the method to attach the LS – Model Riser to the weight at the bottom and the buoy at the top. The grips work by tightening as tension is applied at the end. However, in industry they are mainly used to pull wires and cables, which are able to take the force of the grips tightening, whereas the pipe is hollow and therefore may crush under this pressure. To remedy this, solid PVC rods were made to fit inside the pipe at both ends. This gave the pipe the strength to withstand the force from the grips.

To ensure that the grips worked properly, that they would not slip off of the pipe, and that the plugs were sufficiently strong, a test was performed in the Strength Lab in the Engineering Building at Memorial University. The set up can be seen in Figure 32. As shown, the plugs were placed inside a sample of the Gold Stripe IPEX pipe which was capped with common steel plumbing caps and then the grips were placed over both ends. One end was then bolted to the floor while the other end was attached to an overhead crane, equipped with a load cell, and lifted until the desired tension was reached.

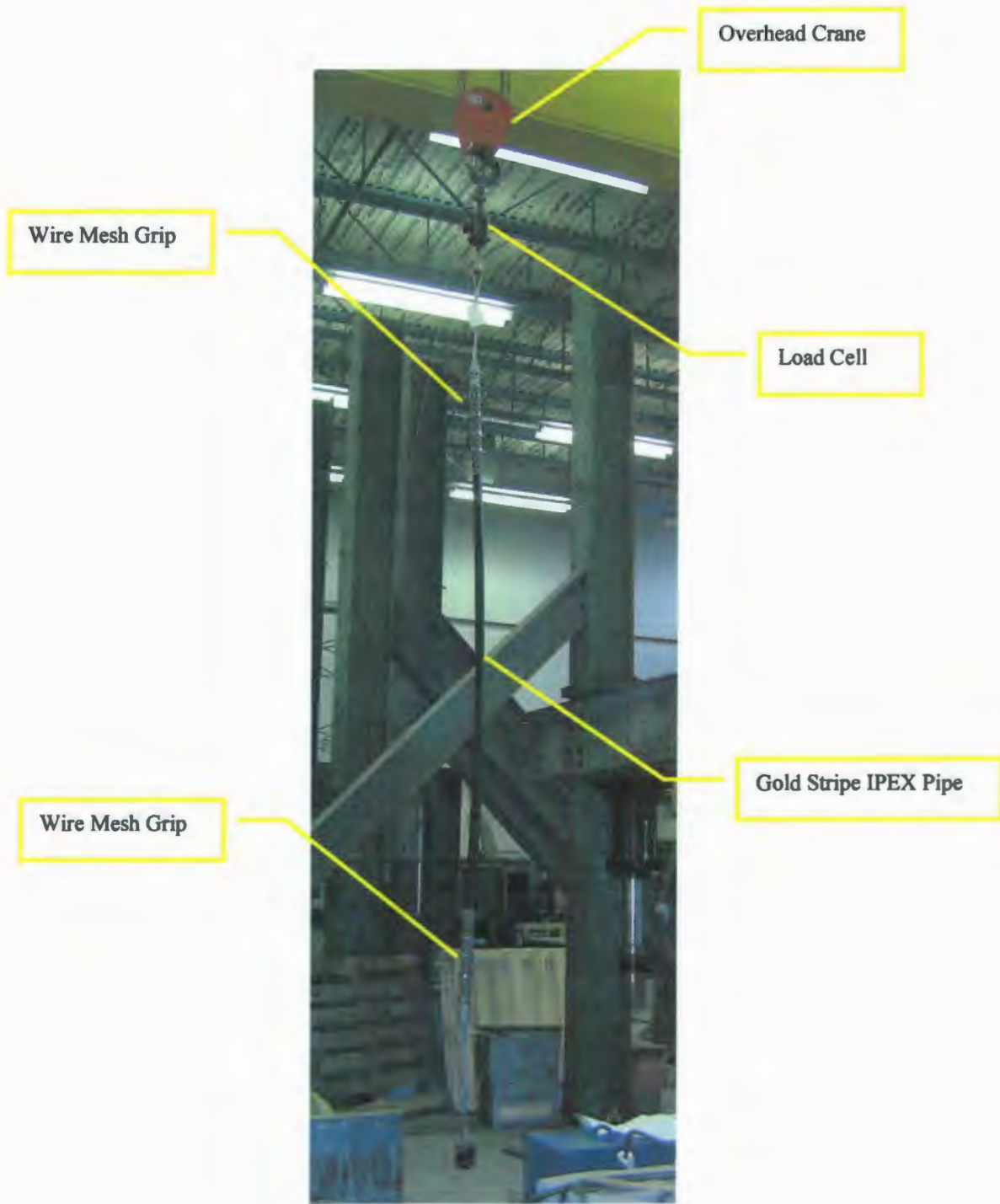


Figure 32: Wire Mesh Grip Strength Test Set-Up

As shown in previous calculations, the expected tension the riser will experience is approximately 10,000 N. Therefore, to err on the side of caution, approximately 14,000 N was applied to the set up and not only did the grips hold, they did not move or slip on

the pipe, the pipe did not crush under the force of the grips and the caps did not move and went undamaged. Therefore, it was felt that the grips, plugs and caps were suitable for use in this project.

4.1.9.3 T Section

Due to the fact that the LS – Model Riser was filled with oil and towed behind the vessel from a buoy, there had to be a watertight way of bringing the power, ground and communication cables out of the model and back to the vessel. Working in conjunction with Kean’s Pump Shop, a local plumbing company in St. John’s Newfoundland, a T Section, shown in Figure 33, was devised for this purpose.

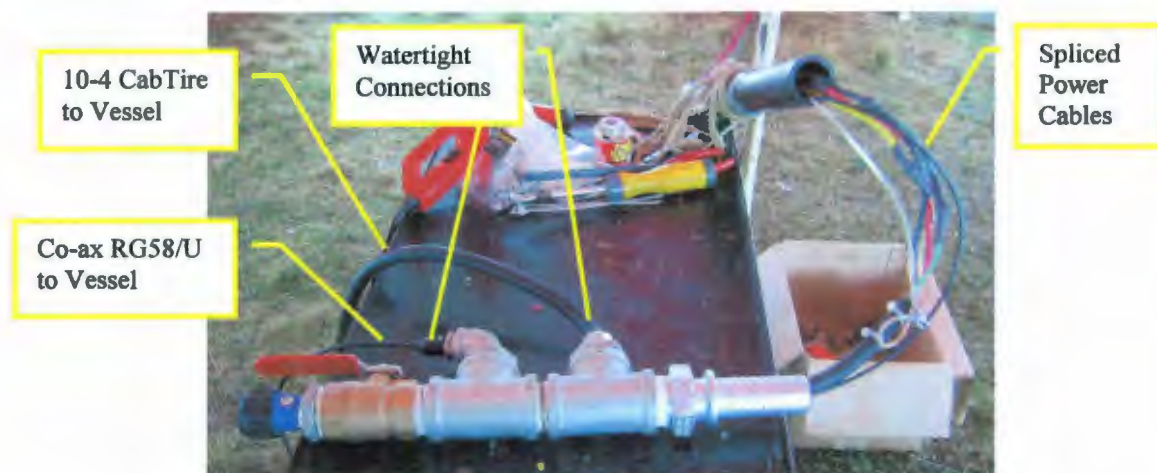


Figure 33: T Section Being Attached to LS - Model Riser

In the above figure, the T Section is being attached to the LS – Model Riser. Firstly, the internal Co-ax RG174/U and the 4 Conductor Submersible 10 Gauge power cables had to be spliced into the external Co-ax RG58/U and the 10-4 CabTire cables respectively. These external cables then go through the T Section and out through a watertight plumbing connection. In Figure 34, the T Section can be seen fully assembled sitting in

the pipe. The end of the T Section that fits inside the pipe is a typical plumbing connection that was clamped on the outside to give extra strength to and to make the joint watertight. On the opposite end of the T Section, there is a ball valve and a connection to hook up the pump system.



Figure 34: Fully Assembled T Section

However, when the T Section was hooked up to the pump system and the UNIVIS BIO 40 was being pumped into the pipe, the clamp joint started to leak, and so a different joint was needed. Figure 35 shows the fully completed T Section with the new joints intact.

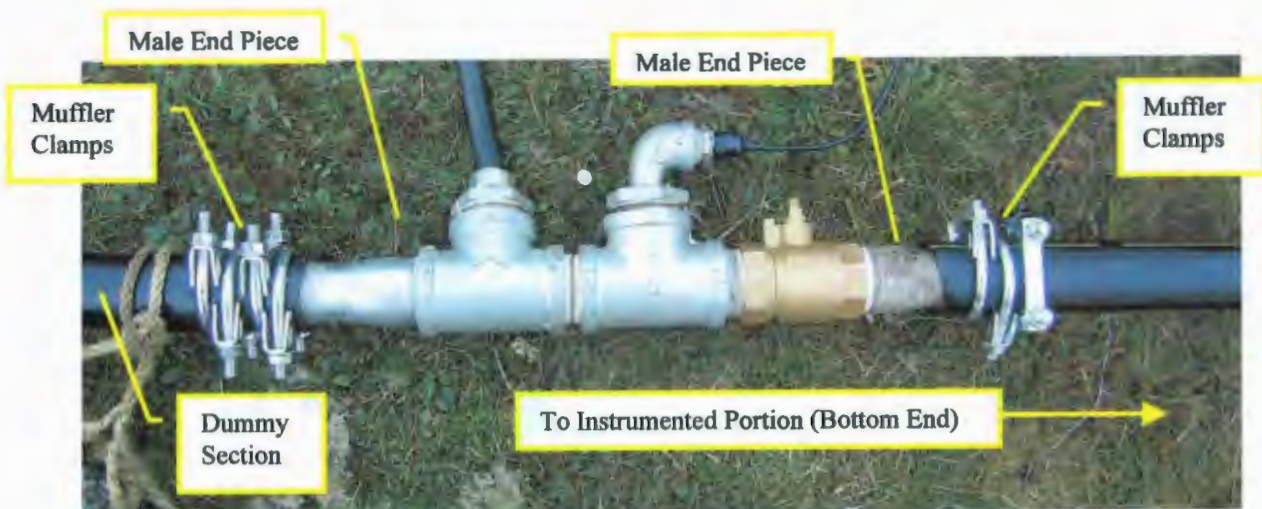


Figure 35: Completed T Section after Fixing Joint Leaks

The problem was fixed by welding an extension of steel tubing onto a common male end plumbing piece to ensure there was ample surface area between the connection and the IPEX pipe. This allowed muffler clamps to be attached on the outside of the IPEX pipe, not only strengthening the joint, but also making it watertight.

4.1.9.4 Dummy Section



Figure 36: Dummy Section

The dummy section that was attached at the top of the LS – Model Riser can be seen in Figure 36. This section replaced the plastic connection that runs to the pump system. The dummy section allows the cables to be taken from the T Section, but gave a section of the IPEX pipe for the mesh grip to be attached.

4.1.9.5 Bottom Section

The bottom section of the LS – Model Riser had to be attached to the railway wheel to provide the necessary tension in the model. Again, a wire mesh grip was fitted over the capped end of the pipe after the PVC plug was fitted inside the pipe. The finished bottom section can be seen in Figure 37.



Figure 37: Bottom Section of the LS - Model Riser

The PVC plug had a hole drilled through its entire length to make it possible to anchor the wire rope. The wire rope was threaded through the plug, and when the plug was fitted inside the pipe, the wire rope was then crimped, not allowing it to be pulled back through the plug.

4.1.10 Railway Wheel

In order to weight down the entire system, and ensure that the riser remained as close to vertical as possible, a railway wheel was attached to the bottom section. The wheel can be seen in Figure 38.



Figure 38: Railway Wheel

The wheel weighed approximately 363 kg or 800 lbs, and had a volume of approximately 0.04617 m^3 . There was also a swivel, shown in Figure 39, located at the top of the wheel. The swivel allowed the wheel to spin in the water while it was being towed, while keeping the LS – Model Riser from twisting.

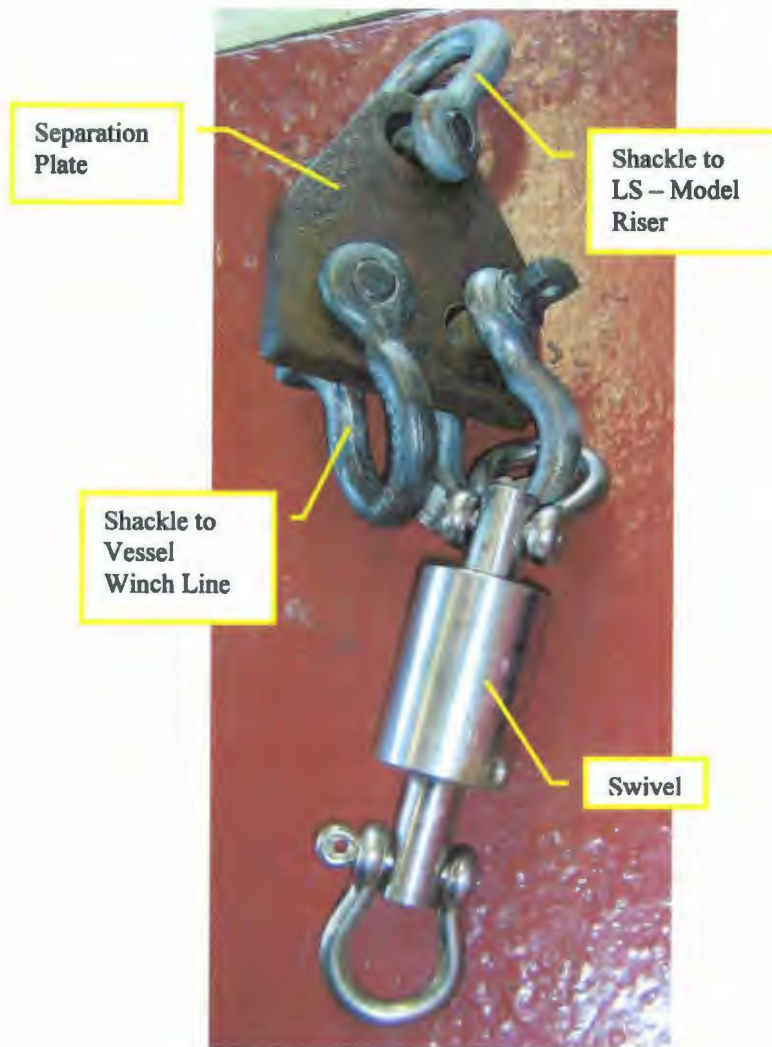


Figure 39: Separation Plate, Shackle and Swivel

4.1.11 Steel Spherical Buoy

At the top of the LS – Model Riser there was a steel spherical buoy that was attached to the vessel winch line at one end and the model at the other end to enable the system to be towed behind the vessel. The buoy allowed the LS – Model Riser to be towed at a distance behind the vessel so that the wake would not have a large effect on the flow the

riser will see. The steel spherical buoy, shown in Figure 40, was 58 inches in diameter, weights 680 lbs and gives 3000 lbs of buoyancy.



Figure 40: Steel Spherical Buoy

4.1.12 Pump System

The pump system, which was hooked up to the ball valve end of the T Section, was used to fill the LS – Model Riser with UNIVIS BIO 40 after all of the instrumentation was placed inside the pipe. The system, shown hooked up to the T Section in Figure 41, consisted of a gear pump, electric motor and hosing to transfer the oil from a 45 gallon (210 liter) oil drum to the pump and into the LS – Model Riser.

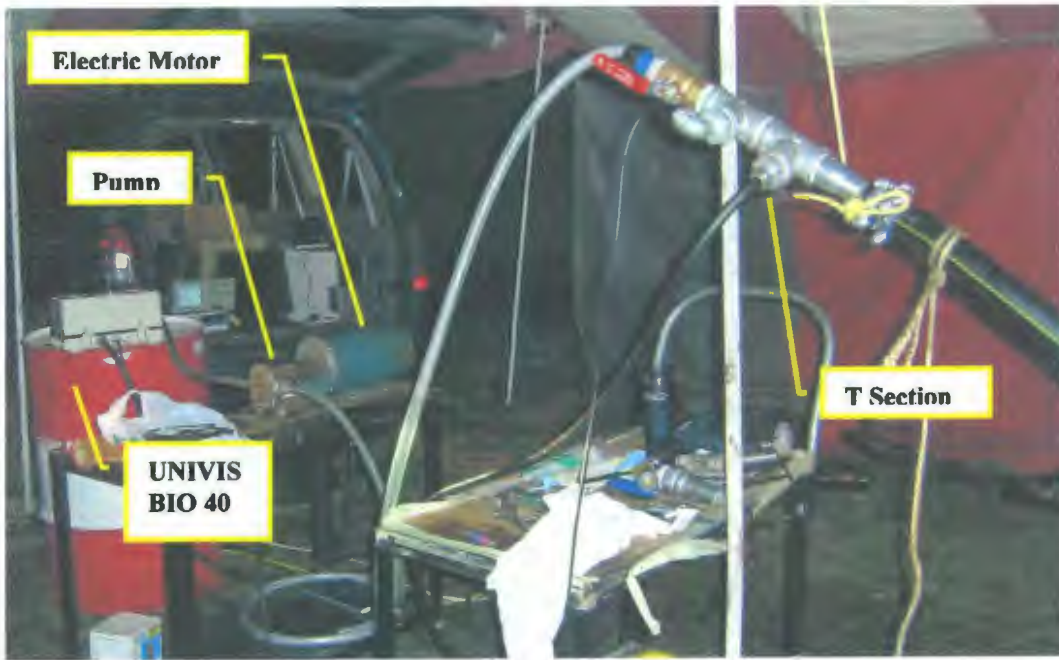


Figure 41: Pump System Set-Up

5 Assembly Process

This section gives the detailed step by step process of how the LS – Model Riser was assembled. As this is the first time a model of this size has been developed by this team at Memorial University, it was a learning process and much insight was gathered along the way about how to best design and assemble a large scale model in a field situation. To help describe the knowledge that was gathered and to make the reasons for any decisions and changes that occurred clear, the assembly steps are listed in chronological order and include any and all information that came as a result of the lessons learned.

1. All instrumentation was built and tested in the Engineering Technical Services Electronics Design and Fabrication Shop and all modules were coated with epoxy before heading out into the field. The epoxy was thought to give each component extra strength, as well as protect each module against water and damage before and during their installation inside the pipe (See Section 4.1.6).
2. After the epoxy was dry, the modules were tested again to ensure they were fully operational before being incorporated into the model. Somewhere between the initial programming of the modules and the process of applying epoxy, 5 of the accelerometer modules did not work and could not be included in the model.

These modules were some of the first to be built, when the process was still new to the technicians assembling the boards. However, after 5 out of the first 17 modules were ruined, which is approximately a 30% failure rate, there were no other drop outs before or after the epoxy was applied. This means only a total of

5 out of the 60 accelerometer modules, or an 8% failure rate was experienced and it was felt that this relatively low failure rate was acceptable. That left 60 modules in total, 56 accelerometer modules and 4 full modules, to be included in the LS – Model Riser.

3. It was felt that the easiest way to pull the instrumentation through the pipe was to first lay the pipe out as straight as possible and then send a small line through the pipe. This small line was then attached to the coated wire rope that held all of the modules together and was finally used to pull the instrumentation through the pipe. Due to the great length of the model, 130m, there was no space available indoors where the pipe could not only be laid out straight, but also could be left for long periods of time unattended. Therefore, with cooperation from the Institute of Ocean Technology (IOT), a field behind their building was used for the assembly of the riser.



Figure 42: Pipe Laid out Behind IOT

To send a small line through the pipe, a vacuum was attached to one end, and a piece of sponge just slightly smaller than the pipe was fed in the other end with the line attached. The vacuum sucked the line through and both ends were tied off until they were needed.

4. With the pipe setup for pulling through the instrumentation, the internal CAN Bus Co-ax RG174/U and the four 10 Gauge Conductor Submersible power cables were laid out on a long sheet of plastic next to the pipe, and the modules were laid out beside them, in numerical order, at 2m increments.



Figure 43: Cables and Instrumentation Laid Out



Figure 44: Modules Laid Out Beside Power Cables

5. In order to expedite the assembly process, the four power cables had been prepared in the lab beforehand, having been stripped at the 2m intervals along the entire length of the cables. The two Type 3051 22 Gauge power and ground cables coming off of each module were then soldered into the four power cables at each 2m. Every second module was connected to either the green/yellow or red/black power cables in turn. This ensured that if a short or any other problem occurred with only one set of power cables, every second module would still be operational.
6. The CAN Bus cables had also been prepared in the shop beforehand, as they needed to have T connectors to join each modules into the system at the 2m interval. The CAN Bus cables were then attached to each other, and to the module by screwing each cable and module into the T connection.

7. The wire rope was then inserted into the placement pucks and crimps were attached at each end of the pucks and the system was ready to be pulled through the pipe.
8. The end of the wire rope was attached to the small line that was already in the pipe. Two men started to pull the system slowly through the pipe from the far end. As they were pulling, UNIVIS BIO 40 was added into the pipe to help lubricate the system. This was done by holding the end of the pipe vertical and pouring the oil into a funnel and approximately 4 to 5 liters of the oil was added at a time. As the instrumentation was being pulled through, it was noticed that the wire rope was in some cases wrapped around the power cables and the CAN Bus cable. This was due to the fact that there were many people helping to set up the system when it was laid out on the ground, and because of a lack of foresight, the importance of keeping this wire free from the cables was not stressed to those helping. This in turn caused the entire assembly to twist inside the pipe as it was being pulled. Since the modules were attached to the power cables at exactly 2m increments, and the T connections were placed at exactly 2m increments on the CAN Bus cables, there was little or no slack in the cables, and the twisting caused the cables to bear the load of being pulled through the pipe. This twisting caused the wire rope to be ineffective, as it was no longer carrying the load as designed. This in turn caused the CAN Bus cables to be ripped out of the T connections in some places, causing complete failure of the modules from the point of failure on along the length of the model. Not only this, but the extreme cold had caused the

modules to be poorly soldered to the power cables, and many of the two Type 3051 power and ground cables were being pulled from the power cables.

9. It was decided that the system would have to be pulled back out of the pipe and fixed before assembly was possible. When the modules were pulled out of the pipe another problem was noticed. The CAN Bus cable and the two Type 3051 cables were only soldered to the module boards and the CAN Bus cable itself had a point of weakness, where the rubber coating on the cables was cut to allow assembly. This can be seen in Figure 45.



Figure 45: Weak Connections on Original Modules

Expected wear and tear on the modules, from actions such as applying epoxy, testing, transporting from the lab to the field and pulling the system into the pipe should not have been a problem if these joints had been designed properly with some sort of clip or other type of durable reinforcement. However, because these joints were not robust, many of them broke from the boards causing the modules

to fail. Again, this was largely due to a lack of experience working in field conditions.

10. The modules were taken out of the pipe, the UNIVIS BIO 40 was cleaned off and repairs were made to the cables that had broken off. As well, using a hot glue gun, glue was applied to each connection on the module to reinforce these joints.

This can be seen in Figure 46.

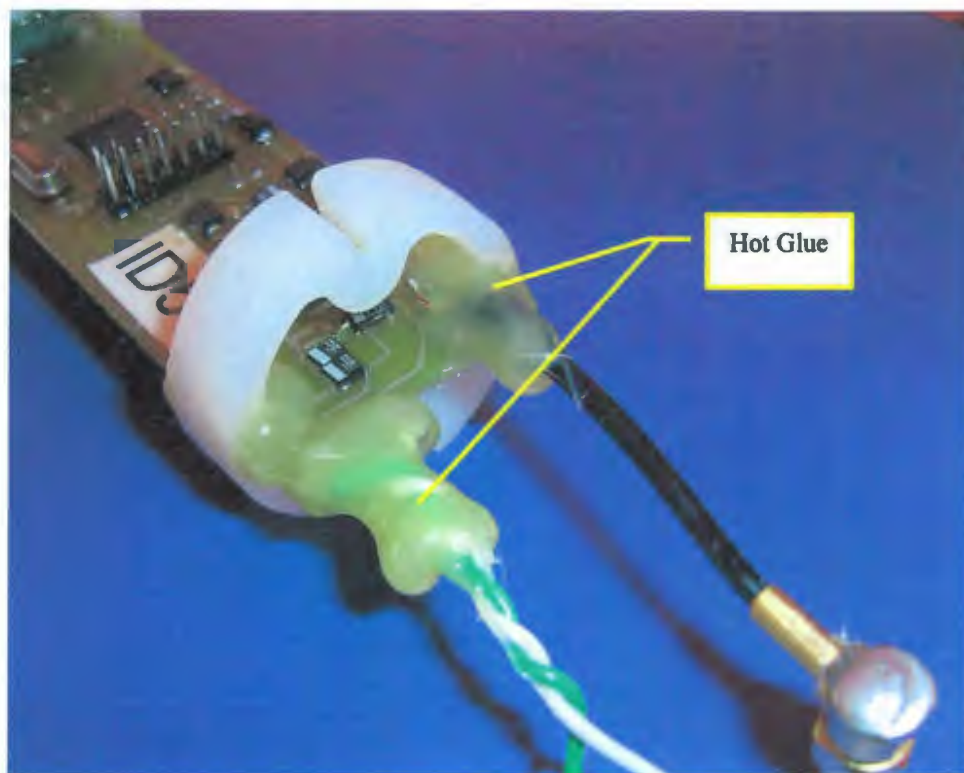


Figure 46: Reinforced Soldered Joints

11. The issue of having no slack on the CAN Bus cable T connections because of the 2m increments was still a problem. To remedy this, the power cables were first thoroughly degreased using a common auto garage degreasing mixture and then carefully dried. Each location where the cables were previously stripped was

wrapped in electrical tape to ensure they could not touch each other and cause a short circuit. This was an issue because originally, the stripped wires were not staggered, and the bare wires of each cable were lying on top of one another. After the tape was applied, the stripped sections were then covered in shrink wrap to fully seal each location.

12. Since the weather was becoming worse by the day, a tent was setup with a propane heater to enable the work to be done more comfortably out of doors.



Figure 47: Tent Setup

This also ensured that any soldering that had to be done would not be negatively affected by the cold temperatures as had previously been a problem. The work of attaching and hooking up each of the modules was also relatively delicate and therefore it was much easier to do without having to wear gloves.

13. With all of the repairs completed, and the tent setup, the instrumentation was again ready to be pulled through the pipe. However, this time, the modules were

connected and the power cables were stripped as they went into the pipe. This process did take much longer, as each module had to be a) attached to the wire rope and crimped on each side, b) each pair of power cables had to be stripped, c) both Type 3051 cables had to be soldered to the stripped power cables, d) the CAN Bus cables had to be attached to the T connection, e) wire ties had to be wrapped around a number of critical points to ensure there was no pulling on the CAN Bus cable, and f) the module had to be pulled into the pipe before the next module could be attached. A completed module just before it enters the pipe can be seen in Figure 48.



Figure 48: Completed Module Ready to Enter the Pipe

By going through this lengthier but thorough process, the modules were not exposed to any rough treatment, and the wire rope remained on top of the entire puck/module assembly and did not get twisted around the power cables. Also, by measuring off the 1.9m spacing and attaching the modules as they were put in the pipe and attaching wire ties, this ensured that the CAN Bus cables had some slack between modules.

14. When the modules were all placed in the pipe, the T Section was then spliced into the external wires (see Section 4.1.9.3) and the LS - Model Riser was ready to fill with UNIVIS BIO 40. The pump system was attached to the T Section and a first attempt was made to fill the pipe. However, as previously mentioned, the clamp joint was leaking. The T Section then had to be removed from the pipe causing the cables to have to be cut, the extended male end piece was put in place, the cables were spliced again and the T Section was reassembled with muffler clamps on the outside of the pipe.
15. At this point, the weather again became an issue, as a snowstorm occurred and stopped work on the project for two days. When the storm had stopped and work was able to continue, other obstacles were found to have occurred. The tent, which was supposed to protect the top end of the riser, had fallen in the storm with the end of the pipe still inside.



Figure 49: The Tent After The Storm

This not only meant that an extra day was needed to dig out the tent but since the storm had torn the tent roof and bent many of the poles, it was unable to be put up

again which meant the work had to again be completed unsheltered in the cold.



Figure 50: After The Storm - Unsheltered Work Setup

16. Another issue caused by the storm was that a plow had cleared an emergency exit behind IOT where the pipe was laid out. This meant that the plow had run over a section of the pipe.



Figure 51: The Buried Pipe Uncovered by a Snow Plow

It was not known if this, or the storm, had caused any damage to the pipe or the instrumentation inside. However, two days after the storm, a warm front occurred causing the weather to change to rain, which melted all of the snow. The LS – Model Riser was then tested, and luckily the storm and plow appeared to have caused little or no damage, other than delaying the project for a number of days.

17. The pump system was again attached to the T Section and the pipe was filled with UNIVIS BIO 40. In order to ensure there were little or no air bubbles in the pipe, two men held the pipe at waist level, starting at the end where the pump was attached and walked slowly along the length of the pipe, shaking it as they went. If any air was caught in the system, it would have been shaken loose and floated to the top of the oil. The opposite end of the pipe, where the pump was not connected, was slightly elevated, so all of the air would naturally seek the highest point and escape from the system. The valve was then closed and the handle

removed to ensure the oil could not escape from the T Section once the pipe was filled.

18. The PVC plug was then slid inside the pipe with the wire rope crimped off at the end to anchor itself inside the pipe. The end of the pipe was then capped using common plumbing fittings and the wire mesh grip was fitted over the end to complete the bottom section.

19. The dummy section was assembled by attaching an extended male end piece, similar to the one used to stop the leak in the T Section, to the end of an empty section of pipe. Muffler clamps were again used to strengthen this joint and make it watertight. At the other end, the PVC plug was inserted into the empty pipe, and it was then capped and the wire mesh grip was fitted over the end, completing the dummy section.

20. At the top end, the plastic fitting to allow the pump system to be connected to the T Section was removed and the dummy end was attached to complete the top section.

This completed the assembly of the LS – Model Riser.

6 Testing VIV with the Large Scale Model Riser

The actual VIV testing with the LS – Model Riser was done on December 15, 2006 off the coast of St. John's, Newfoundland. The LS – Model Riser was fully assembled, calibrated and ready for testing on December 10th, was loaded onto the vessel on December 11th, and tested on December 15th.

6.1 Calibrating the LS - Model Riser

The first step in testing the LS – Model Riser was to calibrate the modules. The calibration was necessary to find the positions of each of the modules inside the pipe relative to each other. If the initial position of the modules is known, the data acquired can then be adjusted for any off centered or tilted modules. It was felt that when all of the instrumentation and the UNIVIS BIO 40 were inside the sealed pipe, there would be little or no movement of the modules afterwards. Therefore, to calibrate the LS – Model Riser, two samples of data were taken for 3 minutes while the model was lying flat on the ground, as straight as possible. The IPEX pipe itself has a gold stripe that runs along the entire length of the pipe, and it was ensured that the stripe was in the same position, that is it was running along one side of the pipe, to get this “0 degree” data sample. The pipe was then turned 90 degrees, by attaching large pipe wrenches along the length and physically turning it until the gold stripe was 90 degrees from the initial position. Two 3 minute samples were again taken to get a “90 degree” data sample.

6.2 Transporting the LS - Model Riser

Transporting the LS – Model Riser was not a trivial task, as the length and weight were significant. Also, the steel spherical buoy and the railway wheel were also heavy and large, and therefore a boom truck had to be hired to transport the complete system. First, the LS – Model Riser had to be manhandled into a loose coil on the ground before it could be lifted by the crane and onto the truck. Four men were required to pick up the LS – Model Riser and walked with it section by section until it was in a coil.



Figure 52: The Coiled LS - Model Riser

A large weight scale was attached to the crane beforehand to get the final weight of the completed LS – Model Riser and then the coil was then lifted onto the boom truck and secured to the bed of the truck for transport. Figure 53 to Figure 57 show the process of lifting the model and placing it on the truck.



Figure 53: Lifting the Coiled LS - Model Riser



Figure 54: Laying the LS - Model Riser on the Truck



Figure 55: Securing the LS - Model Riser to the Truck



Figure 56: LS - Model Riser Secured to the Boom Truck

The boom truck then picked up the spherical buoy and the railway wheel, and transported everything to the vessel.



Figure 57: Truck Loaded with Buoy, Railway Wheel and LS - Model Riser

Once the truck arrived at the vessel, the buoy and railway wheel were lifted in over the aft section of the vessel and secured on deck.



Figure 58: Sphere Buoy Being Lifted On Board

The LS – Model Riser was lifted in over the starboard side of the vessel alongside the pier, as shown in Figure 59 and Figure 60.



Figure 59: LS - Model Riser Being Lifted In Over the Starboard Side



Figure 60: LS - Model Riser Being Lifted In Over the Starboard Side

The equipment was secured on board the vessel, and testing was ready to begin.



Figure 61: Equipment On Board the *Miss Jacqueline IV* Ready for Testing

6.3 Test Setup

The overall test setup can be seen in Figure 62.

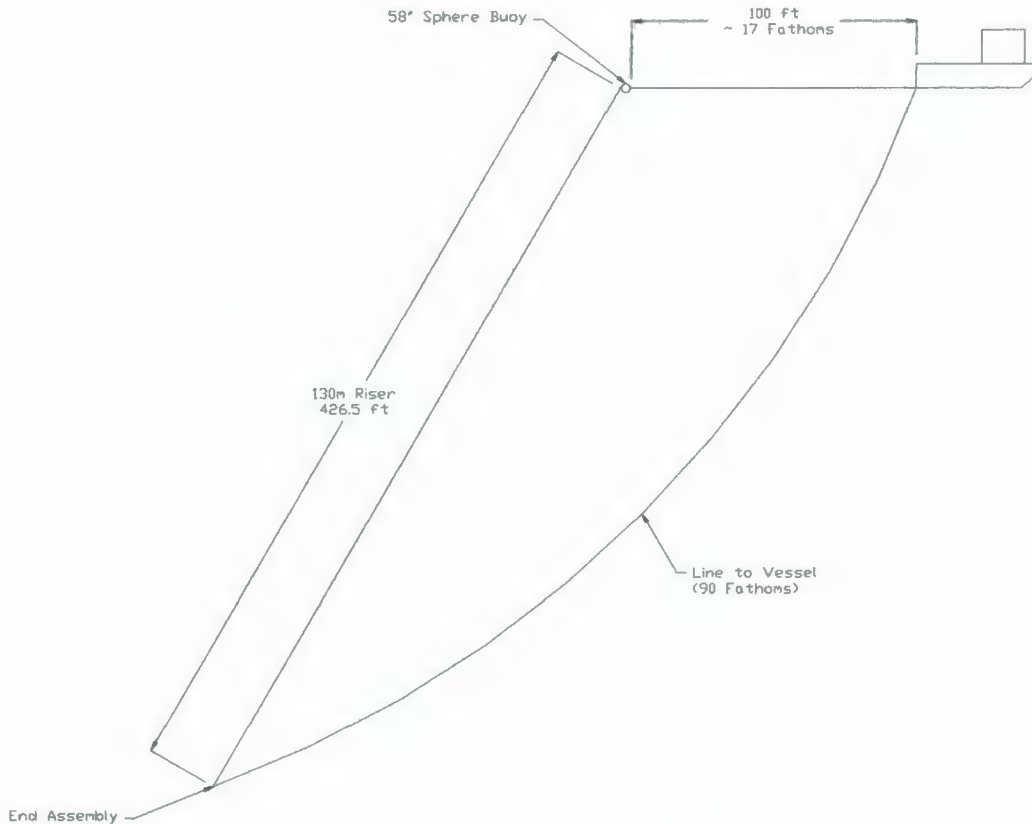


Figure 62: Test Setup

The vessel towed the spherical buoy approximately 100 ft behind its stern to ensure the wake had little or no affect on the current the LS – Model Riser encountered. The buoy was attached to the winch line of the vessel at one end and the LS – Model Riser at the other end, both with a 5/8" shackle. At the bottom end, the LS – Model Riser, the railway wheel and an additional winch line were all attached to a triangular steel

separation plate, also with 5/8" shackles. This bottom end assembly can be seen in Figure 63.

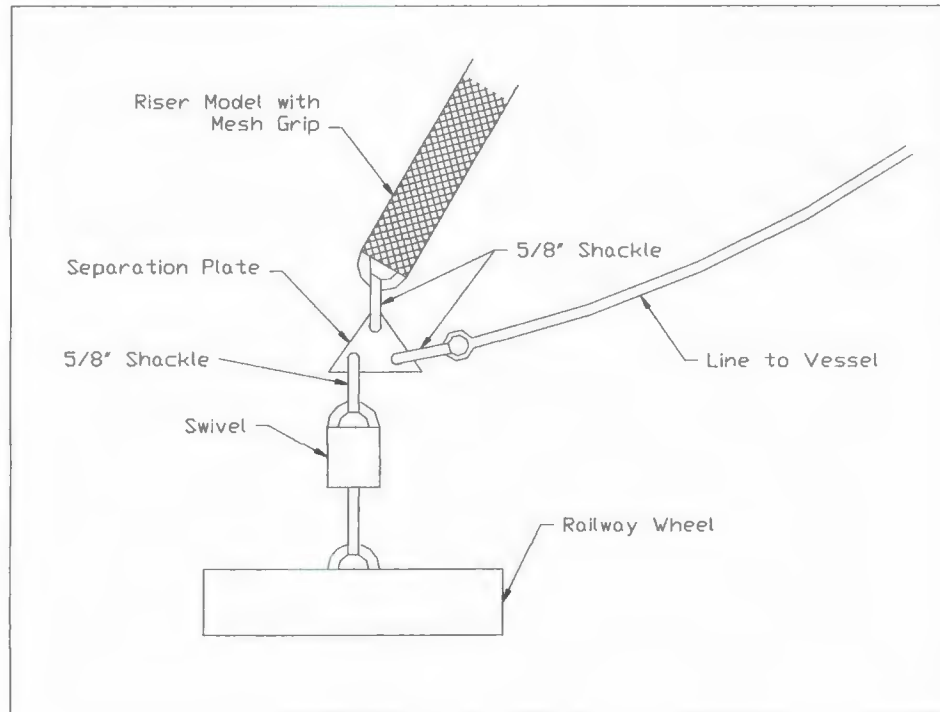


Figure 63: End Assembly Sketch

6.3.1 Test Vessel - *Miss Jacqueline IV*

The vessel used for testing was the *Miss Jacqueline IV*, a local 65' fishing vessel, owned and operated by Mr. Frank Hutchings.



Figure 64: Miss Jacqueline IV

6.3.2 Test Plan

The tests were carried out by keeping the length of the anchor line constant and varying the current speed. The sampling rate was held at a constant 15 hertz and data was sampled for 3 minutes after a steady state speed had been reached. At each speed, two 3 minute samples were taken to give some repeatability to the tests and to catch any irregularity that might occur. Table 8 lists the run number and current speed for an anchor line length of 165m, or 90 fathoms, for each test case that was carried out.

Run #	Current Speed (m/s)	Current Speed (knots)	Anchor Line Length (fathoms)
1	0.15	0.3	90
2	0.45	0.9	90
3	0.75	1.5	90
4	1.05	2.0	90
5	1.25	2.4	90
6	0.9	1.7	90
7	0.6	1.2	90
8	0.3	0.6	90
9	1.35	2.6	90
10	1.45	2.8	90
11	1.5	2.9	90
12	1.4	2.7	90
13	1.3	2.5	90

Table 8: Test Plan

6.4 Test Day

As mentioned, testing took place December 15, 2006 off the coast of St. John's, Newfoundland in a natural trench called The Cordelia Deeps. As the LS – Model Riser was loaded onto the vessel on December 11th, testing was scheduled for December 12th. However due to strong North Easterly winds, the captain of the vessel delayed testing for a number of days. North Easterly winds in Newfoundland are very harsh and cold, and cause a large swell to occur. As well, the spray from the ocean would have been instantly frozen onto the deck of the vessel, causing very slippery and dangerous working conditions. Therefore, it was decided to wait until the wind either died down or changed direction to commence testing. On December 15, 2006, the winds finally subsided enough to make testing safe. The test group gathered on Pier 6 at 6:00am and before leaving the pier, the complete system was hooked up and a quick test was done to ensure everything was working properly and all necessary parts were included in the system.

With everything up and running, the vessel left the pier at 7:00am and reached the The Cordelia Deeps approximately an hour later and the testing began.

The top section of the LS – Model Riser and two winch lines, one to lift the buoy overboard and another to attach the buoy to the vessel while being towed, were attached to the buoy with 5/8” shackles.



Figure 65: Buoy Attachment Details

The buoy was then lifted over the aft of the vessel and the lifting winch line was removed before lowering it completely into the water. This extra winch line enabled the crew to have more maneuverability of the buoy and was not needed after the buoy had been lifted cleared of the aft of the vessel.

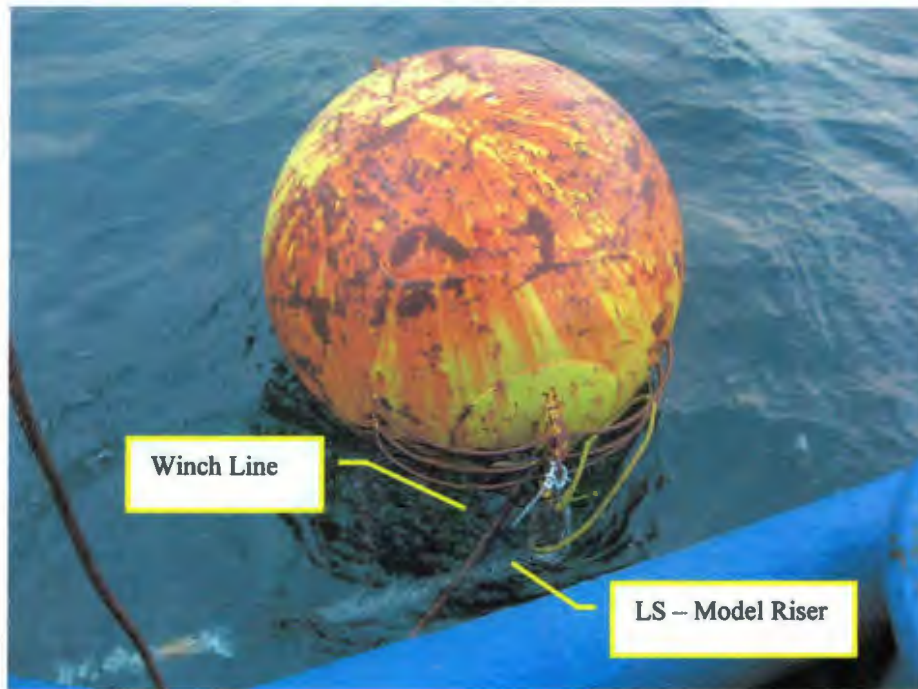


Figure 66: Buoy Lowered Into The Water

The buoy was then winched out approximately 60 feet behind the vessel. This distance, originally 100 feet, was shortened because the CAN Bus cable had to be previously cut in the assembly of the model and only enough remained to tow the buoy at 60 feet. This was not a problem, due to the fact that as previously mentioned, the LS – Model Riser ended up being not instrumented in the top 25m. Therefore it was felt that the small amount of wake that the riser was exposed to at 60 feet behind the vessel would not reach the portion of the model that contained modules. As the buoy was being winched out, the power and CAN Bus cable were attached to the winch line using wire ties, as can be seen in Figure 67.



Figure 67: The Buoy Towed at 60' Behind the Vessel

The bottom section of the LS – Model Riser was then attached to the triangular separation plate that was attached to the swivel and railway wheel and the extra winch line, as shown in the end assembly sketch, Figure 63. The LS – Model Riser was then lowered over the aft of the vessel by hand until the entire length was overboard. This can be seen, along with the end assembly, in Figure 68.

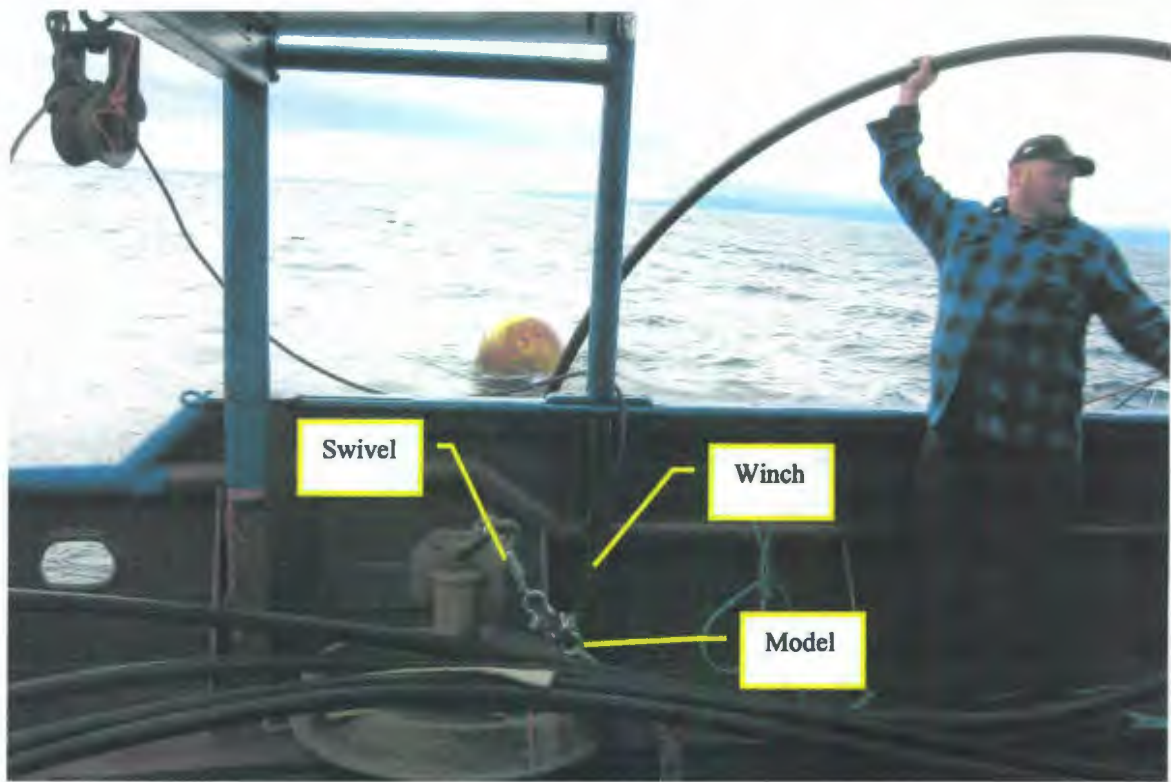


Figure 68: Lowering the LS - Model Riser Overboard

Once the complete LS – Model Riser was in the water, the winch line on the railway wheel was used to lift it overboard and lower it slowly so that no stress was placed on the model.



Figure 69: Lifting the Railway Wheel over the Side



Figure 70: Lowering the Railway Wheel into the Water

At this point, the LS – Model Riser was completely in the water and the launch was complete. Testing then started by setting the vessel speed at 0.15 m/s for Run 1 and two x 3 minute data samples were taken. Vessel speed was then increased to 0.45 m/s for Run 2 and another two x 3 minute data sample was taken. The location/speed of the vessel was measured using the onboard GPS. The vessel speed was then increased to 0.75 m/s and a problem was discovered when trying to obtain a data sample. It could be seen on the oscilloscope that the bundles of data were cutting in and out and were only being received by the computer in a very random and inconsistent way. This indicated that there was a faulty connection or a break somewhere along the length of the CAN Bus cable, causing the flow of data to be disrupted. To troubleshoot this problem, all connections were checked between the computer and the LS – Model Riser, which was found to not be the problem. It was decided that the buoy would be winched into the vessel, as shown in Figure 71, and the CAN Bus cable would be visually inspected.



Figure 71: The Buoy Winched into the Vessel

It was then discovered that the CAN Bus cable had gotten caught between the buoy and one of the shackles causing the cable to become worn. The location where the shackle caught the CAN Bus cable and the worn cable can be seen in Figure 72 and Figure 73.

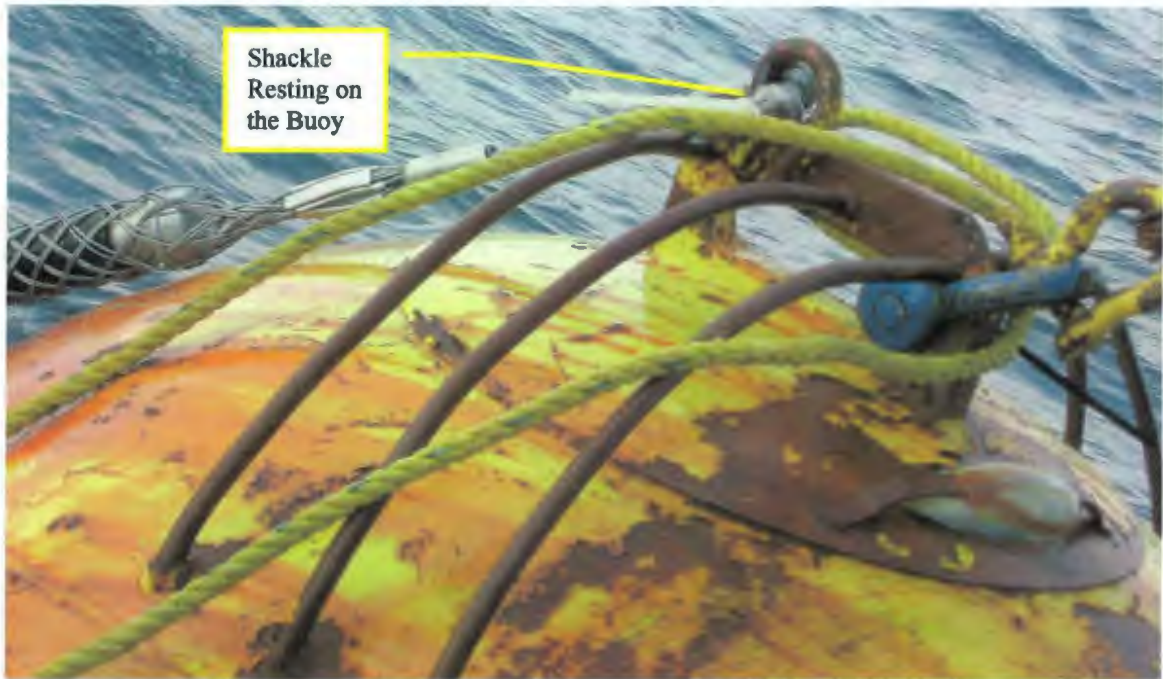


Figure 72: Location of Shackle Causing the CAN Bus to Wear



Figure 73: Worn CAN Bus Cable

The cable, although worn, did not appear to have any damage done to the actual core of the wire, only to the surrounding insulation. Therefore, using a voltmeter, the wire was tested and again was found to not be causing the problem, but since the cable was damaged, it could not be put back out into the ocean even if the problem was finally resolved. It was finally felt, after all other options were exhausted, that when the CAN Bus cable had gotten caught under the shackle, it must have caused the cable to pull and

finally break where it entered the T Section. If this is not the problem, the CAN Bus cable must be broken inside the pipe somewhere. Either way, this problem could not be fixed on the vessel. Therefore, no more data could be gathered and the testing was completed.

The buoy was kept winched tight to the vessel and the railway wheel was slowly winched back and taken onboard. The LS – Model Riser, which was close to neutrally buoyant, was then pulled onto the vessel by hand and coiled on deck as shown in Figure 74 to Figure 76.



Figure 74: Starting to Pull the LS - Model Riser on Board



Figure 75: Pulling the LS - Model Riser on Board



Figure 76: Securing the Completely Coiled LS - Model Riser

The vessel then returned to the Pier at approximately 2:00pm, concluding the Large Scale VIV Testing.

6.5 Accelerometer Data Collected

The 130m long LS – Model Riser was to be outfitted with 65 modules along its length, spaced at a distance of 2.0m. Due to problems during assembly, which are described in detail in Section 5, some of the modules were damaged and only 55 were able to be installed inside the model. As well, assembly issues also meant that the modules that remained were placed at a spacing of 1.9m. The final module locations can be seen in Table 7. Out of the remaining 55 modules placed in the LS – Riser Model, 27 data channels, or sensors, were “dead”, or failed to read data properly when the model was completely assembled. Figure 77 shows the working and dead sensors along the length of the LS – Riser Model once it was complete.

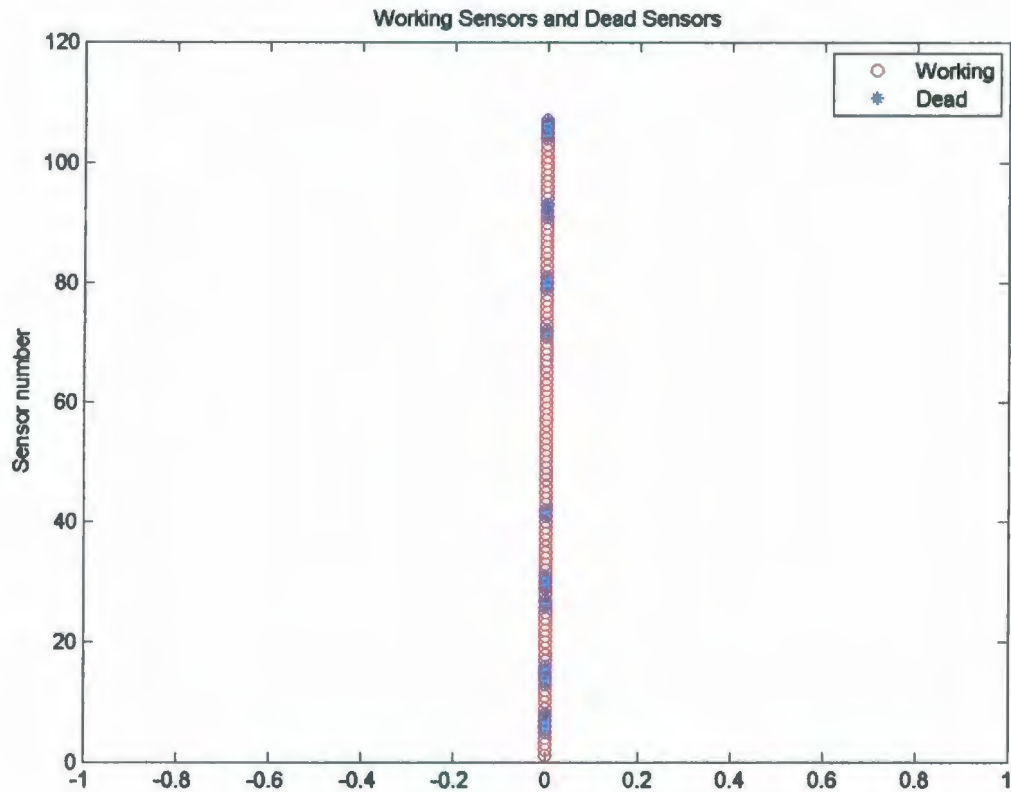


Figure 77: Working and Dead Sensors

Of the 55 modules in the LS – Model Riser, 52 of them were accelerometer modules outputting 2 channels of data each (the acceleration along the axis of the model was not measured to simplify the data acquisition requirements) and 3 of them were full modules outputting 11 channels of data each (the 2 channels of accelerometer data plus 3 channels for the rate sensor and 6 channels for the magnetic sensor). This gave a total of 138 sensors that were installed in the model. Allowing for the 27 “dead” sensors, a total of 111 working sensors were recording data in the model during testing.

Low accelerometer numbers is often a problem when trying to yield high quality, full-scale data from VIV tests [25]. As mentioned, the accelerometer number should be high enough to resolve the mode shapes of the vibration, yet typically, models only have

enough modules to map the lowest mode shapes of risers in shallow water.

Accelerometer modules, however, are quite expensive and fragile, and will drive up the cost of experiments, making a large number of them unattractive to most researchers. By buying the accelerometers in bulk, the cost was kept to a minimum for this project.

For the LS – Model Riser, it was felt that the large drop out rate was unfortunate, but due to the fact that working modules were still located along the entire length of the model, it could still yield useful data and testing was carried out with the remaining working modules.

Four runs were obtained before the LS – Model Riser experienced problems and the testing had to be stopped. Run 1a and 1b were two 3 minute samples at a current speed of 0.15 m/s, and Run 2a and 2b were two 3 minute samples at a current speed of 0.75 m/s. The runs were done twice to ensure their repeatability and that each data set was a good representation of the LS – Model Riser behavior at that current speed. As described previously in Section 6, the LS – Model Riser experienced damage during testing which resulted in these runs being the only data collected on test day.

After the completion of this project, further work, [29] and [30], was completed on the LS – Model Riser and it was rebuilt based on the lessons learned and the recommendations made in this report. Also, the LS – Model Riser was later tested successfully for a range of current speeds and Reynolds numbers, which would not have been possible without the ground work laid by this project.

6.6 Data Analysis

The full analysis of the data acquired during the test was not part of the scope of this research. The purpose of this report was to design, build and run initial tests on a large scale model riser. The information and experience gathered here will be passed on so that others in the VIV Research Group at Memorial University can learn from any knowledge accumulated and either fix the current LS – Model Riser or build another similar system to finish testing at a large range of current speeds. However, the data acquired was analyzed to some extent to determine if it was useful and whether the model could be used in further VIV analysis.

A number of Matlab routines were used to carry out five main computations and plot information regarding the VIV characteristics of the LS – Model Riser. A few of the resulting plots will be presented here to show that the data collected was useful and the instrumentation and design of the LS – Model Riser can be used as a basis for further VIV testing, as can be seen in the further work done [29].

The first computation was to calculate the vibration displacements from the measured accelerations in the in-line and cross-flow directions. Examples of the resulting plots are given in Figure 78 to Figure 81.

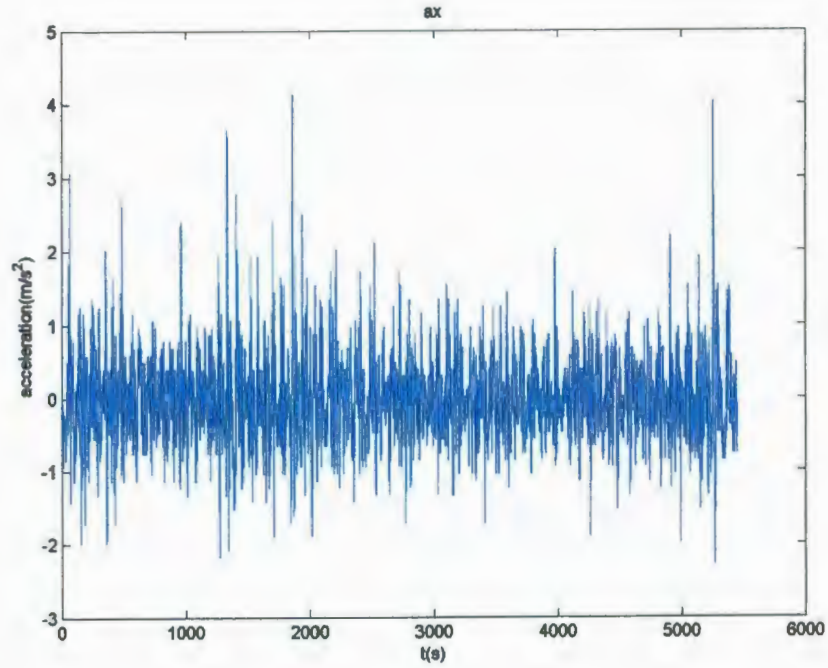


Figure 78: In-Line Acceleration Time History – Node 53 – Current Speed 0.75 m/s

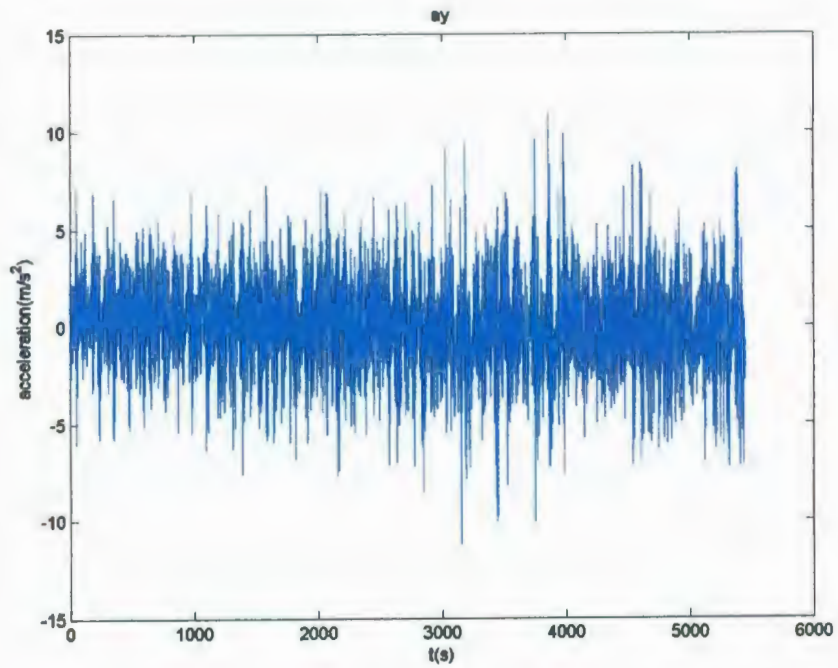


Figure 79: Cross-Flow Acceleration Time History – Node 54 – Current Speed 0.75 m/s

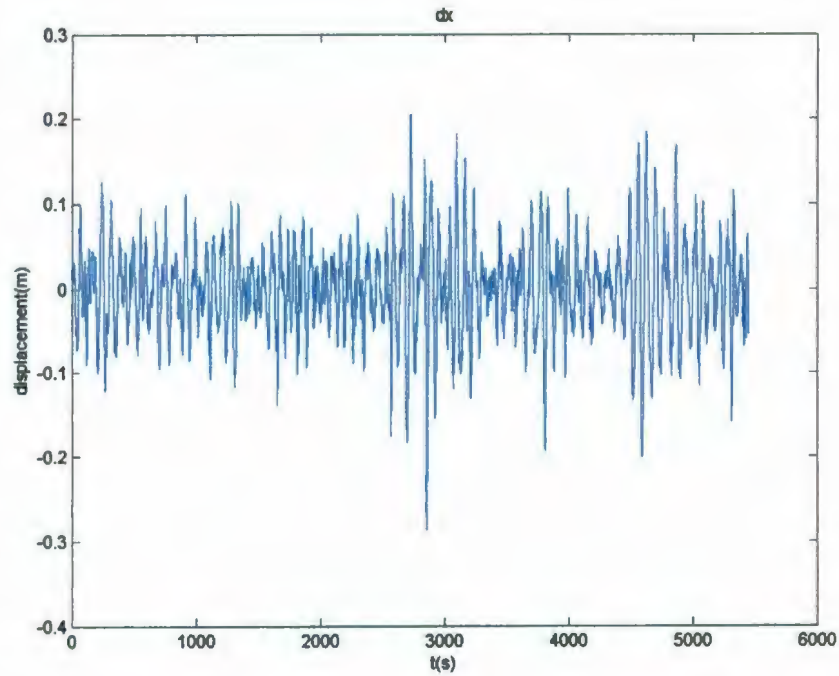


Figure 80: In-Line Displacement Time History – Node 58 – Current Speed 0.75 m/s

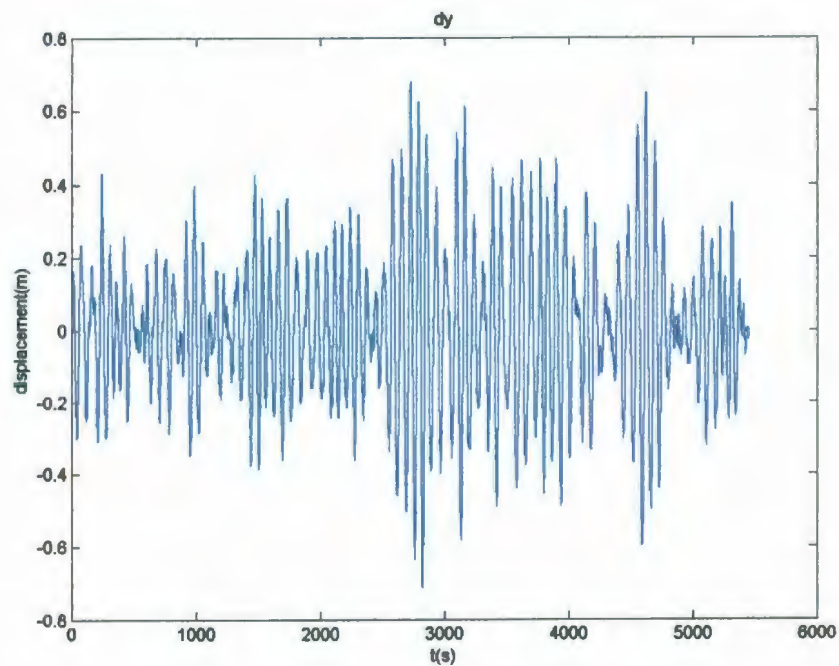


Figure 81: Cross-Flow Displacement Time History – Node 90 – Current Speed 0.75 m/s

The second computation was to calculate the average peak pick-up amplitude and frequency versus reduced velocity in the in-line and cross-flow directions. The non-dimensional amplitude is defined as the amplitude of vibration divided by the outer diameter of the pipe. The non-dimensional frequency is the frequency of vibration divided by the Strouhal frequency from a stationary cylinder at the same Strouhal number. Examples of the resulting plots are given in Figure 82 and Figure 83.

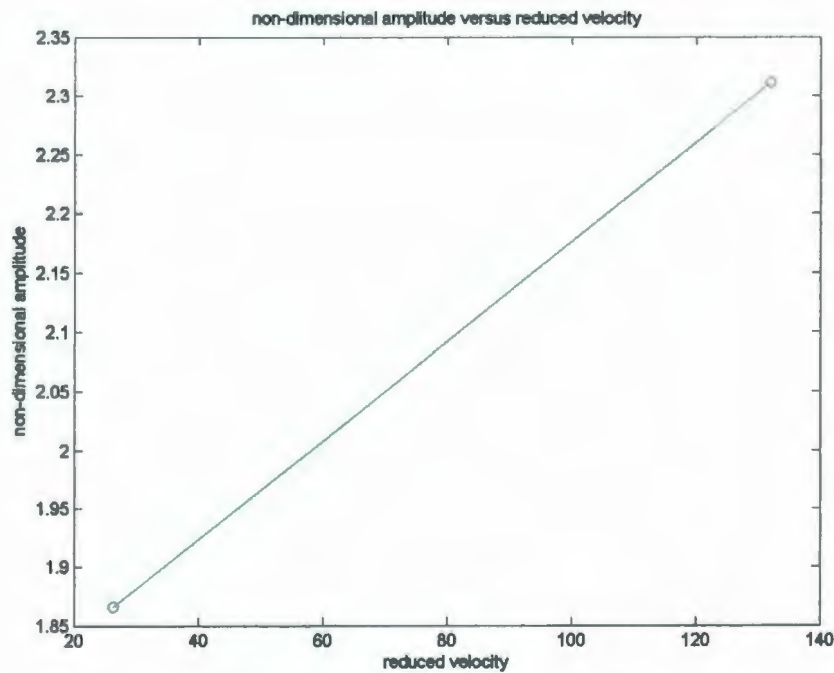


Figure 82: In-Line Amplitude vs. Reduced Velocity

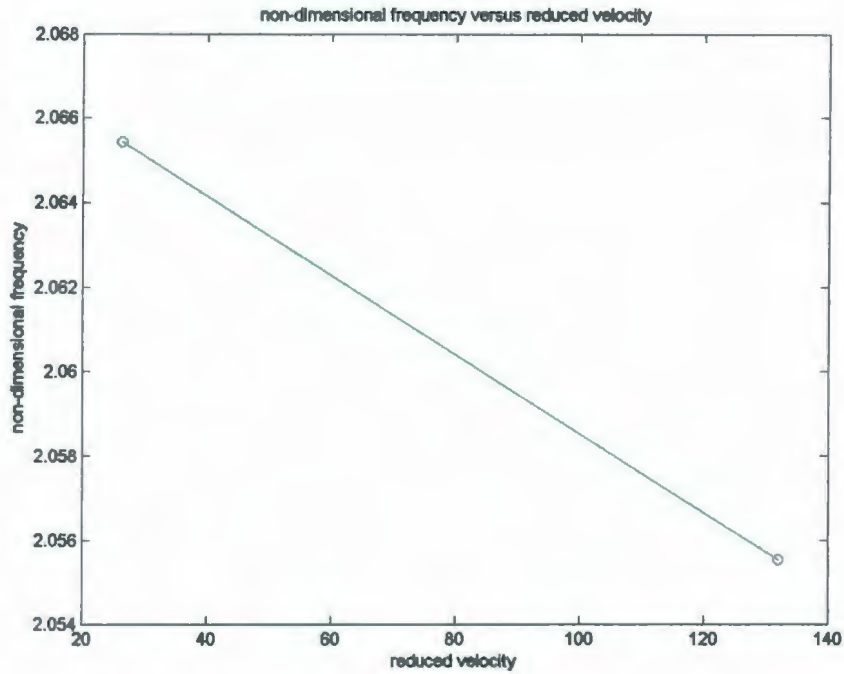


Figure 83: In-Line Frequency vs. Reduced Velocity

The third computation was a modal analysis of the data. The modal component time histories in the in-line (in the direction of the current) and cross-flow (in the direction perpendicular to the current) directions were calculated for up to 25 modes. Examples of the resulting plots are given in Figure 84 to Figure 87.

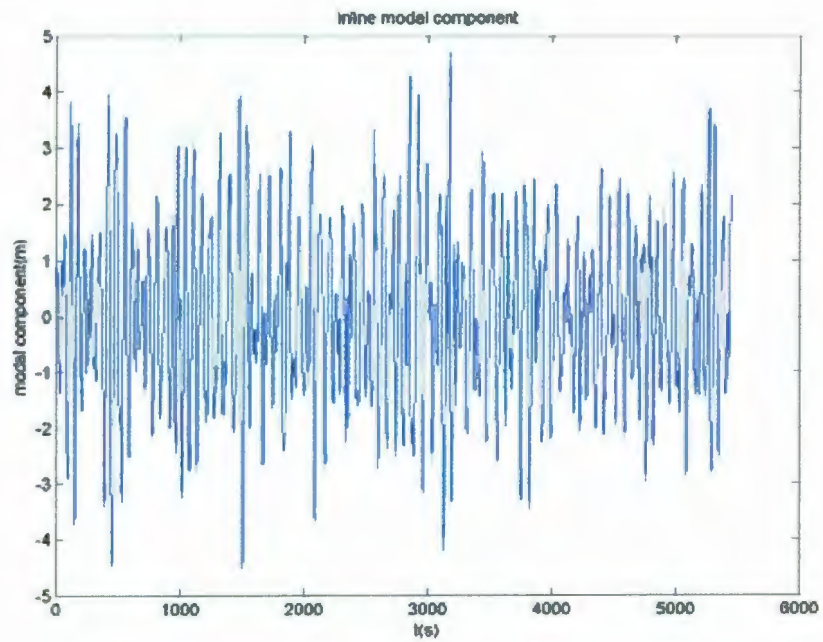


Figure 84: In-Line Modal Component Time History - Mode 1

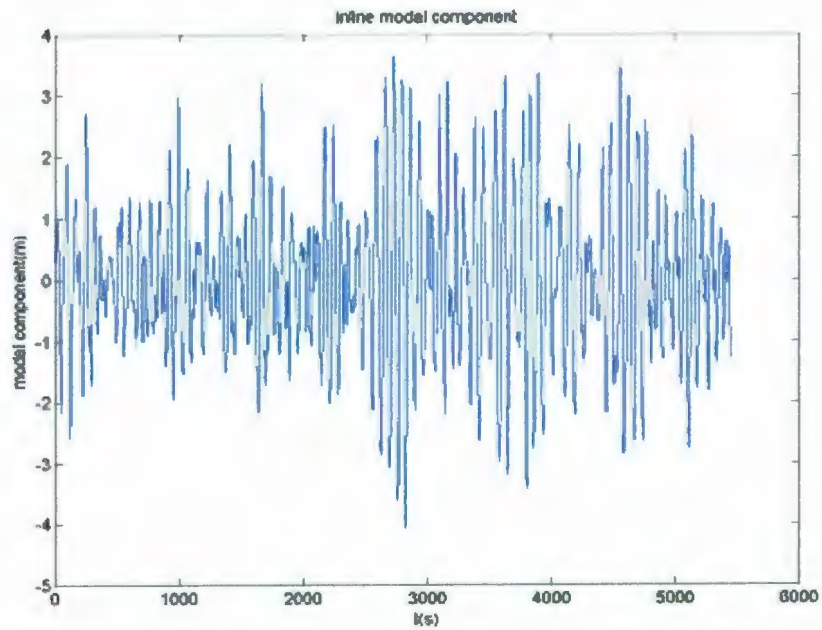


Figure 85: In-Line Modal Component Time History - Mode 25

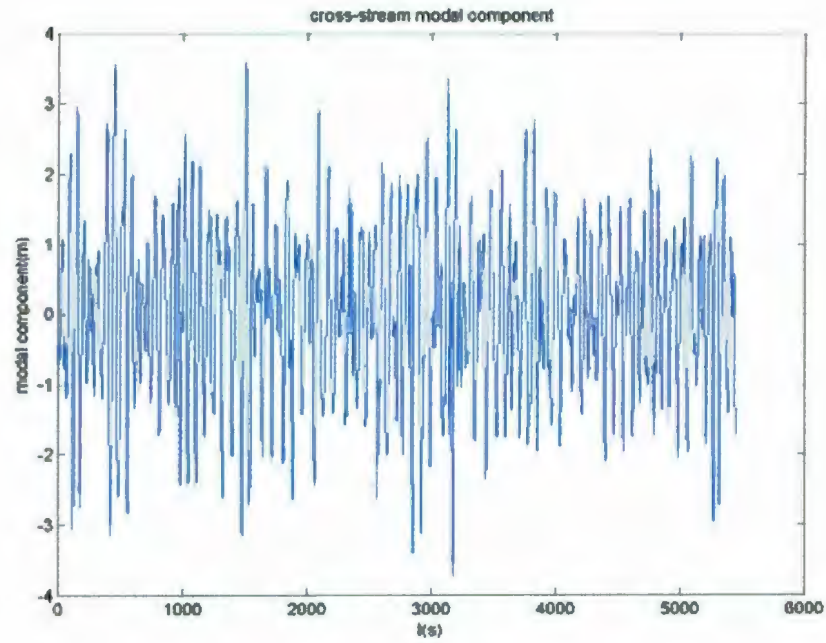


Figure 86: Cross-Flow Modal Component Time History - Mode 1

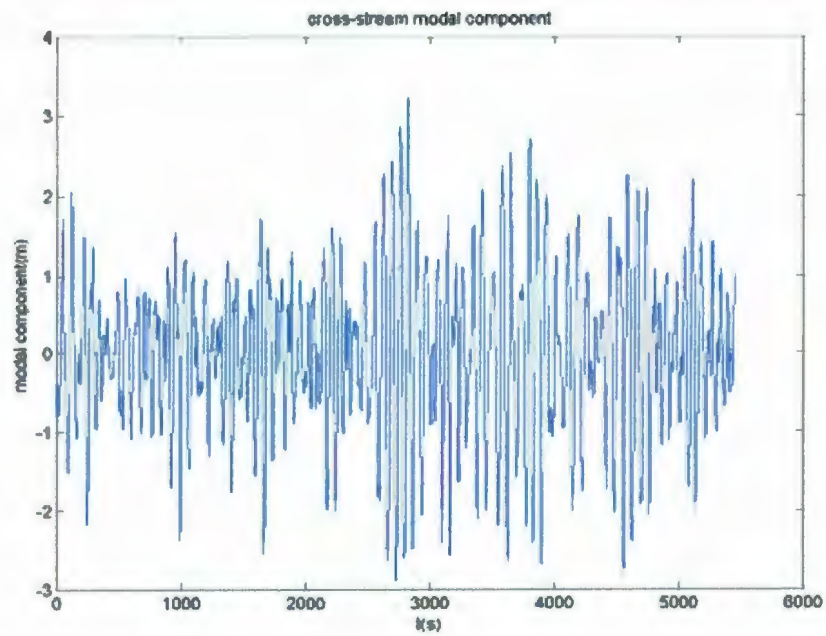


Figure 87: Cross-Flow Modal Component Time History - Mode 25

The fourth computation was a spectral analysis which calculated the spectra of displacement at each location for the in-line and cross-flow directions. An example of the resulting plots for one location along the LS – Model Riser are given in Figure 88 and Figure 89.

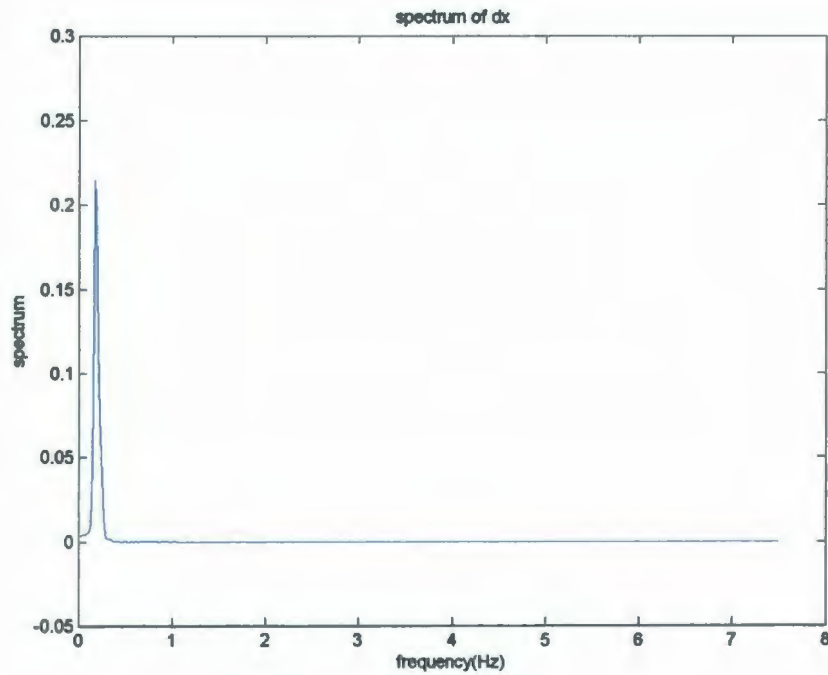


Figure 88: In-Line Displacement Spectra – Node 57

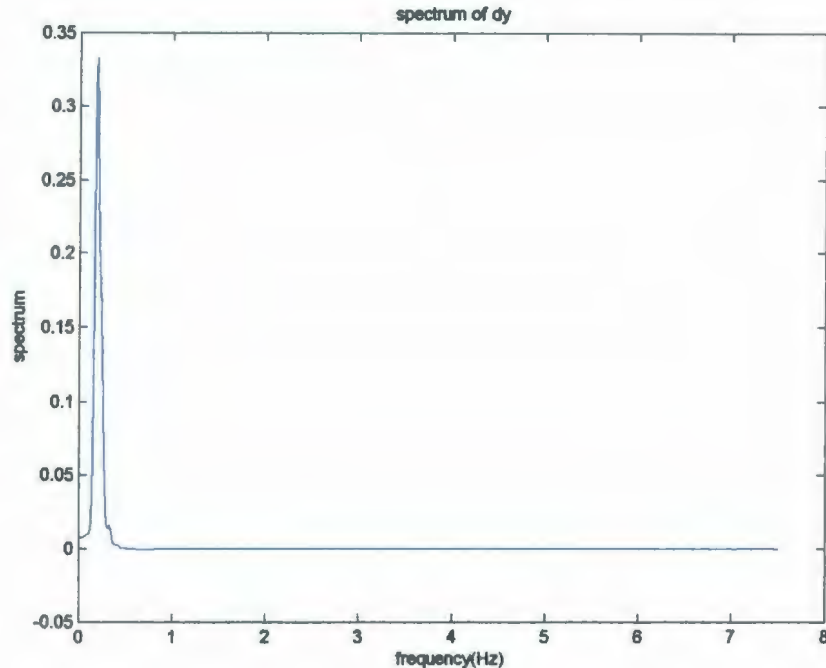


Figure 89: Cross-Flow Displacement Spectra – Node 55

The last computation was to plot the vibration shape and trajectory of the LS – Model Riser. A few examples of the resulting plots are given in Figure 90 to Figure 92.

It can be seen that the trajectories are not following the expected figure “8” shape for cross-flow riser VIV. A possible reason for this is that there were large riser deflections while the LS – Model Riser was being towed. The figure “8” trajectory is usually seen in rigid cylinder VIV simulations, where the riser mean C_d is independent of the riser elevation [26]. A more complex movement occurs when the mean C_d also depends on the riser elevation. When there are large riser deflections, a small change in drag can cause the deflections to fluctuate causing the figure “8” trajectory to be destroyed.

However, the plots are not completely dissimilar to a figure “8” shape. If the run times were extended and given a chance to reach steady state the trajectory may take on the

figure “8” shape, but this is impossible to predict with certainty without further testing. Also, ongoing research on vibration shape and trajectory has shown that other shapes, besides the figure “8” shape, are possible [30].

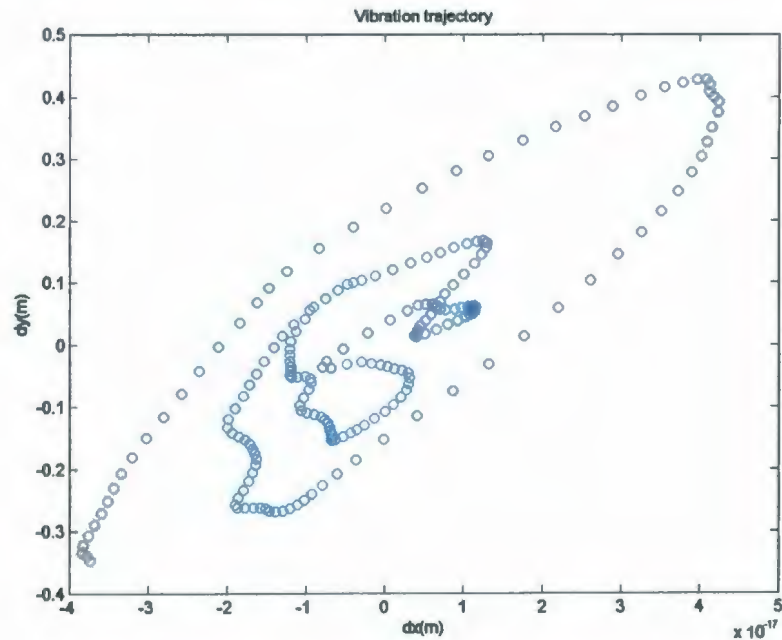


Figure 90: Vibration Trajectory Example 1 – Node 90

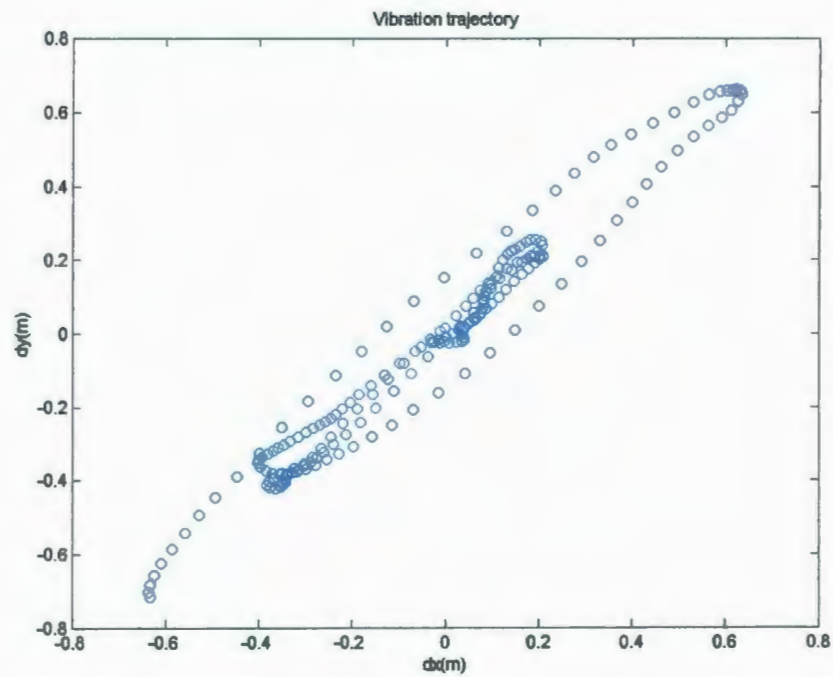


Figure 91: Vibration Trajectory Example 2 – Node 102

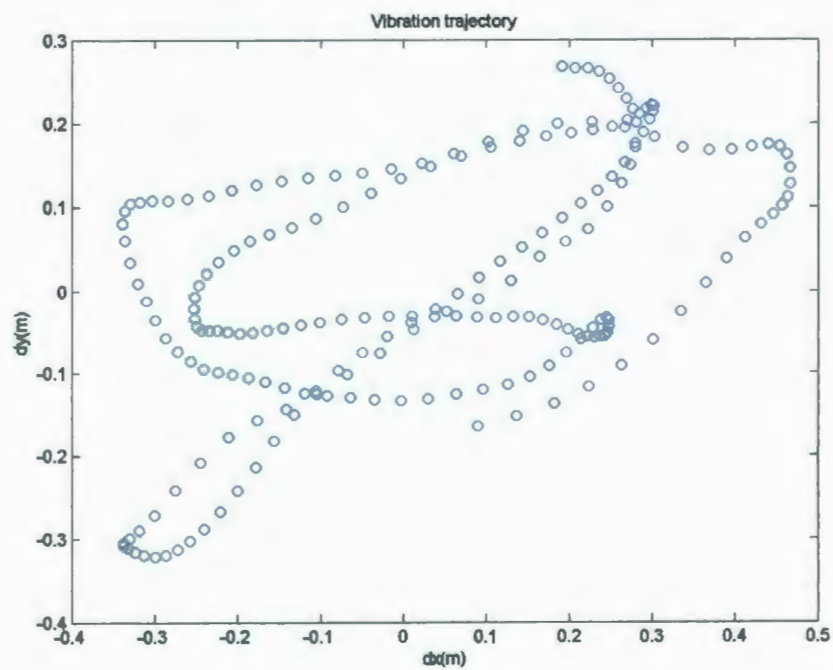


Figure 92: Vibration Trajectory Example 3 – Node 38

7 Conclusions and Recommendations

This section is a summary of the knowledge gathered throughout the design, assembly and testing process. All of the recommendations made throughout this thesis are summarized and final conclusions are drawn regarding different aspects of the project.

7.1 Design Process

The following conclusions and recommendations have been developed through the design process of this project.

- All of the parts and materials used in the LS – Model Riser were chosen to withstand the highest tension of 10,000 N and maximum tensile stress of 6.0×10^6 Pa for the maximum current speed of 1.5 m/s. These values, found using the “IOT Riser Dynamics Code”, were felt to be a good estimate of the complex real life system. With further analysis, higher current speeds may be possible, and in turn, higher mode numbers achieved.
- From the numerical analysis, it was shown that at the maximum current speed of 1.5m/s, a Reynolds number of 68,000 and a maximum mode number of approximately 25 could possibly be achieved by the LS – Model Riser. Due to difficulties during assembly and testing, a sample of data at this maximum current speed was not obtained to verify that these maximum mode numbers were achieved.

- It has been shown, both numerically and by testing, that due to its large length, the bending stiffness of the LS – Model Riser will not greatly affect the resulting vibration. For completeness, additional testing should be done on a sample of the riser model that includes not only the pipe but all model parts, such as the cables and the hydraulic oil, to determine the exact bending stiffness of the overall model. This was completed in conjunction with future work carried out on the LS – Model Riser in [29].
- Once a fully functional large scale riser model has been developed, other areas of VIV research could be explored, such as fatigue and buckling analysis, various realistic catenary shapes and vibration suppression devices.

7.2 Assembly Process

The following conclusions and recommendations have been developed through the assembly process of this project.

- The pipe that was used for the body of the model riser was IPEX Pipe with the Stripe – 160 Series Gold Stripe, a flexible, durable and light weight polyethylene plumbing pipe. This material was chosen as the body of the riser model because:
 - The extremely smooth interior walls allow for the least resistance when pulling the accelerometer units and wiring through the pipe.
 - It is weather resistant in that it has a unique formulation that protects the pipe against excessive ultraviolet rays.

- The Gold Stripe was specifically chosen because it had the highest pressure rating, 160 psi, of all the IPEX pipes considered. This pressure rating will increase by a factor of 1.5 when used at a temperature of 0 degrees Celsius, yielding a test pressure rating of 240 psi.
- The empty pipe was light weight: approximately 1.5 kg/m. This allowed for easy manipulation and placement of the pipe before and during the assembly process.
- The pipe is chemically resistant, which is important due to the fact it was filled with hydraulic oil and permanently capped at both ends.
- The pipe was available in a nominal 2 inch diameter (outer diameter = 0.053m, inner diameter = 0.040m) which was comparable to initial diameter estimates to achieve a maximum mode number of between 20 and 30.

As mentioned, the IPEX pipe pressure rating will increase with decreased temperature and inversely, decrease with increased temperature. If further testing is to be done in the spring or summer, the water temperature around Newfoundland could be relatively warmer than those during testing in December. Therefore, thought should be given to the temperature that the pipe will experience during testing and how this may reduce the pressure rating of the pipe.

- The 160 Series Gold Stripe IPEX pipe is quite specialized and expensive and is only available in 200 and 500 foot coils. A sample of the pipe was not available for strength testing, however, the Blue Stripe 100 Series (rated for 100 psi) was

available and therefore testing was done on a sample of this Blue Stripe pipe. To test the strength of the pipe a common tension test, using ASTM Standard samples made from the wall of the pipe and an automatic tension machine, was performed by stretching the samples at a constant rate until fracture. From the data obtained, the stress and strain were calculated, and stress versus strain curves were developed. The Blue Stripe pipe (outer diameter = 0.053m, inner diameter = 0.040m) was found to have a breaking load of approximately 7,400 N with a resulting modulus of elasticity for the pipe of 4.71×10^7 Pa. The Blue Stripe pipe did satisfy the criteria for testing and therefore, the Gold Stripe pipe, which should be much stronger, was acceptable to use as the body of the LS-riser model. When the Gold Stripe pipe was received, a final test was done to a sample by applying 14,000 N to the pipe, which established that the strength of the pipe was indeed strong enough to withstand the estimated 10,000 N tension in the pipe during testing.

- There were two different modules containing instrumentation used in this experiment, an accelerometer module and a full module. Originally, there were 61 accelerometer modules equipped with a three-axis accelerometer on each to record voltage data that was transferred into acceleration data in the in-line and cross-flow directions. The accelerometers, Analog Devices ADXL330, measured a minimum full-scale range of $\pm 3g$'s, and their small profile of 4mm x 4mm x 1.45mm made them attractive from the point of view of trying to fit the entire system inside a small diameter pipe. There were 4 full modules which each

contained an accelerometer plus an additional rate sensor and magnetic sensor. The rate sensor (gyroscope), Analog Devices ADXRS300, had an output of voltage that could be transferred into angular rate and a reference and temperature to be used for temperature compensation when analyzing the data. This chip was also attractive due to its small size of 7mm x 7mm x 3mm. The magnetic sensor, Honeywell HMC 2003, measured the strength and direction of an incident magnetic field along its length, width and height to provide compass heading and attitude. When assembling modules, it is safe to design for a failure rate of approximately 10 %. Therefore, if some modules do not function properly there are still enough to maintain the 5 modules/cycle design

- It was unknown how the components in the modules would stand up against the pressure of being 150m underwater, therefore, two sample modules were created and tested in the Marine Institute Pressure Chamber. Both modules were coated with epoxy, and then one of the modules was placed inside a sample of the IPEX Gold Stripe pipe which was filled with oil and capped at both ends. The samples were tested at a pressure equal to a water depth of 200m and were found to be functioning properly afterwards. The LS – Model Riser is 130m in length, less than the test 200m water depth, therefore, the pressure at this depth is not expected to influence the modules in a negative fashion.
- The epoxy used to coat the modules was West System epoxy, a high-quality, two part epoxy that will bond to fiberglass, wood, metal, fabrics and other composite materials. It yields superior moisture resistance and high strength and is

especially suited for marine applications. The epoxy coating on each module not only provided protection from the pressure at depth, but also gave each component extra strength, made the modules robust, and protected them against water during installation. Due to these properties, if other modules are produced, it is felt that the epoxy is an invaluable addition to the design of these components.

- The internal set of wires in the LS – Model Riser was used to connect each module to one another. It consisted of one CAN Bus cable, Co-ax RG174/U, a group of 4 power cables, Conductor Submersible Cable, 10 Gauge and one power and one ground wire, Type 3051, 22 Gauge. The current design has all modules connected along the same CAN Bus cable in series. Therefore, if there is a break anywhere in the cable the entire system will stop working from the break point onwards down the riser. In future models, if the modules are connected to four networks in parallel, and one cable breaks, only every fourth module will be lost. This would make the system as a whole much more robust. In the further work, [28] and [29], a category 5 (cat5) network cable which consists of four sets of twisted wire pairs was used so that the sensors could be staggered along the communication cable such that every fourth sensor module was connected to the same twisted pair.
- Placement pucks were made from Delron and served a number of purposes within the LS – Model Riser. The outer diameter was made to be slightly smaller than the inner diameter of the pipe so that the pucks would keep the modules in place

fairly close to the center of the pipe while still allowing them to be pulled through the pipe with little friction when lubricated. The inner diameter of the puck was chosen large enough so that the power, ground and communication cables could all fit under the module when mounted, but still allowed for a wall thickness to be large enough to provide ample strength to support the modules. Furthermore, the pucks allowed the modules to be attached to a coated wire rope, which not only held the module in the correct position along the length of the pipe, but also gave a means for the modules to be pulled into the pipe.

- After the instrumentation was pulled through the pipe, it was filled with the hydraulic oil, UNIVIS BIO 40. The oil was required for the following reasons:
 - The LS-model riser was over 130m in length when completed. The setup required the model to be hung from a steel sphere buoy behind a ship. This meant that at the bottom, the riser saw approximately 200psi of hydrodynamic pressure from the ocean with the pipe itself being rated to only 160 psi. Since there was no evidence to ensure that when testing at 0 degrees Celsius the decrease in temperature would in fact increase the rating of the pipe, it was felt that the pipe could not be assumed to be strong enough to withstand the 200 psi pressure from the ocean. The oil provided extra strength to withstand the hydrodynamic pressure that the pipe was subjected to.
 - The oil is a natural insulator which gave protection to the wiring and instrumentation.

- UNIVIS BIO 40 is a non-toxic, biodegradable, vegetable oil based lubricant. If there was a problem and a leak or break in the pipe occurred during the testing, the oil is not harmful to the environment, which is important when testing in a marine situation. As well, when filling the pipe, any spills that occurred were also not an issue.
- The high viscosity of UNIVIS BIO 40 lends itself well to being used as a lubricant when pulling the instrumentation through the pipe.
- The oil has a flash point of 230 degrees Celsius and a pour point of -36 degrees Celsius. After the pipe was filled with the oil, the ends needed to be heated to allow them to be capped properly. The high flash point allowed this to occur without any danger of fire or explosion. As well, the model was assembled outside in the fall/winter in Newfoundland. Although it was cold, with the lowest temperature estimated to be -10 degrees Celsius, the low pour point ensured that it remained workable even in the coldest temperatures experienced.

The oil was a necessity in the assembly of the LS – Model Riser. The addition of the oil to the model when pulling the instrumentation through made the assembly possible and in the event that the system has to be removed from the pipe in the future, it is recommended that the UNIVIS BIO 40 be added at intervals back into the pipe when pulling the instrumentation back through.

- Wire mesh grips, which work by tightening as tension is applied to one end, were chosen as the method to attach the LS – Model Riser to the weight at the bottom

and the buoy at the top. To ensure that the grips worked properly, that they would not slip off of the pipe, and that the plugs were sufficiently strong, a strength test was performed. Approximately 14,000 N in tension was applied and it was found that the grips held, they did not move or slip on the pipe, the pipe did not crush under the force of the grips and the end caps did not move and went undamaged. Therefore, it was felt that the grips, plugs and caps were suitable for use in this project.

- The lack of experience in a field environment was an issue during the assembly of the LS – Model Riser and many lessons were learned. The following conclusions and recommendations are directly related to the assembly in a field environment.
 - Preparation in the lab to expedite the assembly process should be kept to a minimum. Although it is necessary to assemble the completed setup in the lab to ensure everything is functioning properly, any permanent preparation, such as cutting cable lengths or stripping cables, should not be done until assembly in the field. If items have to be prepared beforehand, proper preparation should include allowances to compensate for the fact that field work is never exact. For example, the CAN Bus cables were cut to exact lengths of 2m. When they were connected in the field, it was found that by pulling through the pipe, more cable was needed so that they did not pull or become tight. This would not have been a problem if excess had been supplied originally.

- The lack of indoor working space available to assemble the riser model had many associated problems, the first of which being the weather. The cold weather and the snow storm not only made it a difficult area in which to work, but it also dampened the spirits of the assembly team and put the instrumentation in danger of not functioning properly. It is felt that if this project was done at another time of the year, in the summer or fall, when Newfoundland weather is at its best, this would not have been an issue. The further work done on the LS – Model Riser was completed indoors and proved to be a more hospitable environment in which to work [29].

Overall, the LS – Model Riser was relatively robust and the assembly went well. The small changes in the parts, instrumentation and assembly process that have been discussed here were needed to help the model function properly. The main purpose of this project was as a learning process for the VIV team at Memorial University and the insight gathered in assembling a large scale model in a field situation was invaluable. The work done in this project provided the necessary ground work for further testing [28], [29]. The LS – Model Riser was rebuilt, taking into account the lessons learned in this project, and tested successfully at many current speeds and Reynolds numbers. This could not have been accomplished without the pioneering work completed here.

7.3 Testing Process and Data Collection/Analysis

The following conclusions and recommendations were developed through the testing process of this project.

- Testing of the LS – Model Riser was done on December 15, 2006 off the coast of St. John’s, Newfoundland. The test setup had a spherical buoy towed approximately 100 ft behind the vessel to ensure the wake had little or no affect on the current the LS – Model Riser encountered. The buoy was attached to the winch line of the vessel at one end and the LS – Model Riser at the other end. At the bottom end of the LS – Model Riser, a railway wheel and an additional winch line were all attached to a triangular steel separation plate. The test setup worked well, however, with the LS – Model Riser located far behind the vessel, there was no way to see the model and therefore it was hard to tell if the setup was working properly. By changing the setup this could be improved. For instance, mounting underwater cameras to the buoy or to an additional structure that is towed in parallel to the riser setup could provide valuable visual data.
- During the launching, testing and retrieval of the LS – Model Riser the following lessons were learned regarding the overall design, assembly and testing:
 - Swivels should be used at each shackle point. The one swivel attached to the railway wheel worked very well, however when the system was winched back aboard, it could be seen that at most of the other shackle points the wires were twisted and could have benefited from a swivel. It

was unknown how much damage, if any, this twisting caused to the LS – Model Riser.

- When the LS – Model Riser was connected onboard and launched behind the vessel, it was found that the buoy could not be winched out the entire 100 feet due to a lack of CAN Bus cable. Again, due to the testing being done in the field, excess CAN Bus and power cables should have been left at the top end of the LS – Model Riser. This would have allowed the riser to be towed at a long distance behind the vessel while still having enough cable to ensure there was slack during testing with no snags, tension or snap loads in any of the instrumentation.
- During testing, the CAN Bus cable was caught between the buoy and one of the shackles causing the cable to become worn. This led to the conclusion that the cables between the vessel and the LS – Model Riser should be protected in some way. A plastic tube or other form of protection should be introduced into the system so that the cables are kept separate from the buoy and winch lines and could not get caught and worn.
- The 130m long LS – Model Riser was outfitted with 65 modules along its length, spaced at a distance of 2.0m. Due to problems during assembly some of the modules were damaged and only 55 were able to be installed inside the model. Assembly issues also caused most of the modules that remained to be placed with a spacing of 1.9m. Out of the remaining 55 modules placed in the LS – Model Riser, 27 data channels, or sensors, were “dead”, or failed to read data properly,

leaving a total of 111 working sensors that were recording data in the model during testing. The large drop out rate was unfortunate, but due to the fact that working modules were still located along the entire length of the model, it could still yield useful data and testing was carried out with the remaining working modules. Four runs were obtained, Run 1a and 1b were two 3 minute samples at a current speed of 0.15 m/s, and Run 2a and 2b were two 3 minute samples at a current speed of 0.75 m/s. The runs were done twice to ensure their repeatability and that each data set was a good representation of the LS – Model Riser behavior at that current speed. The data acquired was analyzed, using Matlab routines to carry out five main computations, to determine that the data was useful and that the model could be used in further VIV analysis. The computations were:

- Calculating the vibration displacements from the measured accelerations in the in-line and cross-flow directions.
- Calculating the average peak pick-up amplitude and frequency versus reduced velocity in the in-line and cross-flow directions.
- Calculating the modal component time histories in the in-line and cross-flow directions were calculated for up to 25 modes.
- A spectral analysis which calculated the spectra of displacement at each location for the in-line and cross-flow directions.
- Plotting the vibration shape and trajectory of the LS – Model Riser.

Overall, the testing of the LS – Model Riser went exceptionally well and the results were useful in preparing the LS – Model Riser for a second test [28], [29]. The

captain, crew and owner of the *Miss Jacqueline IV* were extremely helpful and working with them was an enjoyable experience.

8 References

- [1] Freeman, Bree. "Cold Play" H₂Ops Magazine, Volume 4 Issue 4, 2007.
- [2] Grant, R.G., Litton, R.W., Mamidipudi, P., "Highly Compliant Rigid (HCR) Riser Model Tests and Analysis", Offshore Technology Conference, Houston, Texas, 1999.
- [3] Gupta, H., Finn, L., Halkyard, J., "Spar Alternative for 10,000ft Water Depth", Offshore Technology Conference, Houston, Texas, 2002.
- [4] Hatton, S.A., Willis, N., "Steel Catenary Risers for Deepwater Environments", Offshore Technology Conference, Houston, Texas, 1998.
- [5] Hatton, S.A., Willis, N., "Uncertainties Regarding VIV in the Design of Deep Water Risers" Deeptec 98, Aberdeen, Scotland, 1998.
- [6] Huse, E., Kleiven, G., Nielsen, F.G., "Large Scale Model Testing of Deep Sea Risers" Offshore Technology Conference, Houston, Texas, 1998.
- [7] Kim, Y.H., Vandiver, J.K., Holler, R., "Vortex-Induced Vibration and Drag Coefficients of Long Cables Subjected to Sheared Flows", Fourth International Offshore Mechanics and Arctic Engineering Symposium – Volume I, New York, USA, 1983
- [8] Li, X., Bose, N., Zhu, L., Spencer, D., "Multi-Mode Vortex-Induced Vibration Tests on a Flexible Model Riser", International Symposium on Technology of Ultra Deep Ocean Engineering, Tokyo, Japan, 2005.
- [9] Lie, H., Mo, K., Vandiver, J.K., "VIV Model Test of a Bare-and a Staggered Buoyancy Riser in a Rotating Rig", Offshore Technology Conference, Houston, Texas, 1998.
- [10] Massachusetts Institute of Technology: Department of Ocean Engineering: Vortex-Induced Vibration <http://web.mit.edu/shear7/index.html>
- [11] Vandiver, J.K., Mazel, C.H., "A Field Study of Vortex-Excited Vibrations of Marine Cables", 8th Annual Offshore Technology Conference, Houston, Texas, 1976.

- [12] Vandiver, J.K., "Drag Coefficients of Long Flexible Cylinders", 15th Annual Offshore Technology Conference, Houston, Texas, 1983.
- [13] Vandiver, J.K., Chung, T.Y., "Predicted and Measured Response of Flexible Cylinders in Sheared Flow", ASME Winter Annual Meeting Symposium on Flow-Induced Vibrations, Chicago, December 1988.
- [14] Vandiver, J.K., Marcollo, H., Swithenbank, S., Jhingran, V., "High Mode Number Vortex-Induced Vibration Field Experiments", Offshore Technology Conference, Houston, Texas, 2005.
- [15] Vandiver, J.K., Swithenbank, S., Jaiswal, V., Marcollo, H., "The Effectiveness of Helical Strakes in the Suppression of High-Mode-Number VIV", Offshore Technology Conference, Houston, Texas, 2006.
- [16] Willis, N.R.T. Thethi, K.S., "Stride JIP: Steel Risers in Deepwater Environments – Progress Summary", Offshore Technology Conference, Houston, Texas, 1999.
- [17] www.petro-canada.ca "East Coast Oil, Terra Nova, Photos & Graphics"
- [18] www.shellglobalsolutions.com/exploration/viv/
- [19] Suzuki, Hideyuki et al, "Vortex Induced Vibrations of Compliance Vertical Access Riser", International Symposium on Technology of Ultra Deep Ocean Engineering, Tokyo, Japan. Feb. 1-2 2005.
- [20] "Flexile Pipe Design Presentation" The Life-Cycle of Flexible Risers and Flowlines, Society of Underwater Technology, 2006.
- [21] Trelleborg CRP, "Vortex Induced Vibration Suppression Systems Brochure".
Ref: VIV 08/06
- [22] Bishop, R.E.D., Hassan, A.Y., "The Lift and Drag Forces on a Circular Cylinder in a Flowing Fluid", Proceedings of the Royal Society of London Series A, Mathematical and Physical Sciences Vol. 277 pp.32-50 January 7, 1964.
- [23] Allen, D.W. "Vortex-Induced Vibration of Deepwater Risers", Paper OTC 8703. Offshore Technology Conference, Houston, 1998.
- [24] Sarpkaya, T. "A Critical Review of the Intrinsic Nature of VIV", J. Fluid Struct., 19: 389-447, 2004.

- [25] Vandiver, J.K., "Research Challenges in the Vortex-Induced Vibration Prediction of Marine Risers" Offshore Technology Conference, Houston, Texas, 1998.
- [26] Chen, H-C., et al, "CFD Simulation of a Riser VIV", Offshore Technology Research Center, Texas A&M University, December 2007.
- [27] Gabbai, R.D., Bernaroya, H., "An Overview of Modeling and Experiments of Vortex-Induced Vibration of Circular Cylinders", Journal of Sound and Vibration 282, 2005
- [28] Ordonez, M., Sonnaillon, M., Murrin, D., Bose, N., Qiu, W., 2007, "Characterization in Large-Scale Risers", MTS/IEEE Oceans 2007, Vancouver.
- [29] Murrin, D., Ordonez, M., Stone, G., Bose, N., Qiu, W., 2007, "High Mode VIV Experiments on a Large-Scale Riser", MTS/IEEE Oceans 2007, Vancouver.
- [30] Li, X., Bose, N., Zhu, L., "Experimental Investigation of Multi-Modal VIV on a Flexible Riser", 2008, DRAFT – IN PREPARATION.
- [31] Kundu, P.K., Cohen, I.M., "Fluid Mechanics, 3rd Edition," Elsevier Academic Press, 2004.

Appendix A

Prototype DCR Characteristics

This Appendix contains a complete list of dimensions and characteristics for the Prototype DCR riser that was used as the prototype riser for the design of the LS – Model Riser.

PROTOTYPE RISER CHARACTERISTICS

OTC PAPER NUMBER		14298
Riser Identifier		DCR
Water Depth	m	3,048
Length	m	3,048
Outer Diam	m	0.3239
Outer Casing Thkness	m	0.009525
Outer Casing Pressure ²	psi	3000
Inner Diam	m	0.2445
Inner Casing Thk	m	0.0110
Tubing Outer Diam	m	0.1143
Tubing Thickness	m	0.0069
Inner casing/tubing pressure ³	psi	5,500
Total Wet Weight	kg	440,438
Total Wet Weight per length	kg/m	145
Total Wet Weight per length	N/m	1,418
Tension Factor		1.35
Top Tension	kN	5,834
Bottom Tension	kN	
Net Riser Stiffness	N/m	1,298,857
Cross sectional Area	m ²	3.54E-02
Elastic Modulus (E)	N/m ²	1.12E+11
Moment of Inertia (I)	m ⁴	0.00036459
Bending Stiffness (EI)	N m ²	4.07E+07
Current Velocity	m/s	2.25

Appendix B

Bending Stiffness Calculation

This Appendix contains the simple bending stiffness calculation for the IPEX Gold Stripe 160 Series pipe used to build the LS – Model Riser.

Bending Stiffness Test Report (2006/12/18)

1. Measured data

L=0.39m

No.	Weight(kg)	Height(cm)	$\Delta P(N)$	$\Delta H(m)$
1	7.5	100.7	24.53	0.005
2	5.0	101.2	24.53	0.004
3	2.5	101.6	24.53	0.003
4	0.0	101.9		

2. Formula for estimate of bending stiffness

For a cantilever beam, its bending stiffness can be estimated by

$$k_b = \frac{\Delta PL^3}{3\Delta H}$$

3. Test results

No.	Stiffness (Nm ²)
1	97.0
2	121.3
3	161.7
Average	126.6

Appendix C

Natural Frequency Calculations

This Appendix contains the complete calculations of natural frequency from first principals. This includes two calculations, one including bending stiffness and one without bending stiffness. The % error for all variations in calculations has also been included.

Lastly, a comparison of the large change in bending stiffness has been included.

**Modal Natural Frequencies
(including Bending Stiffness)**

$$\omega_{nk} = \sqrt{\frac{k_b \left(\frac{k\pi}{L}\right)^4 + T \left(\frac{k\pi}{L}\right)^2}{m_s + \frac{\pi}{4} \rho C_m D^2}}$$

kb = bending stiffness

k = mode number

L = length

T = tension

ms = mass/length of structure

Cm = added mass coefficient

ρ = water density

D = outer diameter

*Note: Divide ω by 2PI for Hz

**Modal Natural Frequencies
(Excluding Bending Stiffness)**

$$f_n = \frac{n}{2L} \sqrt{\frac{T}{m + m_a}}$$

n = mode number

L = length

T = tension

m = mass/length of structure

ma = added mass

** For long cylinders where tension dominates the bending stiffness

L = 130 m
 OD = 0.053 m
 ID = 0.040 m
 Wall Tk = 0.007 m
 $\rho = 1025 \text{ kg/m}^3$ (salt water density)
 $C_m = 1.2$ (added mass coefficient)
 Total Wt = 750 lbs
 = 340 kg

 St = 0.15

Minimum Reinforced Cross Sectional Area

$A = 0.0009495 \text{ m}^2$

Minimum Reinforced Moment of Inertia

$I = 2.617\text{E-}07 \text{ m}^4$

Material

$\rho = (\text{kg/m}^3) = 1186$
 $E = (\text{N/m}^2) = 4.84\text{E}+08$
 $m_s = (\text{kg/m}) = 2.617$
 $k_b = (\text{Nm}^2) = 126.6$

Re	1.1E+04	5.7E+04	6.8E+04
Shedding f	0.71	3.54	4.25

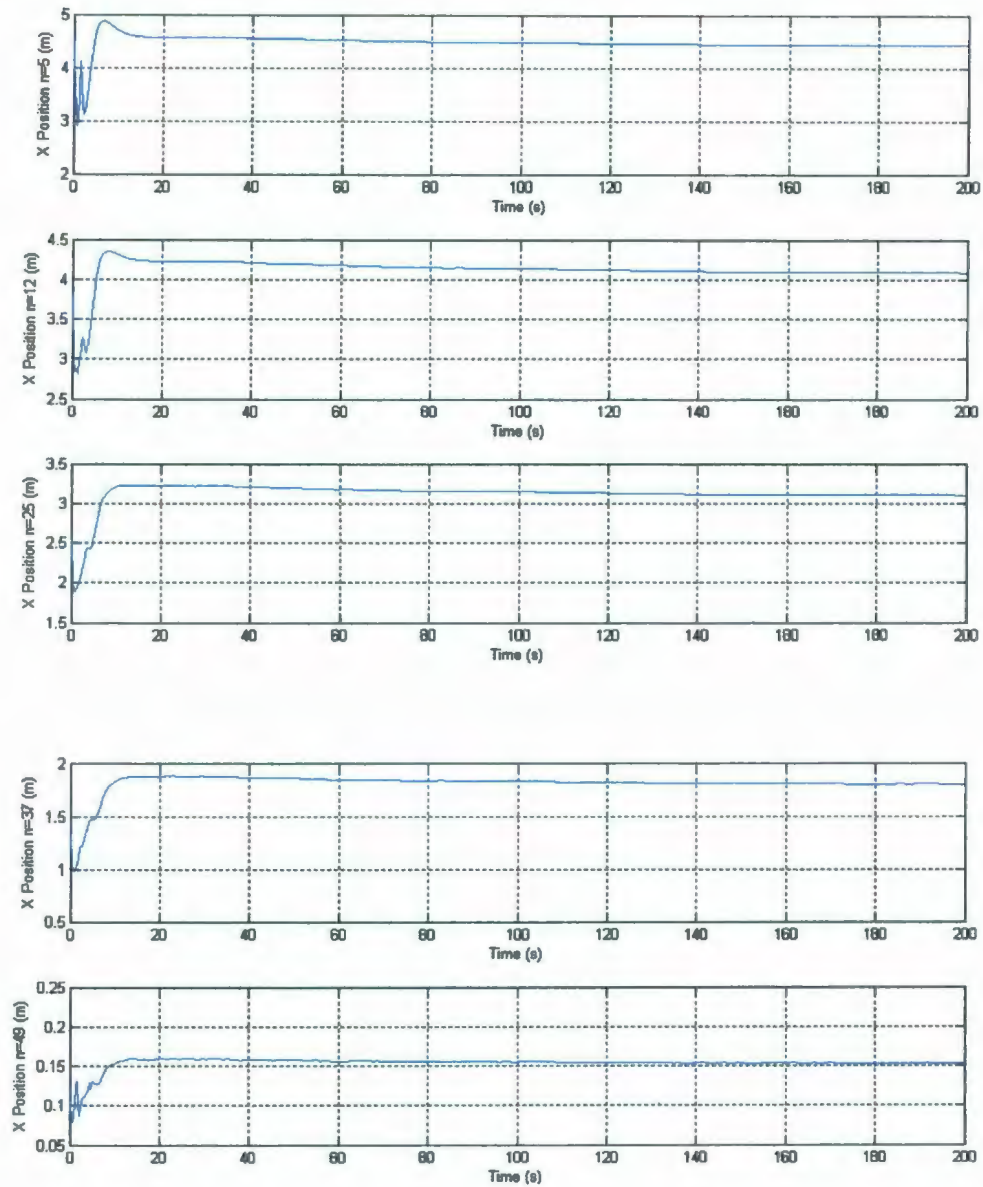
6.8E+04
4.25

Max Speed (m/s)	0.25	1.25	1.50
Tension (N)	5,500	7,500	10,000
Railway wheel (lbs)	800	800	800

1.50
10,000
800

Mode #	Modal Natural Frequencies (Hz) including kb		
1	0.12	0.14	0.17
2	0.25	0.29	0.33
3	0.37	0.43	0.50
4	0.49	0.58	0.67
5	0.62	0.72	0.83
6	0.74	0.87	1.00
7	0.87	1.01	1.17
8	0.99	1.15	1.33
16	1.98	2.31	2.67
17	2.10	2.46	2.84
18	2.23	2.60	3.00
19	2.35	2.75	3.17
20	2.48	2.89	3.34
21	2.60	3.04	3.50
22	2.73	3.18	3.67
23	2.85	3.33	3.84
24	2.98	3.47	4.01
25	3.10	3.62	4.17
26	3.23	3.76	4.34
27	3.35	3.91	4.51
28	3.48	4.06	4.68
29	3.60	4.20	4.85
30	3.73	4.35	5.01

Freq. (Hz) without kb	% Error
0.17	0.00
0.33	0.00
0.50	0.00
0.67	0.01
0.83	0.01
1.00	0.01
1.17	0.02
1.33	0.02
2.67	0.09
2.83	0.11
3.00	0.12
3.17	0.13
3.33	0.15
3.50	0.16
3.66	0.18
3.83	0.19
4.00	0.21
4.16	0.23
4.33	0.25
4.50	0.27
4.66	0.29
4.83	0.31
5.00	0.33



L = 130 m
 OD = 0.053 m
 ID = 0.040 m
 Wall Tk = 0.007 m
 $\rho = 1025 \text{ kg/m}^3$ (salt water density)
 $C_m = 1.2$ (added mass coefficient)
 Total Wt = 750 lbs
 = 340 kg

 St = 0.15

Minimum Reinforced Cross Sectional Area
 A = 0.0009495 m²

Minimum Reinforced Moment of Inertia
 I = 2.617E-07 m⁴

Material
 $\rho = (\text{kg/m}^3) = 1186$
 $E = (\text{N/m}^2) = 4.84\text{E}+08$
 $m_0 = (\text{kg/m}) = 2.617$
 $k_b = (\text{Nm}^2) = 126.6$

Material
 $\rho = (\text{kg/m}^3) = 1186$
 $E = (\text{N/m}^2) = 1.80\text{E}+10$
 $m_0 = (\text{kg/m}) = 2.617$
 $k_b = (\text{Nm}^2) = 4710$

Re	1.1E+04	5.7E+04	8.8E+04
Shedding f	0.71	3.54	4.25
Max Speed (m/s)	0.25	1.25	1.50
Tension (N)	5,500	7,500	10,000
Railway wheel (lbs)	800	800	800
Mode #	Modal Natural Frequencies (Hz) k _b = 126.6 Nm ²		
1	0.12	0.14	0.17
2	0.25	0.29	0.33
3	0.37	0.43	0.50
4	0.49	0.58	0.67
5	0.62	0.72	0.83
6	0.74	0.87	1.00
7	0.87	1.01	1.17
8	0.99	1.15	1.33
16	1.98	2.31	2.67
17	2.10	2.48	2.84
18	2.23	2.60	3.00
19	2.35	2.75	3.17
20	2.48	2.89	3.34
21	2.60	3.04	3.50
22	2.73	3.18	3.67
23	2.85	3.33	3.84
24	2.98	3.47	4.01
25	3.10	3.62	4.17
26	3.23	3.78	4.34
27	3.35	3.91	4.51
28	3.48	4.06	4.68
29	3.60	4.20	4.85
30	3.73	4.35	5.01

Re	1.1E+04	5.7E+04	8.8E+04
Shedding f	0.71	3.54	4.25
Max Speed (m/s)	0.25	1.25	1.50
Tension (N)	5,500	7,500	10,000
Railway wheel (lbs)	800	800	800
Mode #	Modal Natural Frequencies (Hz) k _b = 4710 Nm ²		
1	0.12	0.14	0.17
2	0.25	0.29	0.33
3	0.37	0.43	0.50
4	0.50	0.58	0.67
5	0.62	0.72	0.84
6	0.75	0.87	1.00
7	0.88	1.02	1.17
8	1.00	1.17	1.34
16	2.10	2.41	2.76
17	2.25	2.58	2.94
18	2.40	2.75	3.13
19	2.55	2.92	3.32
20	2.71	3.09	3.51
21	2.87	3.27	3.70
22	3.03	3.44	3.90
23	3.20	3.63	4.10
24	3.37	3.81	4.30
25	3.54	4.00	4.51
26	3.72	4.19	4.72
27	3.90	4.39	4.93
28	4.08	4.58	5.14
29	4.27	4.79	5.36
30	4.46	4.99	5.58

Re	1.1E+04	5.7E+04	8.8E+04
Shedding f	0.71	3.54	4.25
Max Speed (m/s)	0.25	1.25	1.50
Tension (N)	5,500	7,500	10,000
Railway wheel (lbs)	800	800	800
Mode #	% Error		
1	0.02	0.02	0.01
2	0.10	0.07	0.05
3	0.22	0.16	0.12
4	0.39	0.28	0.21
5	0.60	0.44	0.33
6	0.86	0.64	0.48
7	1.17	0.86	0.65
8	1.52	1.12	0.85
16	6.66	4.27	3.25
17	8.35	4.76	3.65
18	7.03	5.31	4.06
19	7.74	5.66	4.50
20	8.47	6.43	4.94
21	9.22	7.02	5.41
22	9.98	7.63	5.89
23	10.76	8.25	6.36
24	11.55	8.88	6.89
25	12.35	9.53	7.41
26	13.16	10.18	7.94
27	13.98	10.85	8.49
28	14.80	11.53	9.04
29	15.63	12.22	9.60
30	16.46	12.91	10.17

C4

Appendix D

IOT Riser Dynamics Code Input Files

This Appendix contains a sample of the input files used in the IOT Riser Dynamics Code.

Three speeds were tested, however, only the input code for the top speed will be included here, as the only difference in coding would be the current speed.

inputs.m file

```

% Input File for riser_dynamics.m : Motion of End Points P0, Pn specified
% Wayne Raman-Nair
% Institute for Ocean Technology, National Research Council
% St. John's, NL, Canada
% July 2005
global g L Ks mp mpb Vseg kE Cs Ds sigma n0
global n m mprime VV d0 CDT_mean CDN_mean CDN0 CL0 phi_drag rhof FP St
nu_seawater
global afi bfi cfi efi hfi gfi mfi VVi

% Other files to edit :
% P0.m P0dot.m Pn.m Pndot.m vfluid.m
n=50;% number of lumped masses
%load cat50;% Elastic Catenary : 100 points
tspan=[0:0.25:200];% Time values for output (s)
m=3*n;
mprime=m-3;% number of degrees of freedom
g=9.81;%acceleration due to gravity (m/s^2)
rhof=1025;%seawater density (kg/m^3)
St=0.15;% Strouhal number
nu_seawater=1e-06;% kinematic viscosity(m^2/s)
kE=10000;% Earth stiffness coefficient (N/m)

% Riser properties - For Model Riser
%L0=Total Natural Length ; rhoriser= mass per unit length ; d0,di = outer and inner
diameters ; E = Young's Modulus
rho_material=1186;% material density (kg/m^3)
L0=130;%unstretched length (m)
for k=1:n
    d0(k)=0.053;%External diameter (m)
    di(k)=0.001;%Internal diameter (m)
    E(k)=1.8e10; %Modulus of Elasticity (N/m^2)
    % Drag and lift coefficients for 3 ranges of Reynolds no.
    % (1) 0 < Re < 40 (2)40 < Re 3e05 (3) Re > 3e05
    CDT_mean(k)=0.2;%Mean Tangential drag coefficient
    CDN_mean(k,:)= [1.2 1.2 1.2];%Mean Normal drag coefficient
    CDN0(k,:)= [0.2 0.2 0.2];%amplitude of oscillating drag coefficient
    phi_drag(k,:)= [0 0 0];%phase angle of oscillating drag coefficient
    CL0(k,:)= [0.8 0.8 0.8];% amplitude of oscillating lift coefficient (mean lift assumed to
be zero)
end
end

```

```

% Internal Fluid Flow properties*****
% 1 barrel =45 U.S. gallons ; 1 U.S. gallon= 3.785 litres; 1 litre= 1e-03 cubic metres
% Flow rate Qflow=20e-03;%20 litres/sec = 10000 barrels/day approx.
% Density of oil = 800 kg/m^3
% Example of linear variation in internal fluid pressure :
% pfi(k)=1e07*(8+(1-k)/(n-1));%Internal fluid pressure in segment Sk (N/m^2)
% Usually about 10000 to 15000 psi . 1 psi= 6897 N/m^2

rho_fi=0;% Internal fluid density (kg/m^3)
Qflow=0;% Internal flow rate (m^3/s)
for k=1:n
    pfi(k)=0;%internal fluid pressure (N/m^2)
end%*****

% zeta= Damping ratio: usually between 5% and 50% of critical damping Ccrit
zeta=0.3;

% Boundary condition at P0 (seabed)
%sigma(1)=6*n*EI(1)/((3*n-1)*L(1));%Cantilever boundary condition at P0
%Ds(1)=zeta*2*L(1)*sqrt(EI(1)*rho(1));% Damping coefficient at P0 for bending
vibrations (N.m.sec)

sigma(1)=0;% Pinned at P0
Ds(1)=0;%Pinned at P0

%External Forces applied to lumped masses
%FP(i,k)= n(i)-component of force on mass m(k) at P(k)
for k=1:n-1
    FP(1,k)=0;
    FP(2,k)=0;
    FP(3,k)=0;
end
%FP(3,1)=-(900/2.2)*g;% 900 lb Vertical load on P1
%No mass for free vibration test

% No applied force on mass at Pn
FP(1,n)=0;
FP(2,n)=0;
FP(3,n)=0;

```

Inputs1 aux.m file

```

% Auxiliary Input File for riser_dynamics.m
% Different initial conditions than in file inputs_aux.m
% Quantities calculated from file inputs.m
% Institute for Ocean Technology (Wayne Raman-Nair)
% June 2005

% Riser properties
%L0=Total Natural Length ; rhoriser= mass per unit length ; d0,di = outer and inner
diameters ; E = Young's Modulus
for k=1:n
    L(k)=L0/n;%segment lengths (m)
    Vseg(k)=pi*d0(k)^2/4*L(k);% segment volume (m^3)
    Asolid(k)=pi/4*(d0(k)^2-di(k)^2);% Solid cross-sectional area (m^2)
    Isolid(k)=(pi/64)*(d0(k)^4-di(k)^4);% Second Moment of Area of cross-section about
neutral axis (m^4)
    rho(k)=rho_material*Asolid(k);% mass per unit length of riser (kg/m)
    EI(k)=E(k)*pi*(d0(k)^4-di(k)^4)/64;%bending stiffness (N.m^2)
end
%Calculating Seg 1 for addition of 800lb railway wheel
rho(1)=(rho_material*(pi/4*(d0(1)^2-di(1)^2)))+(363/2.6); %mass per unit length of seg1
+ anchor(363kg/2.6m) for n=50
Vseg(1)=(pi*d0(1)^2/4*L(1))+ (0.046167); %seg1 volume + anchor volume

% Internal Fluid Flow properties*****
for k=1:n
    Aflow(k)=pi/4*di(k)^2;% Flow area in segment Sk (m^2)
    w(k)=Qflow/Aflow(k);% Internal flow velocity in segment Sk (m/s)
    wdot(k)=0;% Internal flow acceleration in segment Sk (m/s^2) : Steady flow
end%*****
lambda(1)=1;
for k=2:n-1
    lambda(k)=0.5;
end
lambda(n)=1;
for k=1:n-1
    afi(k)=Aflow(k)*(pfi(k)+rho(fi)*w(k)^2-lambda(k)*rho(fi)*L(k)*wdot(k));
    bfi(k)=-rho(fi)*lambda(k)*Aflow(k)*L(k)*w(k);
    cfi(k)=rho(fi)*Aflow(k)*w(k);
    efi(k)=Aflow(k+1)*(-pfi(k+1)-rho(fi)*w(k+1)^2-
lambda(k+1)*rho(fi)*L(k+1)*wdot(k+1));
    hfi(k)=-rho(fi)*lambda(k+1)*Aflow(k+1)*L(k+1)*w(k+1);
    gfi(k)=-rho(fi)*Aflow(k+1)*w(k+1);

```

```

% Lumped internal fluid mass
mfi(k)=rho_fi*( lambda(k)*Aflow(k)*L(k)+lambda(k+1)*Aflow(k+1)*L(k+1) );
end
mfi(n)=0;

% Lumped Mases : Mass of riser without internal fluid
mp(1)=rho(1)*(L(1)+0.5*L(2));
mpb(1)=mp(1)-rho_f*(Vseg(1)+0.5*Vseg(2));
for j=2:n-1
    mp(j)=0.5*rho(j)*(L(j)+L(j+1));
    mpb(j)=mp(j)-0.5*rho_f*(Vseg(j)+Vseg(j+1));
end
mp(n)=0.5*rho(n)*L(n);
mpb(n)=mp(n)-0.5*rho_f*Vseg(n);

%Extensional Stiffness and Damping of segments
% Extensional Stiffness = A*E/L
% Critical Damping = 2*sqrt( E*A*mass per unit length )
% zeta= Damping ratio: usually between 5% and 50% of critical damping Ccrit
for k=1:n
    Ks(k)=Asolid(k)*E(k)/L(k);%segment stiffness (N/m)
    Ccrit(k)=2*sqrt(E(k)*Asolid(k)*rho(k));%critical damping (extensional vibration)
    Cs(k)=zeta*Ccrit(k);% Damping coefficient for extensional (longitudinal) vibrations
    (kg/sec)
end
Ks(1)=0;% Zero stiffness in segment 1
Cs(1)=0;% Zero damping in segment 1

%Bending Stiffness and damping

for k=2:n
    sigma(k)=EI(k)/L(k);
    Ds(k)=zeta*2*L(k)*sqrt(EI(k)*rho(k));% Damping coefficient for bending vibrations
    (N.m.sec)
end
sigma(2)=0;% Zero bending stiffness between segments 1 and 2
Ds(2)=0; % Zero bending damping between segments 1 and 2

VV=zeros(m,m);
VVi=zeros(m,m);
for j=1:n
    VV(3*j-2,3*j-2)=mp(j);
    VV(3*j-1,3*j-1)=mp(j);

```

```

VV(3*j,3*j)=mp(j);

VVi(3*j-2,3*j-2)=mfi(j);
VVi(3*j-1,3*j-1)=mfi(j);
VVi(3*j,3*j)=mfi(j);
end

% Elastic Catenary Initial Conditions*****

%P0zero=P0(0);
%alpha1P0=P0zero(1);
%alpha2P0=P0zero(2);
%alpha3P0=P0zero(3);

%Pnzero=Pn(0);% Initial position of Top End Pn
%beta1Pn=Pnzero(1);
%beta2Pn=Pnzero(2);
%beta3Pn=Pnzero(3);

%P0Q0=[beta1Pn-alpha1P0 beta2Pn-alpha2P0 -alpha3P0];
%P0Q0mod=sqrt( P0Q0(1)^2+P0Q0(2)^2+P0Q0(3)^2 );
%n0=P0Q0/P0Q0mod;
%for k=1:n-1
    %q0(3*k-2)=alpha1P0+xcat(k)*n0(1);
    %q0(3*k-1)=alpha2P0+xcat(k)*n0(2);
    %q0(3*k)=alpha3P0+xcat(k)*n0(3)+zcat(k);
%end
%*****
% The beam segments must not be parallel initially
P0zero=P0(0);% Initial position of bottom end P0
alpha1P0=P0zero(1);
alpha2P0=P0zero(2);
alpha3P0=P0zero(3);

Pnzero=Pn(0);% Initial position of Top End Pn
beta1Pn=Pnzero(1);
beta2Pn=Pnzero(2);
beta3Pn=Pnzero(3);

P0Q0=[beta1Pn-alpha1P0 beta2Pn-alpha2P0 -alpha3P0];
P0Q0mod=sqrt( P0Q0(1)^2+P0Q0(2)^2+P0Q0(3)^2 );
bb0=P0Q0mod/n;
aa0=0.5*beta3Pn/n;
dd0=2/(n-1)*( beta3Pn/n-aa0 );

```

```

%Unit vector n0 in inertial coordinates
% May need to be defined as a function of time.
n0=P0Q0/P0Q0mod;
for k=1:n-1
    q0(3*k-2)=alpha1P0+k*bb0*n0(1);
    q0(3*k-1)=alpha2P0+k*bb0*n0(2);
    q0(3*k)=alpha3P0+k*bb0*n0(3)+(k/2)*( 2*aa0+(k-1)*dd0 );
end

u0=zeros(1,mprime);
for r=1:mprime
    x0(r)=q0(r);
    x0(mprime+r)=u0(r);
end
%*****
% Plot of initial profile*****
xriser0(1)=alpha1P0;
yriser0(1)=alpha2P0;
zriser0(1)=alpha3P0;

for k=1:n-1
    xriser0(1+k)=q0(3*k-2);
    yriser0(1+k)=q0(3*k-1);
    zriser0(1+k)=q0(3*k);
end
xriser0(n+1)=beta1Pn;
yriser0(n+1)=beta2Pn;
zriser0(n+1)=beta3Pn;

%plot3(xriser0,yriser0,zriser0),...
%title('Initial Profile'),...
%xlabel('x-axis'),...
%ylabel('y-axis'),...
%zlabel('z-axis'),...
%grid
%*****

```

P0.m file

```
% Position of Point P0
function point0=P0(t)
point0(1)=5;
point0(2)=0;
point0(3)=0;
```

Pn.m file

```
% Position of Point Pn (Top End of Riser)
function pointn=Pn(t)
pointn(1)=0;
pointn(2)=0;
pointn(3)=150;
```

P0dot.m file

```
% Velocity of Point P0
function VP0=P0dot(t)
VP0(1)=0;
VP0(2)=0;
VP0(3)=0;
```

Pndot.m file

```
% Velocity of Point Pn (Top End of Riser)
function VPn=Pndot(t)
VPn(1)=0;
VPn(2)=0;
VPn(3)=0;
```

vfluid.m file

```
% Fluid Velocity Field
function vfield=vfluid(t,x)
% Inertial components of fluid velocity field at point x at time t
% Output is a row vector
% x(3) measured from seabed

vfield=[1.5 0 0];
%if x(3)<=2
    %vfield=[1 0 0];
%elseif x(3) < 112
    %vfield=[1 0 0];
%else
    %vfield=zeros(1,3);
%end
```

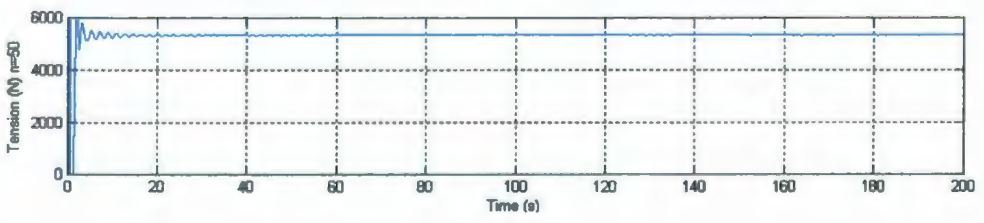
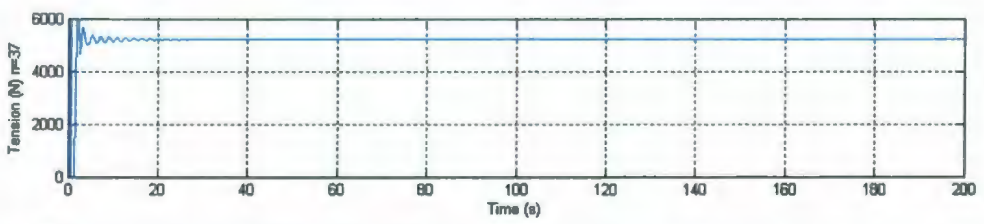
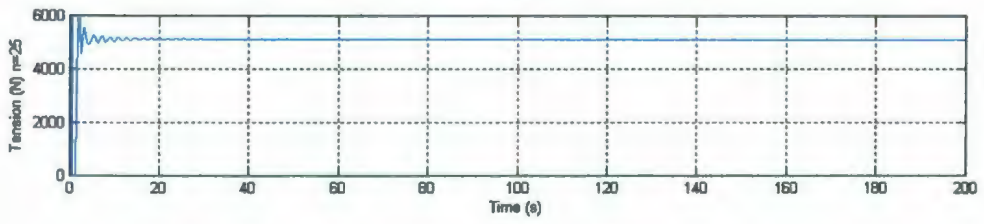
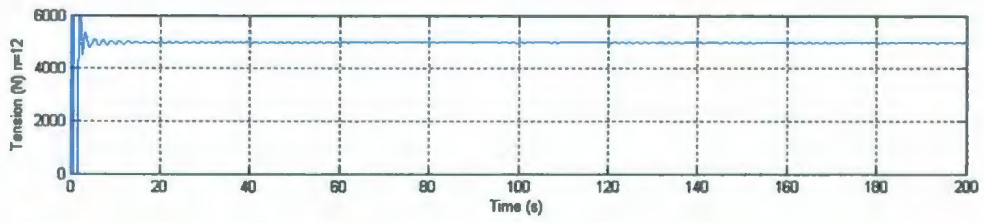
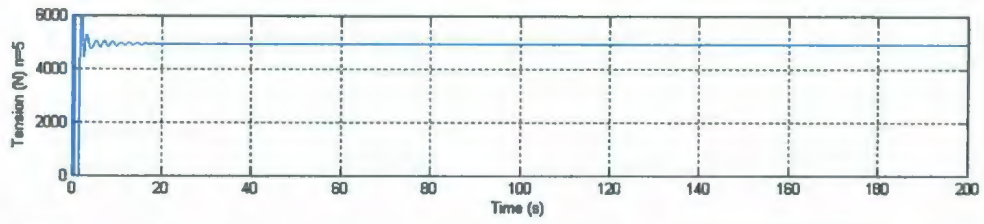
Appendix E

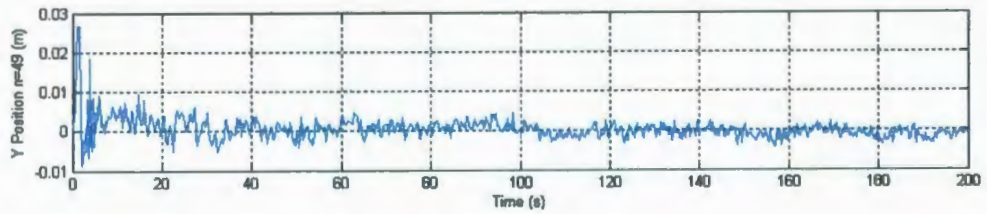
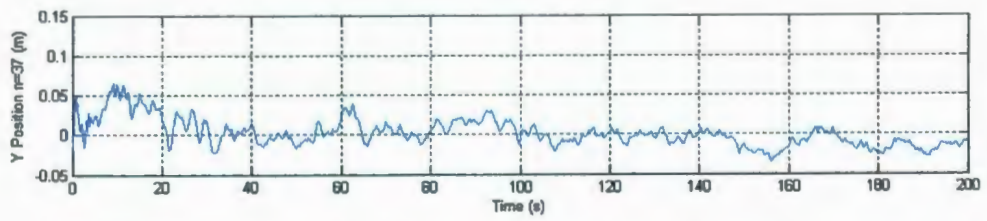
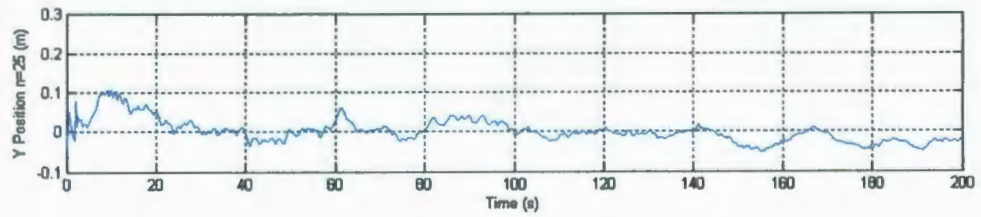
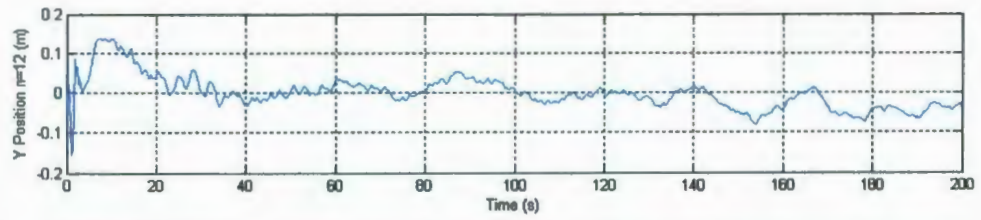
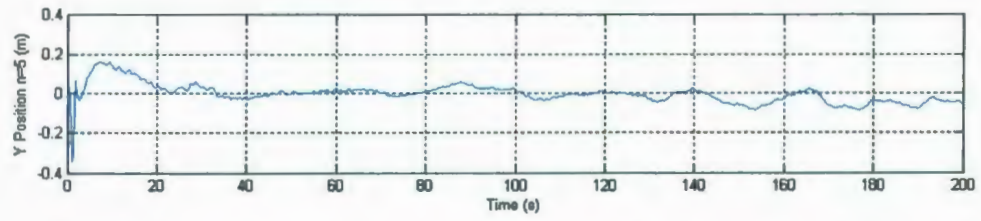
IOT Riser Dynamics Code Output

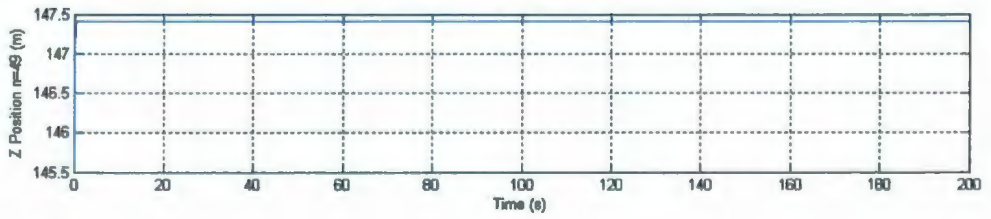
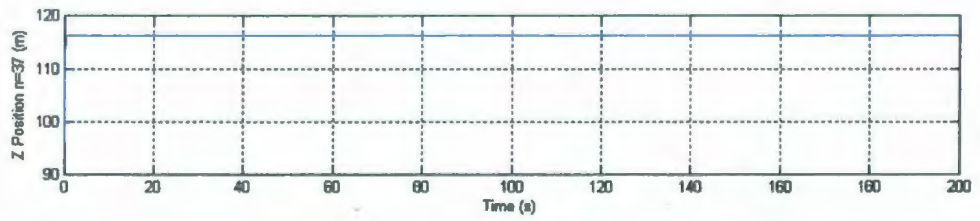
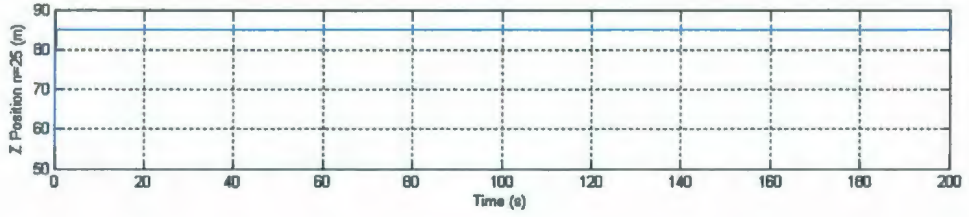
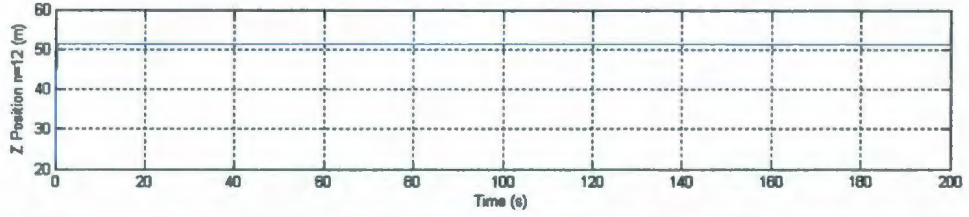
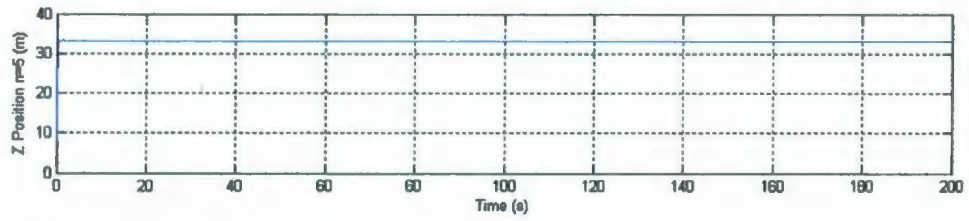
This Appendix contains the output data yielded from the IOT Riser Dynamics Code for the two current speeds, 0.25 and 1.25m/s that were not included in the body of this report.

This includes the tension vs. time, maximum tensile stress vs. time, and x, y and z positions vs. time.

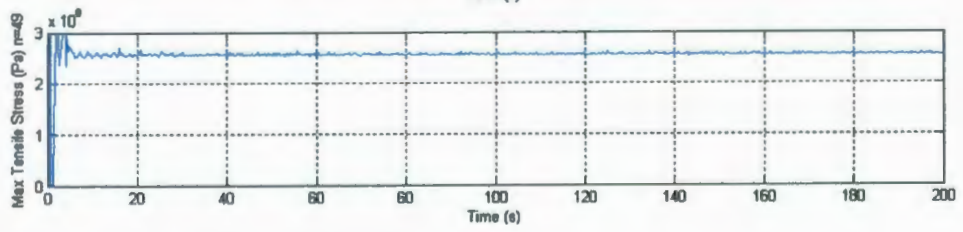
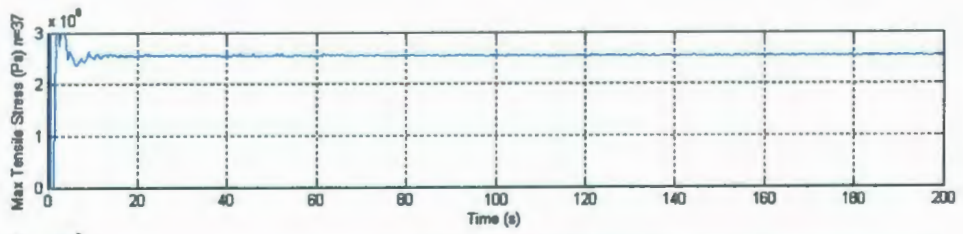
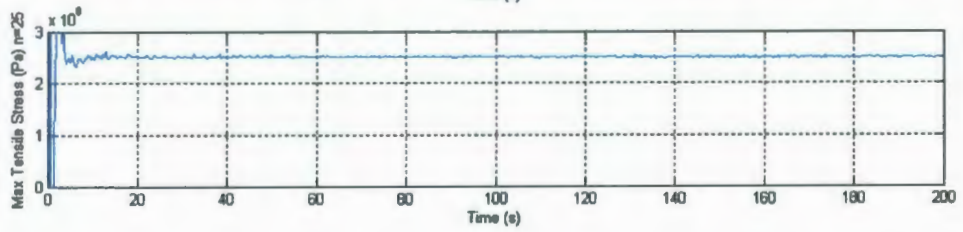
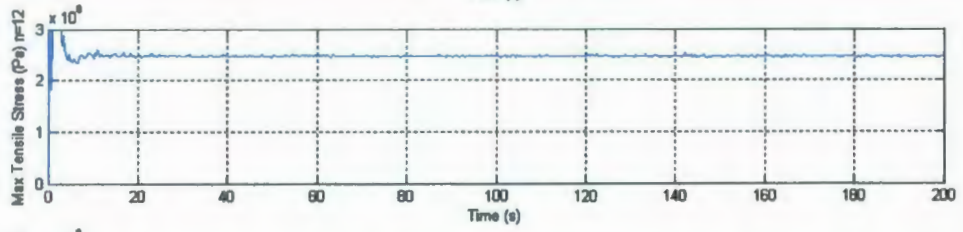
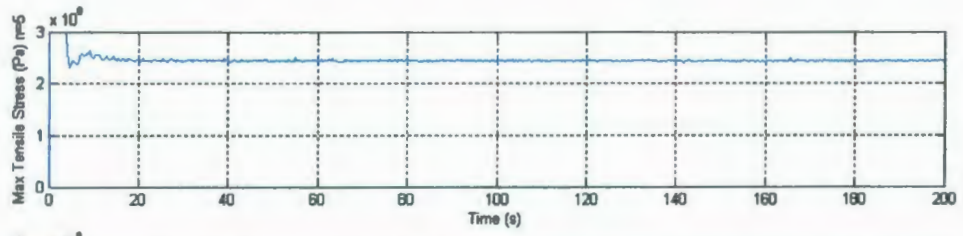
CURRENT SPEED 0.25m/s

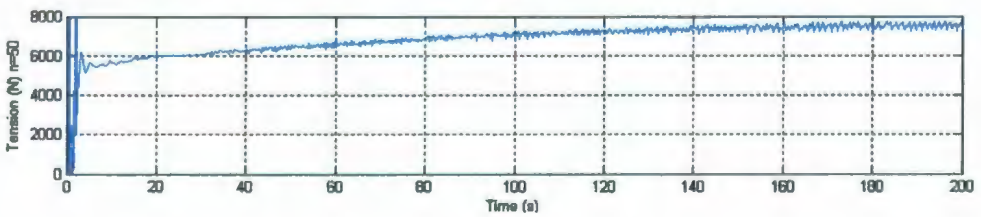
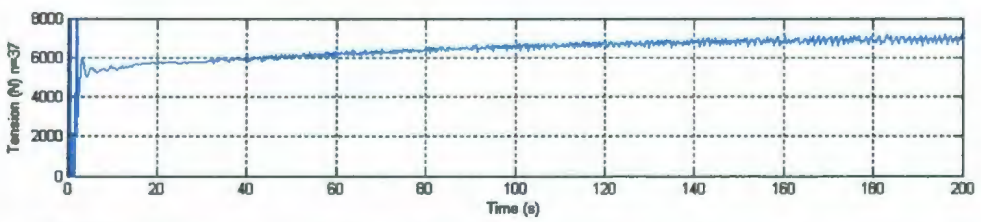
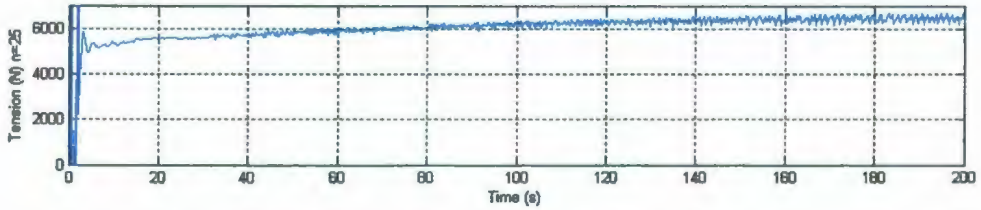
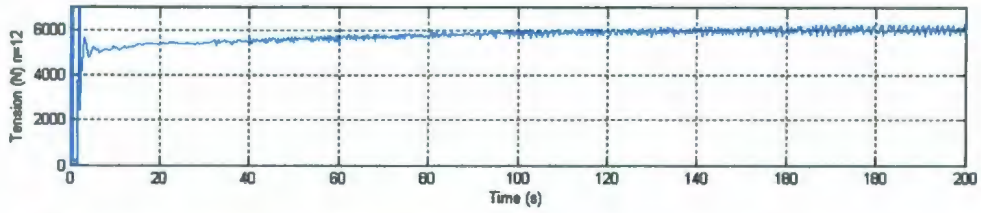
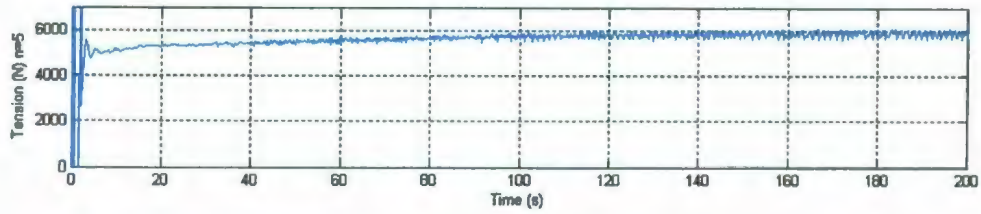


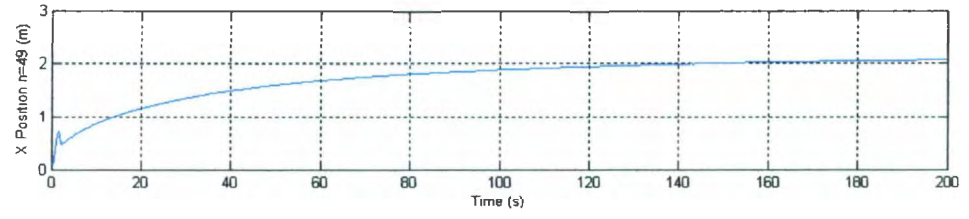
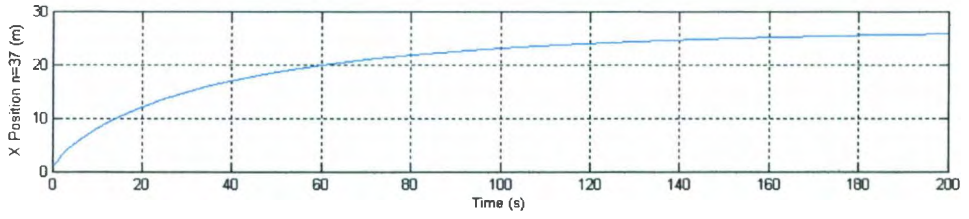
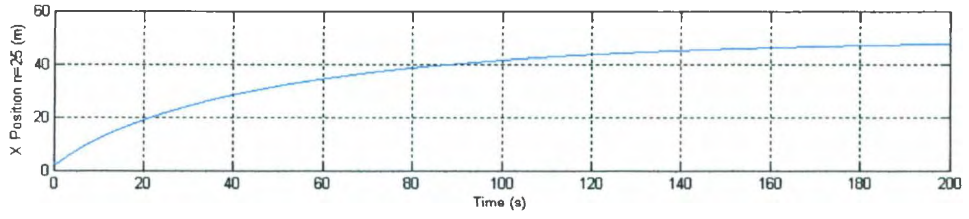
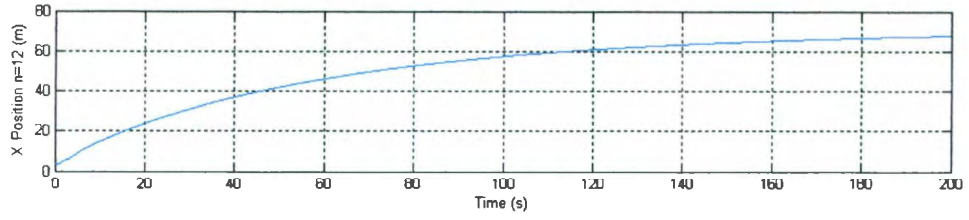
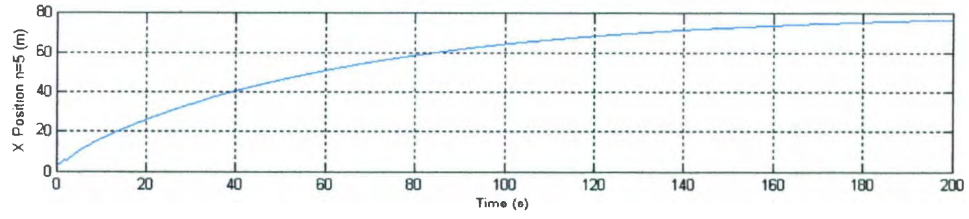


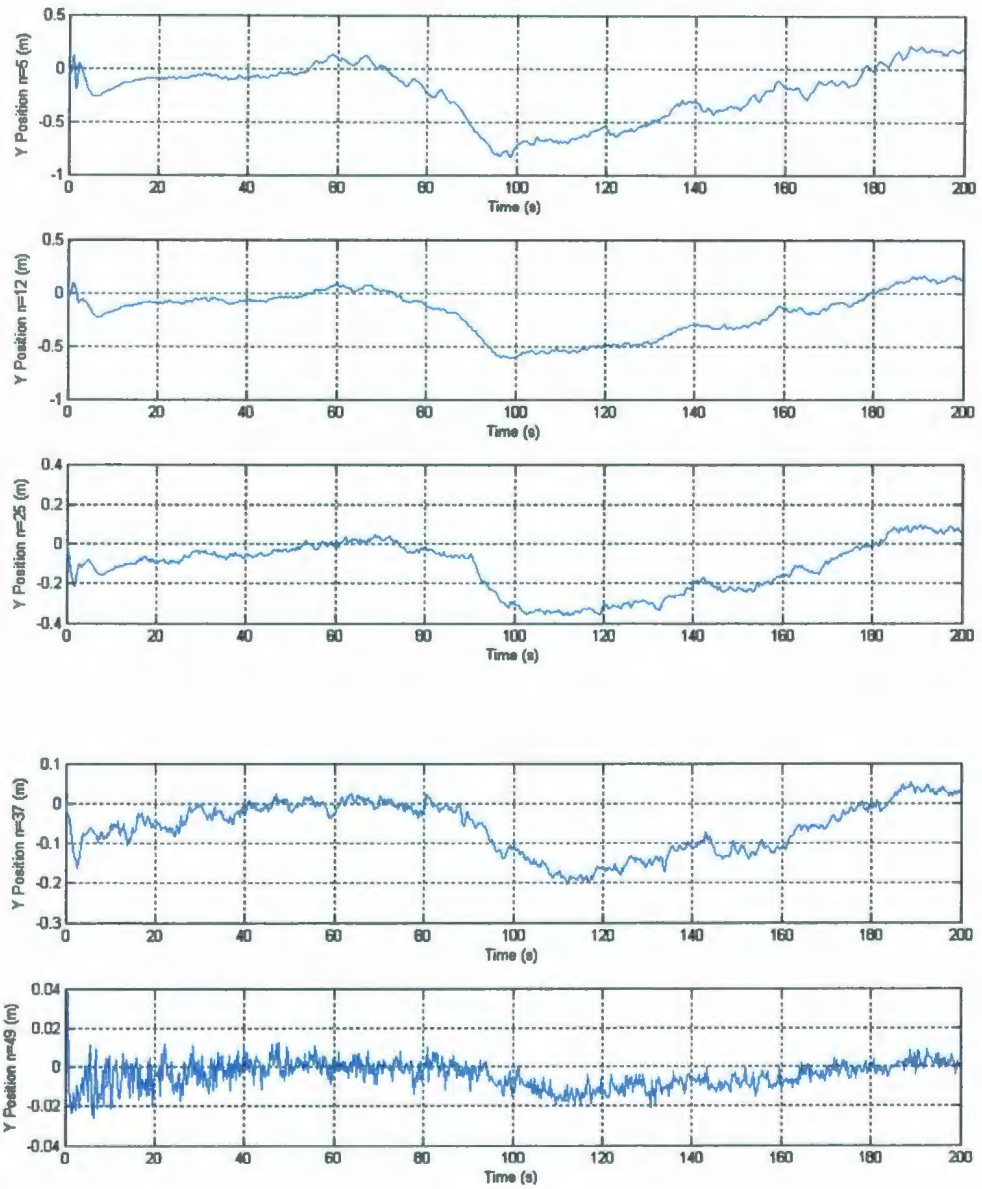


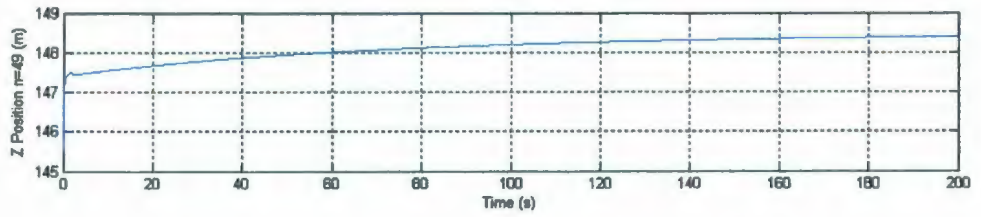
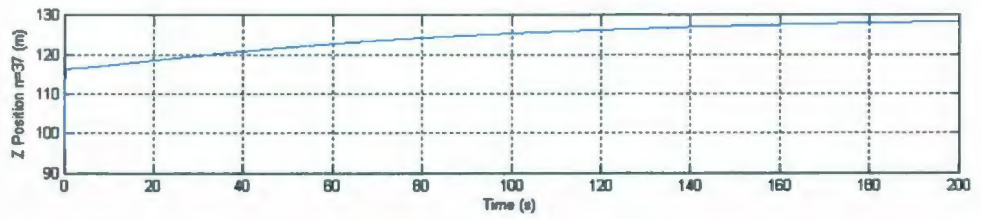
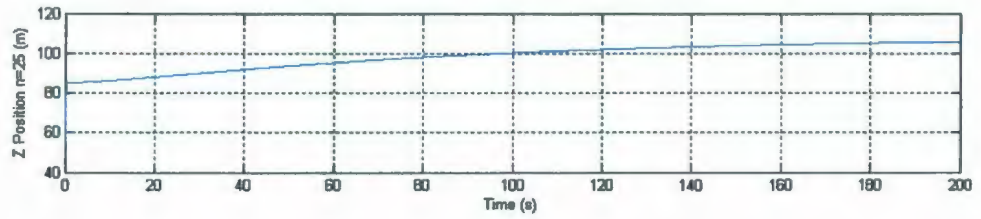
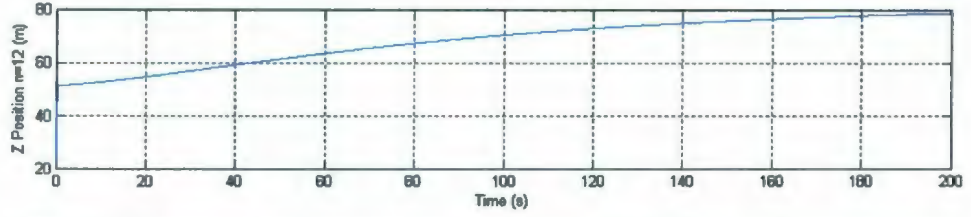
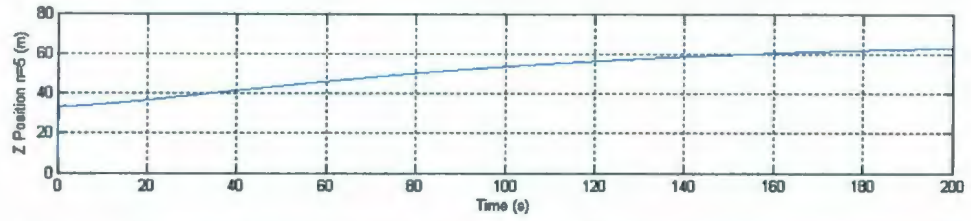
3

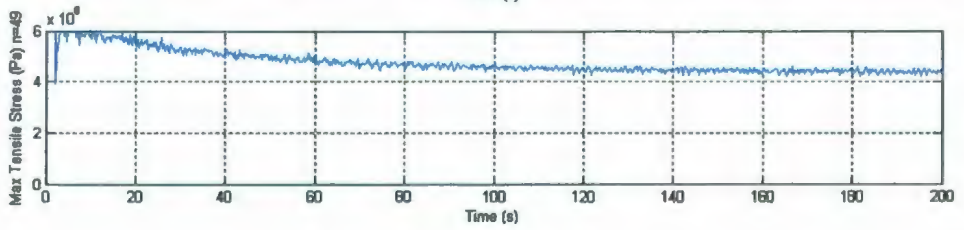
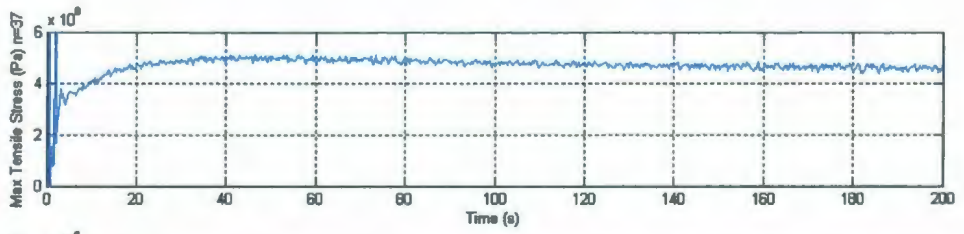
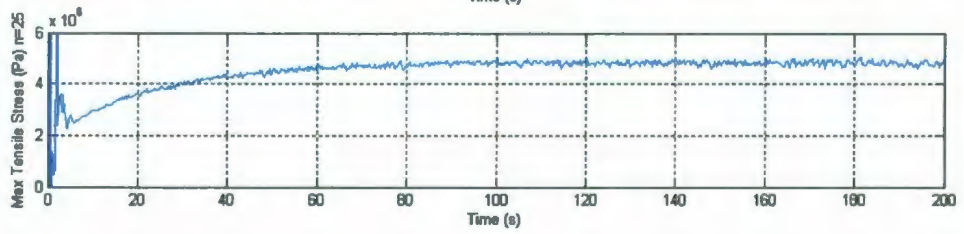
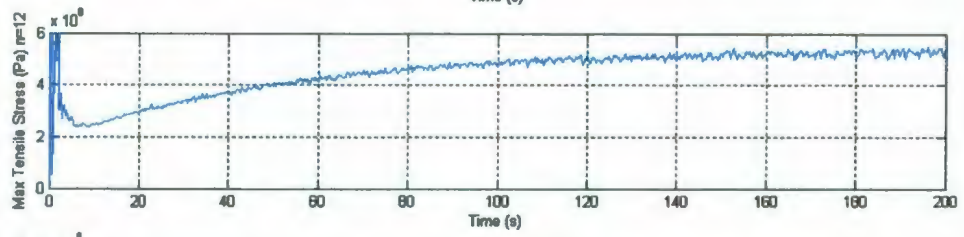
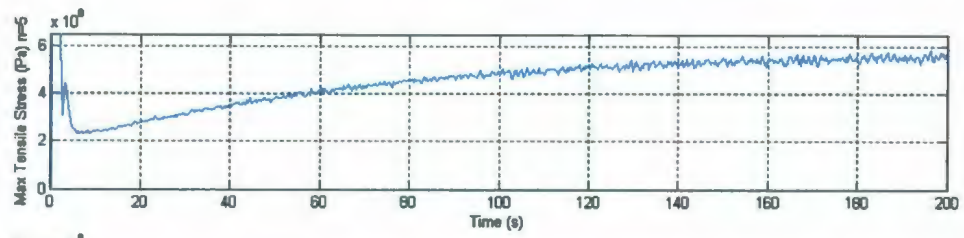


CURRENT SPEED 1.25m/s









Appendix F

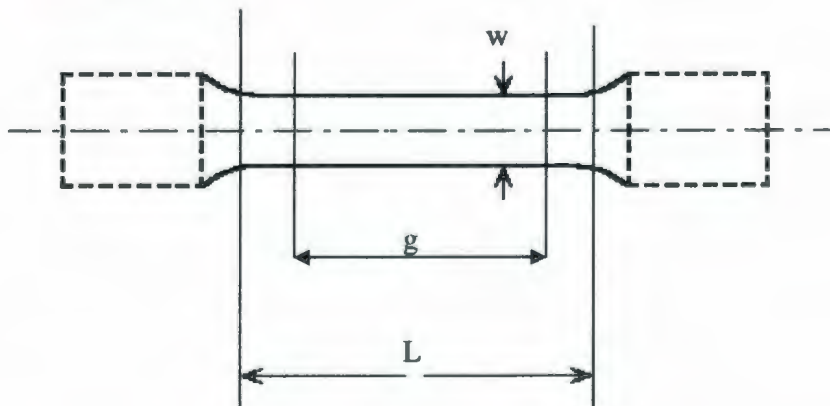
Tension Test Data and Calculations

This Appendix contains all of the data acquired and the completed calculations to determine the strength of the IPEX Blue Stripe 100 Series pipe.

Tension Test Summary Table

Sample		3	4	5	6
Width (w)	mm	10.472	10.446	10.648	9.944
Thickness	mm	6.575	6.433	6.46	6.932
gauge length (g)	mm	25	25	25	25
gauge length (g)	m	0.025	0.025	0.025	0.025
overall length (L)	mm	49.8	44.6	49.7	45.05
CS Area	mm ²	68.853	67.199	68.786	68.932
CS Area	m ²	6.885E-05	6.720E-05	6.879E-05	6.893E-05
Load Rate	cm/min	10	5	5	5
Chart Rate	cm/min	5	5	5	5
Ultimate Tensile Strength	kPa	11,398	10,219	9,983	9,635
Ultimate Tensile Strength	Pa	11,398,130	10,218,884	9,983,124	9,634,948
Modulus of Elasticity ²	kPa	189,969	51,094	49,916	40,146
Pipe CS Area	m ²	7.18E-04	7.18E-04	7.18E-04	7.18E-04
Ultimate Tensile Strength	N	8,179	7,333	7,164	6,914
Average Ultimate	N	7,398			
Avg Modulus of Elasticity ³	Pa	4.71E+07			

Specimen Dimensions



The thickness, not shown on the above diagram, represents the 3 dimensional aspect of the sample. It is the dimension of the sample "into" the page.

Sample 3

CS Area	m ²	6.8853E-05
g	m	0.025

Load (kg)	Load (N)	Stress (Pa)	Stress (kPa)	extension (cm)	extension (m)	Strain
0	0.00	0	0	0.00	0	0.00
20	196.20	2,849,532	2,850	0.00	0	0.00
50	490.50	7,123,831	7,124	0.05	0.0005	0.02
70	686.70	9,973,364	9,973	0.10	0.001	0.04
80	784.80	11,398,130	11,398	0.15	0.0015	0.06
81	794.61	11,540,607	11,541	0.20	0.002	0.08
81	794.61	11,540,607	11,541	0.30	0.003	0.12
79	774.99	11,255,653	11,256	0.40	0.004	0.16
79	774.99	11,255,653	11,256	0.65	0.0065	0.26
66	647.46	9,403,457	9,403	1.10	0.011	0.44
66	647.46	9,403,457	9,403	1.40	0.014	0.56
67	657.27	9,545,934	9,546	2.10	0.021	0.84
0	0.00	0	0	2.10	0.021	0.84

Ultimate Tensile Strength	11,398	kPa	11398129.9	Pa
Modulus of Elasticity	189,969	kPa	1.900E+08	Pa

Sample 4

CS Area	m ²	6.7199E-05
g	m	0.025

Load (kg)	Load (N)	Stress (Pa)	Stress (kPa)	extension (cm)	extension (m)	Strain
0	0.00	0	0	0.00	0	0.00
20	196.20	2,919,681	2,920	0.00	0	0.00
30	294.30	4,379,522	4,380	0.07	0.00067	0.03
40	392.40	5,839,362	5,839	0.13	0.00134	0.05
50	490.50	7,299,203	7,299	0.20	0.002	0.08
60	588.60	8,759,044	8,759	0.30	0.003	0.12
65	637.65	9,488,964	9,489	0.40	0.004	0.16
70	686.70	10,218,884	10,219	0.50	0.005	0.20
72	706.32	10,510,852	10,511	0.70	0.007	0.28
72	706.32	10,510,852	10,511	1.50	0.015	0.60
73	716.13	10,656,836	10,657	1.80	0.018	0.72
73	716.13	10,656,836	10,657	2.40	0.024	0.96
70	686.70	10,218,884	10,219	2.90	0.029	1.16
66	647.46	9,634,948	9,635	3.20	0.032	1.28
64	627.84	9,342,980	9,343	3.40	0.034	1.36
63	618.03	9,196,996	9,197	3.60	0.036	1.44
64	627.84	9,342,980	9,343	5.00	0.05	2.00
66	647.46	9,634,948	9,635	9.00	0.09	3.60
68	667.08	9,926,916	9,927	14.40	0.144	5.76
70	686.70	10,218,884	10,219	16.40	0.164	6.56
72	706.32	10,510,852	10,511	17.20	0.172	6.88
72	706.32	10,510,852	10,511	17.40	0.174	6.96
60	588.60	8,759,044	8,759	17.70	0.177	7.08
0	0.00	0	0	17.79	0.1779	7.12

Ultimate Tensile Strength	10,219	kPa	10218884.1	Pa
Modulus of Elasticity	51,094	kPa	5.109E+07	Pa

Sample 5

CS Area	m ²	6.8786E-05
g	m	0.025

Load (kg)	Load (N)	Stress (Pa)	Stress (kPa)	extension (cm)	extension (m)	Strain
0	0.00	0	0	0.00	0	0.00
20	196.20	2,852,321	2,852	0.00	0	0.00
30	294.30	4,278,482	4,278	0.07	0.00067	0.03
40	392.40	5,704,643	5,705	0.13	0.00134	0.05
50	490.50	7,130,803	7,131	0.20	0.002	0.08
60	588.60	8,556,964	8,557	0.30	0.003	0.12
70	686.70	9,983,124	9,983	0.50	0.005	0.20
71	696.51	10,125,741	10,126	0.70	0.007	0.28
71	696.51	10,125,741	10,126	2.40	0.024	0.96
70	686.70	9,983,124	9,983	2.60	0.026	1.04
66	647.46	9,412,660	9,413	3.20	0.032	1.28
62	608.22	8,842,196	8,842	3.60	0.036	1.44
62	608.22	8,842,196	8,842	4.40	0.044	1.76
63	618.03	8,984,812	8,985	6.20	0.062	2.48
64	627.84	9,127,428	9,127	7.40	0.074	2.96
65	637.65	9,270,044	9,270	10.30	0.103	4.12
60	588.60	8,556,964	8,557	10.50	0.10501	4.20
0	0.00	0	0	10.50	0.10501	4.20

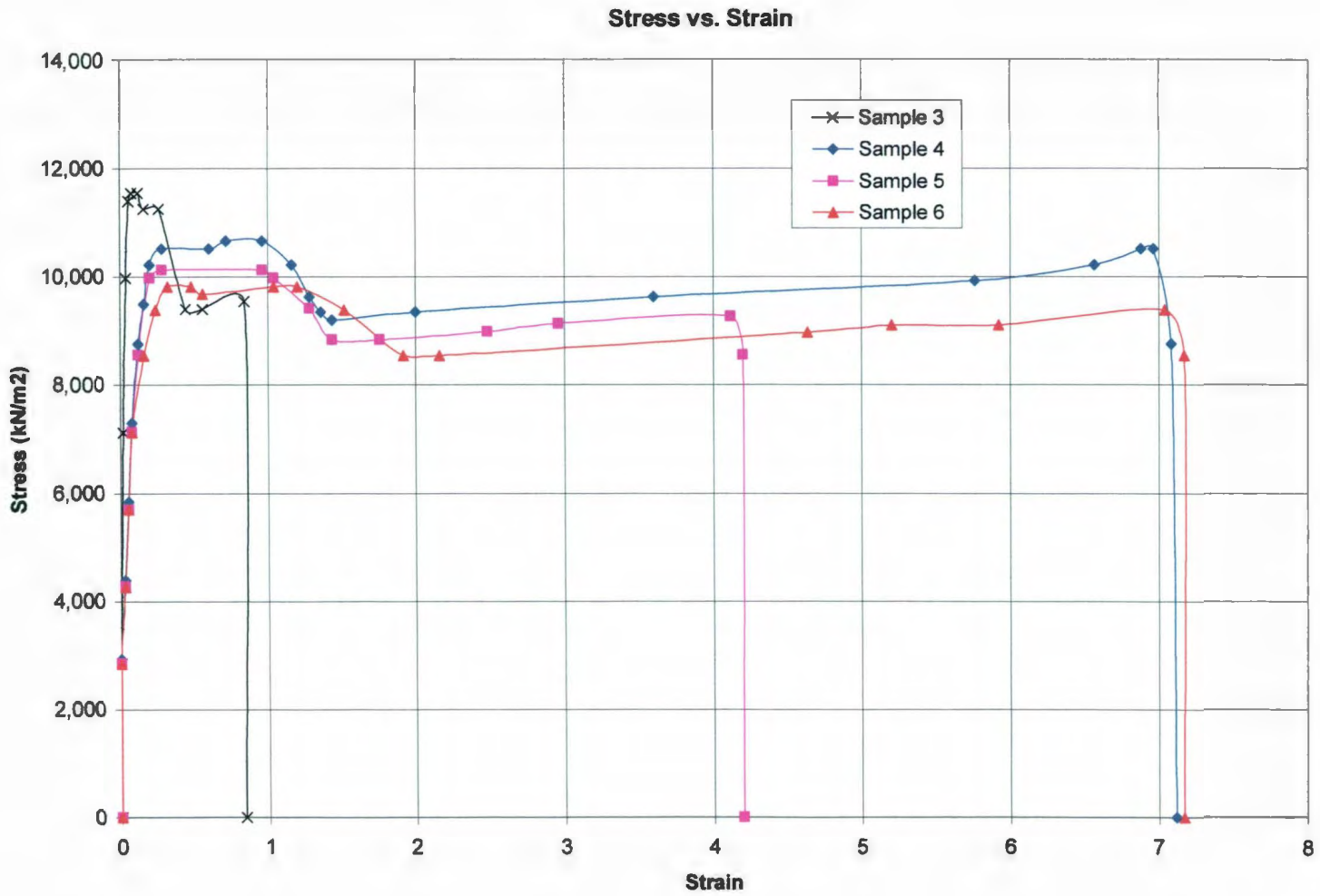
Ultimate Tensile Strength	9,983	kPa	9983124.49	Pa
Modulus of Elasticity	49,916	kPa	4.992E+07	Pa

Sample 6

CS Area	m ²	6.8932E-05
g	m	0.025

Load (kg)	Load (N)	Stress (Pa)	Stress (kPa)	extension (cm)	extension (m)	Strain
0	0.00	0	0	0.00	0	0.00
20	196.20	2,846,291	2,846	0.00	0	0.00
30	294.30	4,269,437	4,269	0.07	0.00067	0.03
40	392.40	5,692,582	5,693	0.13	0.00134	0.05
50	490.50	7,115,728	7,116	0.20	0.002	0.08
60	588.60	8,538,874	8,539	0.40	0.004	0.16
66	647.46	9,392,761	9,393	0.60	0.006	0.24
69	676.89	9,819,705	9,820	0.80	0.008	0.32
69	676.89	9,819,705	9,820	1.20	0.012	0.48
68	667.08	9,677,390	9,677	1.40	0.014	0.56
69	676.89	9,819,705	9,820	2.60	0.026	1.04
69	676.89	9,819,705	9,820	3.00	0.03	1.20
66	647.46	9,392,761	9,393	3.80	0.038	1.52
60	588.60	8,538,874	8,539	4.80	0.048	1.92
60	588.60	8,538,874	8,539	5.40	0.054	2.16
63	618.03	8,965,817	8,966	11.60	0.116	4.64
64	627.84	9,108,132	9,108	13.00	0.13	5.20
64	627.84	9,108,132	9,108	14.80	0.148	5.92
66	647.46	9,392,761	9,393	17.60	0.176	7.04
60	588.60	8,538,874	8,539	17.92	0.1792	7.17
0	0.00	0	0	17.92	0.1792	7.17

Ultimate Tensile Strength	9,393	kPa	9392761.03	Pa
Modulus of Elasticity	39,137	kPa	3.914E+07	Pa



Appendix G

Instrumentation Product Data Sheets

This Appendix contains product data sheets for some of the major parts of the accelerometer and full modules.



$\pm 300^\circ/\text{s}$ Single Chip Rate Gyro Evaluation Board

ADXRS300EB

GENERAL DESCRIPTION

The ADXR300EB is a simple evaluation board that allows the user to quickly evaluate the performance of the ADXR300ABG yaw rate gyro. No additional external components are required for operation. The ADXR300EB has a 20-lead dual-in-line (0.3 inch width by 0.1 inch pin spacing) interface that allows the user to easily prototype products without having to deal with BGA soldering. The 0.4 square inch outline of the ADXR300EB is still among the smallest gyros available today.

CIRCUIT DESCRIPTION

The schematic of the ADXR300EB is shown in Figure 1. It is identical to the suggested application shown in the ADXR300ABG data sheet.

The analog and power grounds (AGND and PGND) have separate ground planes and are joined at one point. The user may cut this trace if separate ground schemes are desired.

Note that the analog supply voltage and charge pump supply voltage (AVCC and PDD) are not connected on the ADXR300EB, and the user must connect these as appropriate to the application.

The parts layout of the ADXR300EB is shown in Figure 2, and the part list for the ADXR300EB is shown in Table 1. As delivered, the ADXR300EB is set for 40 Hz bandwidth ($C_{cut1} = 22 \text{ nF}$). The user may add an additional external capacitor to further reduce the bandwidth and improve the noise floor.

SPECIAL NOTES ON HANDLING

Note that the ADXR300EB is not reverse polarity protected. Reversing the power supply, or applying inappropriate voltages to any pin (outside the ADXR300 data sheet's Absolute Maximum Ratings), may damage the ADXR300EB.

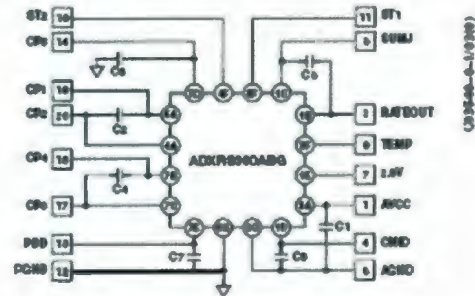


Figure 1. ADXR300EB Schematic

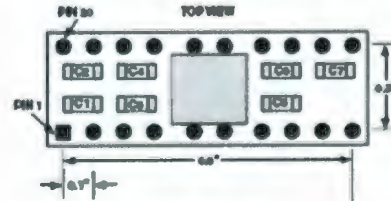


Figure 2. ADXR300EB Parts Layout

Table 1. ADXR300EB Component Values

Component	Values (nF)
C1	100
C2	22
C3	22
C4	22
C5	100
C6	47
C7	100

REV. 0

Information furnished by Analog Devices is believed to be accurate and reliable. However, no responsibility is assumed by Analog Devices for its use, nor for any infringements of patents or other rights of third parties that may result from its use. No license is granted by implication or otherwise under any patent or patent rights of Analog Devices. Trademarks and registered trademarks are the property of their respective companies.

One Technology Way, P.O. Box 9106, Norwood, MA 02062-9106, U.S.A.
Tel: 781/329-4700 www.analog.com
Fax: 781/326-8700 © 2003 Analog Devices, Inc. All rights reserved.



Small, Low Power, 3-Axis $\pm 3g$ iMEMS® Accelerometer

ADXL330

FEATURES

- 3-axis sensing
- Small, low-profile package
4 mm x 4 mm x 1.45 mm LFCSP
- Low power
180 μ A at $V_s = 1.8$ V (typical)
- Single-supply operation
1.8 V to 2.6 V
- 10,000 g shock survival
- Excellent temperature stability
- BW adjustment with a single capacitor per axis
- RoHS/WEEE lead-free compliant

APPLICATIONS

- Cost-sensitive, low power, motion- and tilt-sensing applications
- Mobile devices
- Gaming systems
- Disk drive protection
- Image stabilization
- Sports and health devices

GENERAL DESCRIPTION

The ADXL330 is a small, thin, low power, complete 3-axis accelerometer with signal conditioned voltage outputs, all on a single monolithic IC. The product measures acceleration with a minimum full-scale range of $\pm 3g$. It can measure the static acceleration of gravity in tilt-sensing applications, as well as dynamic acceleration resulting from motion, shock, or vibration.

The user selects the bandwidth of the accelerometer using the C_x , C_y , and C_z capacitors at the XOUT, YOUT, and ZOUT pins. Bandwidths can be selected to suit the application, with a range of 0.5 Hz to 1600 Hz for X and Y axes, and a range of 0.5 Hz to 550 Hz for the Z axis.

The ADXL330 is available in a small, low profile, 4 mm x 4 mm x 1.45 mm, 16-lead, plastic lead frame chip scale package (LFCSP_LQ).

FUNCTIONAL BLOCK DIAGRAM

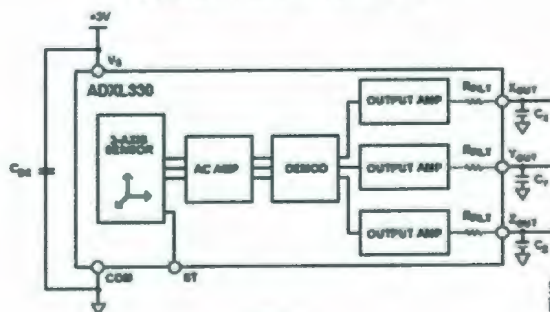


Figure 1.

NOTES

Information furnished by Analog Devices is believed to be accurate and reliable. However, no responsibility is assumed by Analog Devices for its use, nor for any infringements of patents or other rights of third parties that may result from its use. Specifications subject to change without notice. No license is granted by implication or otherwise under any patent or patent rights of Analog Devices. Trademarks and registered trademarks are the property of their respective owners.

One Technology Way, P.O. Box 9106, Norwood, MA 02062-0106, U.S.A.
Tel: 781.329.4700 www.analog.com
Fax: 781.461.3113 ©2006 Analog Devices, Inc. All rights reserved.



Three-Axis Accelerometer Evaluation Board

EVAL-ADXL330Z

DESCRIPTION

The EVAL-ADXL330Z is a simple evaluation board that allows quick evaluation of the performance of the ADXL330 dual-axis accelerometer. The EVAL-ADXL330Z has a 5-pin, 0.1 inch spaced header for access to all power and signal lines that the user can attach to a prototyping board (breadboard) or wire using a standard plug. Four holes are provided for mechanical attachment of the EVAL-ADXL330Z to the application.

The EVAL-ADXL330Z is 20 mm x 20 mm with mounting holes set 15 mm x 15 mm at the corners of the PCB.

CIRCUIT DESCRIPTION

The schematic of the EVAL-ADXL330Z is shown in Figure 1. Analog bandwidth can be set by changing Capacitors C2, C3, and C4. See the ADXL330 data sheet for a complete description of the operation of the accelerometer.

The part layout of the EVAL-ADXL330Z is shown in Figure 2. The EVAL-ADXL330Z has three factory installed 100 nF capacitors (C2, C3, and C4) at Xout, Yout, and Zout to reduce the bandwidth to 50 Hz. Many applications require a different bandwidth, in which case, the user can change C2, C3, and C4 as appropriate.

SPECIAL NOTES ON HANDLING

The EVAL-ADXL330Z is not reverse polarity protected. Reversing the +V supply and ground pins can cause damage to the ADXL330.

Dropping the EVAL-ADXL330Z on a hard surface can generate several thousand g of acceleration and might exceed the data sheet absolute maximum limits. See the ADXL330 data sheet for more information.

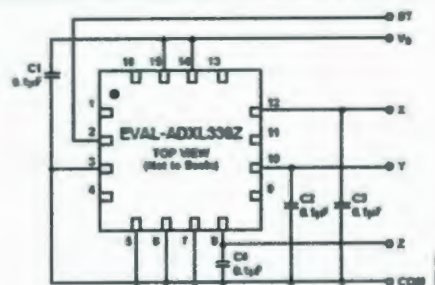


Figure 1. EVAL-ADXL330Z Schematic

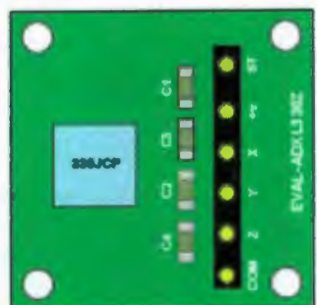


Figure 2. EVAL-ADXL330Z Physical Layout

ORDERING GUIDE

Model	Package Description
EVAL-ADXL330Z ¹	Evaluation Board

¹ Z = Pb-free part.

Rev. 0
Information furnished by Analog Devices is believed to be accurate and reliable. However, no responsibility is assumed by Analog Devices for errors or for copyright infringement of patents or other rights of third parties that may result from their use. Specifications are subject to change without notice. No license is granted by implication or otherwise under any patent or patent rights of Analog Devices. Trademarks and registered trademarks are the property of their respective owners.

One Technology Way, P.O. Box 9106, Norwood, MA 02062-9106, U.S.A.
Tel: 781.329.4700 www.analog.com
Fax: 781.461.3113 ©2006 Analog Devices, Inc. All rights reserved.

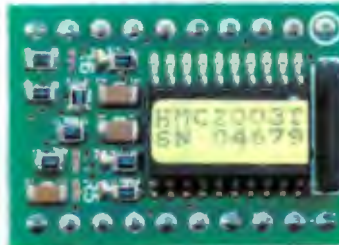
HMC2003

Honeywell
SENSOR PRODUCTS

THREE-AXIS MAGNETIC SENSOR HYBRID

Features

- 20-pin Wide DIP Footprint (1" by 0.75")
- Precision 3-axis Capability
- Factory Calibrated Analog Outputs
- 40 micro-gauss to ± 2 gauss Dynamic Range
- Analog Output at 1 Volt/gauss (2.5V @ 0 gauss)
- Onboard +2.5 Volt Reference
- +6 to +15 Volt DC Single Supply Operation
- Very Low Magnetic Material Content
- -40° to 85°C Operating Temperature Range



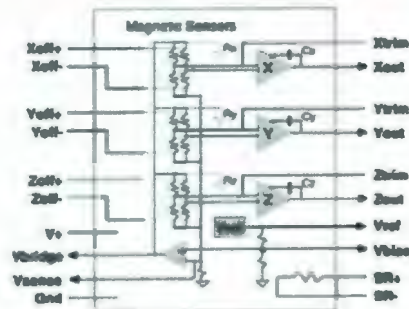
General Description

The Honeywell HMC2003 is a high sensitivity, three-axis magnetic sensor hybrid assembly used to measure low magnetic field strengths. Honeywell's most sensitive magneto-resistive sensors (HMC1001 and HMC1002) are utilized to provide the reliability and precision of this magnetometer design. The HMC2003 interface is all analog with critical nodes brought out to the pin interfaces for maximum user flexibility. The internal excitation current source and selected gain and offset resistors, reduces temperature errors plus gain and offset drift. Three precision low-noise instrumentation amplifiers with 1kHz low pass filters provide accurate measurements while rejecting unwanted noise.

APPLICATIONS

- Precision Compassing
- Navigation Systems
- Attitude Reference
- Traffic Detection
- Proximity Detection
- Medical Devices

BLOCK DIAGRAM



Appendix H

UNIVIS BIO 40 Product Data Sheet

This Appendix contains the product data sheet for the hydraulic oil, UNIVIS BIO 40, which was used to fill the LS – Model Riser.



Product Data Sheet

UNIVIS BIO 40

BIODEGRADABLE HYDRAULIC FLUID

October 2003

UNIVIS[®] BIO 40 was developed to meet the growing global demand for more environmentally friendly hydraulic fluids. UNIVIS BIO 40 offers the following features and benefits:

- ♦ Non-toxic, biodegradable, vegetable oil based lubricant designed to meet hydraulic equipment requirements
- ♦ Provides the high performance characteristics of a premium quality conventional hydraulic oil with the added assurance of reduced environmental impact
- ♦ UNIVIS BIO 40 can help achieve your environmental awareness objectives and, should accidental release occur, will lessen the damage and facilitate spill management.

Primary Applications

UNIVIS BIO 40 is suitable for applications demanding a high performance hydraulic fluid in woodland, construction, mining, marine and industrial hydraulics as well as lubricant applications wherever critical environmental concerns exist. The excellent anti-wear characteristics of UNIVIS BIO 40 ensure extended pump life in hydraulic systems.

Performance Features

Biodegradability

UNIVIS BIO 40 meets and exceeds the requirements of biological degradation as defined by the OECD guideline and the CEC L-33-T-82 hydrolysis test method. The CEC procedure measures the natural biodegradability of a substance using non-acclimated, naturally occurring organisms. This test method tracks the disappearance of the hydraulic oil over a period of time using infrared techniques. UNIVIS BIO 40 is biodegradable at not less than 97% within 21 days, minimizing harm to soil or water by released fluid. Biodegradable as defined by the OECD guideline and the CEC L-33-T-82 test method.

Ecotoxicity

UNIVIS BIO 40 is non-toxic as defined by the following tests:

[®]Trademarks of Imperial Oil Limited, Imperial Oil, Licensee. Lubricants and Specialties, Marketing Technical Services
[™]Trademark of Exxon Corporation, Imperial Oil, Licensee. Helpline: 1-800-268-3183

Oral Limit Test OECD 401	Non-toxic LD50>2000 mg/kg
Dermal Limit Test OECD 402	Non-toxic LD50>2000 mg/kg
Skin Irritation OECD 404	Non-Irritating to skin
Eye Irritation OECD 405	Non-Irritating to eyes
Ames Test	Not mutagenic

High Viscosity Index

The naturally high viscosity index of UNIVIS BIO 40 provides excellent shear stability, thus enabling optimum performance over a wide temperature range.

Load Carrying Ability

UNIVIS BIO 40 exhibits excellent load carrying ability. This ensures exceptional protection against wear and scuffing.

Rust and Corrosion Protection

UNIVIS BIO 40 provides excellent rust and corrosion protection to help protect expensive system components.

Demulsibility

The good demulsibility characteristics of UNIVIS BIO 40 ensure clean water separation.

Compatibility

UNIVIS BIO 40 is compatible with conventional mineral oils. It should be noted that contamination of UNIVIS BIO 40 with other fluids may lead to a reduction in the biodegradability and other performance characteristics and could

increase the product toxicity. The degree of quality degradation will vary with the level and type of contamination. UNIVIS BIO 40 is compatible with Nitrile, Viton and Acrylate. It is not suitable with Crude-Buryl or SBR elastomers.

Precautions

UNIVIS BIO 40 is blended using vegetable oil base stocks combined with selected additives. As with all petroleum products, good personal hygiene and careful handling should always be practiced. Avoid prolonged exposure with the skin, splashing into the eyes, ingestion or vapour inhalation. Please refer to the Material Safety Data Sheet for further information. Additional questions regarding this and all products should be directed to your local Sales Representative.

UNIVIS BIO 40 is not controlled under the Canadian WHMIS legislation.

*Trademarks of Imperial Oil Limited, Imperial Oil, Licensee. Lubricants and Specialties, Marketing Technical Services
 **Trademark of Exxon Corporation, Imperial Oil, Licensee. Helpline: 1-800-268-3183

Typical Properties

	UNIVIS BIO 40
Kinematic Viscosity	
cSt @ 40 °C	38
cSt @ 100 °C	9
Viscosity Index	240
Density @ 15 °C, kg/m ³	920
Flash Point, °C	230
Pour Point, °C	-36
Rust Protection	Pass
Oxidation Stability	180
Demulsibility	41-30-0
Slow Cool Data,	
Viscosity @ -30 °C, cSt	
after one day	1300
after three days	3400
after seven days	2400
Load Carrying Capacity, FZG pass stage	12

The values shown above are representative of current production. Some are controlled by manufacturing and performance specifications while others are not. All may vary within modest ranges.

*Trademarks of Imperial Oil Limited. Imperial Oil, Licensee. Lubricants and Specialties, Marketing Technical Services

**Trademark of Exxon Corporation. Imperial Oil, Licensee. Helpline: 1-800-268-3163





